



HAL
open science

The bromine and chlorine isotope composition of primary halite deposits and their significance for the secular isotope composition of seawater

H. G. M. Eggenkamp, P. Louvat, P. Agrinier, Magali Bonifacie, A. Bekker, V Krupenik, J Griffioen, J Horita, J JBrocks, R Bagheri

► To cite this version:

H. G. M. Eggenkamp, P. Louvat, P. Agrinier, Magali Bonifacie, A. Bekker, et al.. The bromine and chlorine isotope composition of primary halite deposits and their significance for the secular isotope composition of seawater. *Geochimica et Cosmochimica Acta*, 2019, 264, pp.13-29. 10.1016/j.gca.2019.08.005 . hal-02395315

HAL Id: hal-02395315

<https://hal.science/hal-02395315>

Submitted on 13 Dec 2019

HAL is a multi-disciplinary open access archive for the deposit and dissemination of scientific research documents, whether they are published or not. The documents may come from teaching and research institutions in France or abroad, or from public or private research centers.

L'archive ouverte pluridisciplinaire **HAL**, est destinée au dépôt et à la diffusion de documents scientifiques de niveau recherche, publiés ou non, émanant des établissements d'enseignement et de recherche français ou étrangers, des laboratoires publics ou privés.

1 **The bromine and chlorine isotope compositions of primary halite deposits and**
2 **their significances for the secular isotope compositions of seawater**
3

4 HGM Eggenkamp^{a,b,*}, P Louvat^a, P. Agrinier^a, M Bonifacie^a, A Bekker^c, V Krupenik^d, J Griffioen^{e,f},
5 J Horita^g, JJ Brocks^h, R Bagheriⁱ
6

7 a Institut de Physique du Globe de Paris, Sorbonne Paris Cité, UMR 7154, CNRS, 1 rue Jussieu,
8 75238 Paris Cedex 05, France

9 b Eberhard Karls Universität Tübingen, FB Geowissenschaften, AG Petrologie, Wilhelmstraße 56,
10 72074 Tübingen, Germany

11 c Department of Earth Sciences, University of California, Riverside, CA 92521, USA

12 d Sector of Precambrian Geology, A.P. Karpinsky Russian Geological Research Institute, 74
13 Sredny Prospect, 199106, St. Petersburg, Russia

14 e TNO Geological Survey of the Netherlands, P.O. Box 80015, Utrecht, the Netherlands

15 f Copernicus Institute of Sustainable Development, Utrecht University, P.O. Box 80115, Utrecht,
16 the Netherlands

17 g Department of Geosciences, Texas Tech University, Texas, 79409-1053, USA

18 h Research School of Earth Sciences, The Australian National University, Canberra, ACT 2601,
19 Australia

20 i Faculty of Earth Sciences, Shahrood University of Technology, Shahrood, Iran
21

22 *Corresponding author, email hans@eggenkamp.info
23

24 Keywords: Bromine isotopes, chlorine isotopes, isotope fractionation, halite, secular variation, salt
25 deposits
26

27 Abstract

28

29 We determined the chlorine and bromine isotope compositions of 83 halite samples from nine
30 different geological periods between the Orosirian and the Pliocene in order to study the secular Cl
31 and Br isotope variations in the ocean during the last 2 billion years. Relatively large Cl (-0.24 to
32 +0.51‰ vs. SMOC) and Br (-0.24 to +1.08‰ vs. SMOB) isotope variations are found in these
33 halite samples. Two different methods, one in which the isotope fractionation between the brine and
34 the salt is used, and a second in which the relationship between the isotope compositions and the
35 Br/Cl ratios in the halite samples is used were applied to establish the original Cl and Br isotope
36 compositions of the ocean. Both approaches showed that the Cl and Br isotope compositions of the
37 ocean have always been close to the modern value (which is by definition 0‰ for both isotope
38 systems) and that at most very small variations in Br and Cl isotope composition of seawater have
39 occurred during the last 2 billion years. This indicates that, unlike in other isotope systems that
40 often show significant isotope variations over geologic time, Cl and Br isotope compositions can be
41 used directly to determine processes that occurred in the deposits of interest without need for
42 correction for secular variations.

43

44 1. INTRODUCTION

45

46 Of the geochemically significant halogen elements (fluorine, chlorine, bromine and iodine) only
47 chlorine (Cl) and bromine (Br) have two stable isotopes. It is only of these two that the stable
48 isotope geochemistry can be studied. Chlorine consists of the isotopes ³⁵Cl and ³⁷Cl which exist in a
49 ratio of approximately 3:1. Bromine consists of the isotopes ⁷⁹Br and ⁸¹Br which exists at about
50 equal abundances. For both elements the internationally accepted standard is the isotope ratio of
51 seawater (Standard Mean Ocean Chloride, SMOC (Kaufmann, 1984) for chlorine and Standard
52 Mean Ocean Bromide (Eggenkamp and Coleman, 2000) for bromine. Their isotope variations are
53 reported as δ³⁷Cl and δ⁸¹Br values that indicate the per mil (‰) difference of the ratio of the isotope
54 of interest, relative to that ratio in the international standard. δ³⁷Cl is defined as:

55

$$56 \delta^{37}\text{Cl} = \left(\frac{{}^{37}\text{Cl}/{}^{35}\text{Cl}}{({}^{37}\text{Cl}/{}^{35}\text{Cl})_{\text{standard}}} \right) - 1$$

57

58 where (³⁷Cl/³⁵Cl)_{sample} is the Cl isotope ratio in the sample and (³⁷Cl/³⁵Cl)_{standard} in the standard.
59 δ⁸¹Br is defined as:

60

$$61 \delta^{81}\text{Br} = \left(\frac{{}^{81}\text{Br}/{}^{79}\text{Br}}{({}^{81}\text{Br}/{}^{79}\text{Br})_{\text{standard}}} \right) - 1$$

62

63 where (⁸¹Br/⁷⁹Br)_{sample} is the Br isotope ratio in the sample and (⁸¹Br/⁷⁹Br)_{standard} in the standard.

64 The chlorine isotope geochemistry of evaporite deposits has been studied extensively. The chlorine
65 isotope fractionation has been studied experimentally in individual evaporite minerals and brines
66 (Eggenkamp et al., 1995, 2016, Luo et al., 2012, 2014) and isotope variations have been studied in
67 detail both in marine evaporites (Eastoe and Peryt, 1999, Eastoe et al., 1999; 2001, 2007,
68 Eggenkamp et al., 2019) and terrestrial evaporites (Xiao et al., 1994; 1997; 2000; Liu et al., 1997,
69 Tan et al., 2005; 2006; 2009; Luo et al., 2012; Eastoe, 2016). As a result, the chlorine isotope
70 behaviour of an evaporating seawater body is now quite well understood. During evaporation of
71 modern seawater, the chlorine isotope ratio of the precipitated halite decreases from slightly
72 positive values in the first precipitated halite to fairly negative values when other salts start to
73 precipitate after halite. This effect is due to a Rayleigh-type fractionation because the precipitated
74 halite has a higher chlorine isotope ratio than the brine. As the heavier chlorine isotope is removed
75 preferentially from the brine the remaining brine becomes lighter, and halite that precipitates later
76 have thus lighter isotope compositions. This effect has recently been confirmed to exist in natural

77 salt sequences by Eggenkamp et al. (2019) in a study on Cl and Br isotope variations in a fully
78 developed Zechstein (Upper Permian) salt sequence from the Netherlands. The Cl isotope data
79 observed in both natural salt deposits (Eggenkamp et al., 1995; 2019) and experimental evaporation
80 of seawater (Eastoe et al., 1999) indicate that salt precipitates from brine in an open system. If salt
81 were to precipitate in a closed system this would indicate that its isotope ratio could not be lower
82 than the original isotope ratio of the brine, and these studies already showed that lower ratios are
83 possible in significantly evolved salt deposits.

84 The chlorine isotope composition of an extensive set of Late Proterozoic to Miocene salts has been
85 previously measured by Eastoe et al. (2007) who concluded that the chlorine isotope composition of
86 the ocean could not have varied significantly from its modern composition. They observed that all
87 $\delta^{37}\text{Cl}$ values of marine evaporites were in the range of $0.0\pm 0.9\%$ relative to SMOC (Standard Mean
88 Ocean Chloride, equivalent to the Cl isotope composition of the modern ocean) with most of the
89 data in the range of $0.0\pm 0.5\%$, but with larger ranges observed in smaller basins. On average, lower
90 Cl isotope values were found in potash-rich basins. These data suggest that no detectable change in
91 Cl isotope ratio of seawater has taken place during the Phanerozoic. Cl isotope values measured in
92 Precambrian cherts, barite, dolomite and halite confirmed that values must have been relatively
93 constant during the Precambrian too, although the data suggest a possibly wider range than for the
94 Phanerozoic (Sharp et al., 2007, 2013).

95 The isotope fractionation of chlorine during precipitation of chloride salts from saturated solutions
96 has been studied extensively (Eggenkamp et al., 1995, 2016; Luo et al., 2012, 2014). Based on the
97 isotope fractionation factors for halite (NaCl), it is possible to estimate, within an approximate
98 range of 0.5% , what was the original Cl isotope composition of seawater if the Cl isotope
99 composition of halite salts of a marine evaporite deposit is measured. This approach makes it
100 possible to impose a better constraint on and explore some limited variations in the original Cl
101 isotope composition of the ocean during the Phanerozoic and to resolve whether limited Cl isotope
102 variations in the seawater compositions occurred.

103 In their recent paper Eggenkamp et al. (2019) showed that the chlorine isotope composition within a
104 single salt sequence correlates very well with its Br/Cl ratio. As a consequence, the combination of
105 the Cl isotope ratio with the Br/Cl ratio for a sample makes it possible to estimate the original Cl
106 isotope composition of the brine from which a salt precipitated as the Br/Cl ratio of the first
107 precipitating halite is known for the Phanerozoic (Siemann, 2003). Consequently, combining Cl
108 isotope values and Br/Cl ratios, it might be possible to determine the original Cl isotope ratio of a
109 brine more precisely than with other techniques.

110 Compared to Cl, our knowledge of the Br isotope composition of evaporites and ancient seawater is
111 very limited. This knowledge was only based on a small number of Br isotope determinations of
112 formation waters with very low Br/Cl ratios (Eggenkamp, 2014), which, as a consequence, should
113 have most of their Cl and Br content from the dissolution of Br-poor (and halite-rich) evaporite
114 deposits. Only eight such samples were recognised and published prior to 2016 (Shouakar-Stash et
115 al., 2007; Boschetti et al., 2011; Bagheri et al., 2014) and they suggest an average $\delta^{81}\text{Br}$ value of
116 $+0.60\pm 0.29\%$ for evaporites. This value is at first sight not consistent with Br precipitation from
117 modern seawater with a value of 0% vs. SMOB, as an almost negligible Br isotope fractionation
118 was expected (Eggenkamp, 1995, Eggenkamp et al., 2016), indicating either a significantly more
119 positive Br isotope ratio in ancient seawater or a significant isotope fractionation accompanying
120 incorporation of bromide into chloride minerals during precipitation of salt from brine. The Br
121 isotopes in a salt sequence from the Dutch Zechstein deposit seems even more complex
122 (Eggenkamp et al., 2019). From slightly positive $\delta^{81}\text{Br}$ values ($+0.2\%$) in the samples with the
123 lowest Br/Cl ratios, $\delta^{81}\text{Br}$ values decreased sharply (to -0.5%) in samples with slightly higher Br/Cl
124 values, and increases again (to $0.1 \pm 0.3\%$) in samples with very high Br/Cl ratios (carnallite- and
125 bischofite-dominated samples). This effect was explained as a competition effect between Br^- and
126 Cl^- ions in solution for incorporation into a chloride salt. Due to its slightly larger size, Br^- ions are

127 more difficult to be incorporated into the salt and will thus concentrate in the brine. This effect has
128 been explained to produce a considerably larger isotope fractionation factor than the equilibrium
129 between Br^- in solution and Br^- in a pure bromide salt (Eggenkamp et al., 2016, 2019). This effect
130 must be related to the fact that there is only 1 Br^- ion for 600 Cl^- ions in seawater as compared to Br^-
131 ions only in pure bromide brine.

132 For the present study, we collected a total of 83 presumably primary (unaltered) salt samples
133 dominated by halite so that it could be expected that they were precipitated during early stages in
134 salt precipitation. The geologic ages of the samples range from the Paleoproterozoic to recent salt
135 pans, covering approximately 2 billion years. For all samples, chemical compositions and Cl and if
136 possible Br isotopic compositions were determined in order: 1/ to assess if it were possible to
137 constrain the Cl isotope variations to a narrower band than had been done before by Eastoe et al.
138 (2007); 2/ to assess if the Br isotope composition of the ocean was as stable as the Cl isotope
139 composition; and 3/ to refine the understanding on the Br isotope variations observed in halite-
140 dominated salt samples.

141

142 **2. MATERIAL**

143

144 We collected 73 salt samples from various evaporite deposits from Pliocene to Orosirian ages, as
145 well as 10 recent salt pan samples for comparison with the ancient samples. The ancient samples are
146 from 16 different geological stages and were sampled from different locations in North America,
147 Europe, Asia, and Australia. Some samples were individual samples, while others were related
148 samples taken from a single drill-core or from within a restricted area. A brief description of the
149 samples used in this study follows, sorted by age from the most recent to the most ancient. The
150 analytical results are presented in Table 1. In the discussion, the samples from each geological
151 period are combined in order to have a large enough set of samples per time period to properly
152 estimate Cl and Br isotope trends. The samples often originate from several subperiods as discussed
153 below.

154

155 **2.1 Recent samples**

156

157 10 samples of modern sea salts were mostly bought from supermarkets in France and the
158 Netherlands. The salts are from different locations, most of them in Europe with a focus on France.
159 Of these MO1 is JOZO salt (AKZONobel) of unknown origin, MO2 is from the Mediterranean
160 coast of France (La Baleine), MO3 is Maldon salt from the United Kingdom, MO4 is from the
161 South Coast of Portugal (Atlantis salt), MO5 and EVA27 are Fleur de Sel from Gu erande, MO6 is
162 from Le Saunier, and MO7 is from Noirmoutier. The last three are from France, MO6 from the
163 Mediterranean coast (Camargue), while MO5 and MO7 are from the Atlantic coast. EVA 6 and
164 EVA10 are from Sicily (Mediterranean Sea). All samples except MO3 are produced from salt pans,
165 where seawater is introduced into individual pans and left to evaporate by the sun. Evaporation is
166 enhanced by regularly turning the salt. MO3 is produced by seething, a process by which seawater
167 is filtered and boiled in salt pans until it crystallises (see <http://www.maldonsalt.co.uk/The-Story-How-Maldon-Salt-is-made.html>).

168

170 **2.2 Neogene**

171

172 *2.2.1 Plio-Pleistocene (about 2.6 Ma)*

173

174 One sample (H1) was taken from the Sedom salt deposit in Israel (Zak, 1967; Weinberger et al.,
175 1997; Stein et al., 2000).

176

177 2.2.2 *Messinian (about 6.3 Ma)*

178

179 Nine samples from Messinian salt deposits were analysed. EVA2, EVA9, EVA12, and EVA24 are
180 from Sicily in Italy: EVA 2 (Pe38 3D) and EVA12 (Pe38 6D) from borehole Porto Empedocle 38,
181 (Caltanissetta basin), EVA9 (Mess1) from Realmonte Mine and EVA24 (Cat5) from Cattolica
182 Eraclea borehole. EVA15 (L4 212) and EVA23 (L4 228) are from Lorca in Spain (Paris et al.,
183 2010). IR1, IR2 and IR3 are from the Garmsar Salt Dome in North Iran (Alijani, 2000), deposited in
184 a lagoon during the Ghom sea regression. Upon analysis, sample IR1 happened to be a KCl salt and
185 was not used as a primary source in the following study to determine the original Cl isotope
186 composition of the Messinian Ocean.

187

188 2.2.3 *Serrevalian (about 12.7 Ma)*

189

190 Two samples (EVA5 and EVA7) from Serravallian salt deposits in Poland, taken from the section
191 Woszczyce IG-1, were analysed (Paris et al., 2010).

192

193 **2.3 Paleogene**

194

195 2.3.1 *Eocene-Oligocene transition (about 33.9 Ma)*

196

197 The three samples EVA8 (EZ8 1229), EVA14 (EZ8 1230.7) and EVA18 (EZ8 1400) were from the
198 Eocene-Oligocene salt deposits from Bresse in Eastern France (Paris et al., 2010).

199

200 2.3.2 *Priabonian (about 35.9 Ma)*

201

202 The three samples EVA16 (BI 436/1), EVA20 (BI 436/2) and EVA21 (BI 427) were from
203 Priabonian salt deposits from the Lower Evaporite Unit of the Biurrun borehole in Navarra, Spain
204 (Paris et al., 2010).

205

206 **2.4 Triassic**

207

208 2.4.1 *Carmian/Norian (about 227 Ma)*

209

210 One French Keuper sample from the Paris Basin was analysed (H2).

211

212 2.4.2 *Anisian (about 245 Ma)*

213

214 Seven samples (NL02 to NL08) were taken from the drill-core TWR-515 from depths between
215 418.3 and 424.2 m. These samples are from Röt (Triassic) deposits of Anisian age. The core was
216 drilled in 2000 by AKZO in order to explore for table salt. The description of the core can be found
217 at the Dutch Oil and Gas Portal (<http://www.nlog.nl/en>): click on "boreholes" and "listing boreholes"
218 then search for TWR-515. The purest halite samples were selected from this core based on their
219 translucency.

220

221 **2.5 Permian**

222

223 2.5.1 *Changhsingian (about 253 Ma)*

224

225 One sample (H3) is taken from the Changhsingian Salado salt deposit in New Mexico (Maley and
226 Huffington, 1953; Pierce and Rich, 1962).

227
228
229
230
231
232
233
234
235
236
237
238
239
240
241
242
243
244
245
246
247
248
249
250
251
252
253
254
255
256
257
258
259
260
261
262
263
264
265
266
267
268
269
270
271
272
273
274
275
276

2.5.2 *Wuchiapingian (about 257 Ma)*

Six of the samples described in Eggenkamp et al. (2019), which are halite salt samples are incorporated in this study. These samples were recently taken the core TCI-2, which was described and studied earlier by Eggenkamp et al. (1995). A general description of this core was given in Coeleweij et al. (1978) and Buyze and Lorenzen (1986).

2.6 Late Ordovician to Middle Devonian

2.6.1 *Givetian (about 385 Ma)*

The three samples EVA1 (15.34.93.24W4), EVA4 (6.80.36.13W4) and H4 were taken from the Givetian (Mid-Devonian) Canadian Prairie Formation (Grobe, 2000). EVA1 and EVA4 were made available from the collection of the Muséum Nationale de Histoire Naturelle in Paris.

2.6.2 *Late Ordovician / Early Silurian (about 444 Ma)*

One sample (H5) was taken from the Western Australian Caribuddy Formation of the Late Ordovician to Early Silurian age (Haines, 2009). As this sample was visibly heterogeneous, containing white and red parts, it was split into two, H5a containing the white salt and H5b containing the red salt.

2.7 Ediacaran to Early Cambrian

2.7.1 *Terreneuvian (about 531 Ma)*

One sample (H6) was taken from the East Siberian Angarskaya Formation (Petrychenko et al., 2005).

2.7.2 *Ediacaran (about 545 Ma)*

One sample (H7) is taken from the Ara Formation in Oman (Mattes and Conway Morris, 1990; Schröder et al., 2005) and three (IR4, IR5 and IR6) from the Iranian Hormuz Formation (Kent, 1979; Alavi, 2004). These samples are of comparable age are lateral equivalent to each other.

2.8 Tonian (about 820 Ma)

Six samples (AU1 to AU6) were collected from the Gillen Formation of the Bitter Springs Group, Amadeus Basin in central Australia. The Gillen Formation was, until recently, the oldest known massive salt deposit (Naughton et al., 1968; Stewart, 1979). Samples AU1 AU3 were collected from drill core Mt Charlotte-1 at depths of 1875.34 to 1875.44, 1877.85 to 1877.92 and 2060.14 m respectively. Samples AU4 to AU6 were collected at depths of 556', 306' and 600' from diamond drill core Mt Liebig-1 and represent massive, orange-coloured halite.

2.9 Orosirian (about 2000 Ma)

This deposit represents a recently discovered massive and thick evaporite (halite and anhydrite) deposit that is only recognised in the Onega parametric well in Russia (Morozov et al., 2010; Krupenik and Sveshnikova, 2011; Gorbachev et al., 2011; Glushanin et al., 2011). These are the

277 oldest currently known massive halite deposits on Earth. They are described as marine evaporites
278 (Blätter et al., 2018). It is not known yet if their thickness in the drill core represents stratigraphic
279 thickness or the thickness of the evaporite interval in a salt diapir. 23 samples from this core were
280 available for this study. Magnesium and calcium isotopes of this evaporite deposit have recently
281 been studied and interpreted to record the Great Oxidation Event that can explain the high sulphate
282 contents in these deposits (Blättler et al., 2018). Several of the samples analysed in the study from
283 this deposit were previously measured for their Cl isotope composition by Sharp et al. (2013).

284

285 3. METHODS

286

287 All samples, except those labelled "EVA" were available as solid salt samples. The "EVA" samples
288 were available as solutions prepared previously with approximately seawater chloride
289 concentrations (see Paris et al., 2010). Solid salt samples were dissolved in water in a ratio of 1:9 (1
290 gram of salt and 9 grams of distilled water) for Cl and Br isotope measurements. This 1:9 solution
291 was diluted by an extra 1000 times to obtain solutions diluted enough for ICP-OES and ICP-MS
292 measurement of the chemical composition. All dissolved samples were analysed for the
293 determination of chemical (Cl^- , Br^- , SO_4^{2-} , Na^+ , K^+ , Mg^{2+} and Ca^{2+}) and isotopic ($\delta^{37}\text{Cl}$ and $\delta^{81}\text{Br}$)
294 compositions at the Institut de Physique du Globe de Paris, France.

295 Cl^- and Br^- concentrations were measured by ICP-MS on an Agilent Technologies 7900 ICP-MS.
296 The cations and sulphate (measured as S) were analysed by ICP-OES on a Thermo Scientific iCAP
297 6000 Series ICP Spectrometer. The results were calculated back to the chemical composition of the
298 salts and are reported in Table 1 in the unit of g per kg salt.

299 The chlorine isotope composition was measured according to the method described by Kaufmann
300 (1984), Eggenkamp (1994) and Godon et al. (2004). In short, Cl^- is precipitated as AgCl by adding
301 AgNO_3 , which was reacted with CH_3I to form CH_3Cl . CH_3Cl is separated from CH_3I by two gas
302 chromatograph runs using a PÉrichrom IGC-11 gas chromatograph (with dry pure He at 130 °C, 2.1
303 bar and 15 ml/min) in two identical packed columns (Porapak-Q 80–100 mesh, 2 m length and
304 3.175 mm outer diameter). A thermal conductivity detector is used to check the progress of this
305 purification and to detect any leaks. $^{37}\text{Cl}/^{35}\text{Cl}$ ratios were subsequently determined on the CH_3Cl
306 with dual-inlet mass spectrometry on a ThermoFisher Delta PlusXP mass spectrometer (IRMS). The
307 results are reported in the δ notation (as $\delta^{37}\text{Cl}$) in ‰ relative to SMOC (Standard Mean Ocean
308 Chloride, Kaufmann et al., 1984), with a standard deviation (1σ) of 0.05‰.

309 The bromine isotope composition was measured on a Neptune (ThermoFisher) multicollector ICP
310 mass spectrometer (MC-ICP-MS). Due to the low Br/Cl ratios of the halite samples, it was not
311 possible to extract the bromide using the classic ion-exchange method (Louvat et al., 2016);
312 bromine was extracted through oxidative distillation following Murphy et al. (1954) as described by
313 Eggenkamp and Louvat (2018). Bromide is oxidised to bromine gas by a 14% boiling nitric acid
314 solution and distilled into a 0.5N ammonia solution, where bromine is trapped and
315 disproportionated into bromide and bromate. Due to the reducing nature of the ammonia solution,
316 bromate is reduced to bromide. The extraction efficiency of this distillation is about 50%. As shown
317 by Eggenkamp and Louvat (2018) no isotope fractionation was observed during the distillation
318 process. This solution can be measured directly by MC-ICP-MS as a wet plasma as described by
319 Louvat et al. (2016). Results are reported in the δ notation (as $\delta^{81}\text{Br}$) in ‰ relative to SMOB
320 (Standard Mean Ocean Bromide, Eggenkamp and Coleman, 2000) with an average standard
321 deviation (1σ) of about 0.1‰.

322 For both Cl and Br isotope measurements ocean water sampled in the Indian Ocean (sampled in
323 January 2010 during the MD 175 cruise, latitude 32.45°S, longitude 84.01°E) was prepared and
324 measured 13 times for its $\delta^{37}\text{Cl}$ composition (with better than 0.05‰ 1σ standard deviation, which
325 is comparable to the typical long-term external reproducibility of $\delta^{37}\text{Cl}$ measurements obtained at
326 IPGP on both seawater and unknown samples; e.g., Godon et al., 2004 and Bonifacie et al., 2005)

327 and prepared and measured 5 times for its $\delta^{81}\text{Br}$ composition (with better than 0.10‰ 1 σ standard
328 deviation).

329 Results of the $\delta^{37}\text{Cl}$ and $\delta^{81}\text{Br}$ measurements are also reported in Table 1. The accuracy of the
330 measurements is indicated in the Table showing the 1 σ standard deviation of multiple (mostly two)
331 preparations and measurements of the same sample.

332

333 4. RESULTS

334

335 Data reported in Table 1 show that all samples except one (IR1) are predominately composed of
336 halite. Varying amounts of K, Mg and Ca are present, indicating that the evaporates formed during
337 various stages of halite-dominated precipitation. As the Br/Cl ratio can be used as a proxy for the
338 evaporation stage (Valyasko, 1956; Braitsch, 1962; Herrmann et al., 1973; McCaffrey et al., 1987;
339 Eggenkamp et al., 2019), it was calculated for all samples and included in table 1. The samples
340 show a considerable range in Br/Cl ratios, from <0.00001 to 0.00091. All samples with very low
341 Br/Cl ratios (<0.00005) are taken from the Onega parametric well in Russia (A02 to A21), and due
342 to their low Br content and insufficient amount of sample available it was only possible to analyse
343 two of these samples for Br isotopes. The total range of Cl isotope ratios in the sample set ranges
344 from -0.24 to +0.51‰, while the range of Br isotope ratios is from -0.24 to +1.08‰. The total range
345 of Br isotope ratios is thus considerably larger than that for Cl isotope ratios.

346

347

Table 1

348

349

350 5. DISCUSSION

351

352 Based on a set of 132 salt samples with ages ranging from the Late Neoproterozoic (ca. 550 Ma) to
353 the Messinian (ca. 6.3 Ma), Eastoe et al. (2007) concluded that significant variations in the Cl
354 isotope composition of the ocean were unlikely during this period. They reported no range within
355 which the Cl isotope composition could have varied (however small it may have been), which was
356 based on the observation that the overwhelming majority of salt samples had $\delta^{37}\text{Cl}$ values between -
357 0.50 and +0.50‰ relative to SMOC. We expect that it should be possible to constrain the $\delta^{37}\text{Cl}$
358 secular trend of the ocean within a narrower limit using our recent constraints for the isotope
359 fractionation of chloride during chloride salt precipitation from saturated brine. There are several
360 studies that determined the isotope fractionation of chlorine during precipitation from saturated
361 brine (Eggenkamp et al., 1995, 2016, Luo et al., 2012, 2014). The fractionation factors obtained in
362 these studies varied considerably. Eggenkamp et al. (1995) reported a value of $\alpha=1.00026$,
363 Eggenkamp et al. (2016) reported 1.00035 and the average of the values reported by Luo et al.
364 (2012, 2014) is 1.00049. This relatively large variability has to be taken into account, if the original
365 $\delta^{37}\text{Cl}$ of seawater is to be determined. If the fractionation factor is larger, the $\delta^{37}\text{Cl}$ values of the
366 precipitated halite diverge progressively with precipitation (see e.g. the discussion by Eggenkamp
367 (2015a) and Luo et al. (2015)). Thus, the estimate of secular seawater $\delta^{37}\text{Cl}$ values requires
368 relatively large corrections, if the larger fractionation factors are assumed. The Br isotope data in
369 the present paper are the first of a notable number of halite samples, and the seawater record of the
370 Br isotopes will be discussed despite our limited knowledge of Br isotope fractionation during sea-
371 salt precipitation.

372

373 5.1 Estimate of the secular $\delta^{37}\text{Cl}$ values of seawater

374

375 Here we apply two methods to estimate the original $\delta^{37}\text{Cl}$ of the ocean based on the $\delta^{37}\text{Cl}$ values of
376 the analysed halite samples. At first, an approach solely based on $\delta^{37}\text{Cl}$ values is applied, and the

377 second approach is based on the Br/Cl ratio used as a parameter in combination with the $\delta^{37}\text{Cl}$ of
378 the samples to infer the original $\delta^{37}\text{Cl}$ of the ocean from which the halite was precipitated.
379

380 5.1.1 Estimate based on $\delta^{37}\text{Cl}$ of halite salt only

381
382 When salt precipitates from a saturated solution it removes heavy chlorine isotope from the brine
383 that, as a result, becomes enriched in the lighter isotope. This effect is a classic Rayleigh effect that
384 has been described before (Eggenkamp et al., 1995, Luo et al., 2014, Eggenkamp 2015). As long as
385 halite is the only chloride-precipitating mineral, this process is gradual. The previous studies have
386 demonstrated that the first halite that precipitates is heavier in Cl isotopes than that of seawater, and
387 that it becomes progressively lighter until 82.5% of all chloride is precipitated and the first
388 potassium chloride (kainite [$\text{K}_4\text{Mg}_4\text{Cl}_4(\text{SO}_4)_4 \cdot 11\text{H}_2\text{O}$]) starts to precipitate (Braitsch, 1962). From
389 this stage, precipitating salt is no longer a pure halite so that isotope fractionation, as well as Br
390 distribution, will be different from there on. Thus, if we use the $\delta^{37}\text{Cl}$ of a primary halite to infer the
391 seawater composition it must have precipitated before 82.5% of the chloride present in the brine has
392 been precipitated. The $\delta^{37}\text{Cl}$ composition of salt that precipitated from modern seawater with a
393 $\delta^{37}\text{Cl}$ value of 0‰ decreases depending on the fractionation factor that is used. For example, if we
394 assume a fractionation factor of 1.00026, the halite precipitated initially will have a $\delta^{37}\text{Cl}$ of
395 +0.26‰ and the last batch (when potassium-bearing chloride starts to precipitate) will have a $\delta^{37}\text{Cl}$
396 of -0.19‰. If we use a fractionation factor of 1.00035, $\delta^{37}\text{Cl}$ of the precipitated halite decreases
397 from +0.35‰ to -0.26‰ due to the Rayleigh effect. Similarly, if we use a fractionation factor of
398 1.00049, the $\delta^{37}\text{Cl}$ of the halite decreases from +0.49‰ to -0.36‰. To know the $\delta^{37}\text{Cl}$ composition
399 of the original seawater, these $\delta^{37}\text{Cl}_{\text{halite}}$ values need to be inverted. That means that in the case of a
400 fractionation factor of 1.00026 the original $\delta^{37}\text{Cl}$ value of the ocean was somewhere between
401 0.26‰ lower and 0.19‰ higher than the $\delta^{37}\text{Cl}$ of the halite sample, depending on where the sample
402 was precipitated on the Rayleigh curve. For higher fractionation factors, these numbers are between
403 0.35‰ lower and 0.26‰ higher for $\alpha=1.00035$ and between 0.49‰ lower and 0.36‰ higher for
404 $\alpha=1.00049$. This result in fairly large potential ranges for the original $\delta^{37}\text{Cl}$ of the oceans, as it is
405 unknown at what point on the Rayleigh curve the samples precipitated. Figure 1 shows how this
406 process is applied to seawater with a $\delta^{37}\text{Cl}$ of 0‰ and halite with a fractionation factor of 1.00035.
407 However, since we have measured multiple halite samples for each geological period, it is possible
408 to decrease the calculated range of $\delta^{37}\text{Cl}$ in seawater.
409

410 Figure 1

411
412 Indeed, assuming primary, unaltered $\delta^{37}\text{Cl}$ values of the salt samples, the possible range of $\delta^{37}\text{Cl}$ in
413 the ocean must be the overlapping part of all the $\delta^{37}\text{Cl}$ ranges from the individual samples
414 corresponding to the concerned geological period. Figure 2 illustrates how this works for one of the
415 geological periods, the Permian, a period from which we analysed eight samples. For each of the
416 eight samples we calculate the maximum range of possible original $\delta^{37}\text{Cl}$ of the seawater for
417 $\alpha=1.00035$. This figure shows that the range, within which the original $\delta^{37}\text{Cl}$ must have layed,
418 decreases significantly when more samples from a period were measured. In the case a smaller or
419 larger value for α used the original $\delta^{37}\text{Cl}$ range will be smaller or larger. It is clear from this figure
420 that the effective range of $\delta^{37}\text{Cl}$ of the seawater is where all eight $\delta^{37}\text{Cl}$ of the seawater ranges of the
421 samples overlap. In the case of the Permian the figure shows that assuming a fractionation factor α
422 of 1.00035 the original $\delta^{37}\text{Cl}$ of the oceans must have been between -0.10‰ and +0.14‰. This
423 range would be smaller (between -0.01‰ and +0.07‰) assuming $\alpha=1.00026$, or larger (between -
424 0.24‰ and +0.24‰) assuming $\alpha=1.00049$.
425

426 Figure 2

427
428
429
430
431
432
433
434
435
436
437
438
439
440
441
442
443
444
445
446
447
448
449
450
451
452
453
454
455
456
457
458
459
460
461
462
463
464
465
466
467
468
469
470
471
472
473
474
475
476

Table 2

These calculations were made for all the geologic periods considered here and the results are summarised in Table 2. This table highlights also weaknesses of this approach. For two periods, the Recent and the Neogene, the range in $\delta^{37}\text{Cl}$ of the seawater was larger than the possible isotope variation if we assume $\alpha=1.00026$. As a consequence, the minimum value in this approach is higher than the maximum value, and that means that the seawater $\delta^{37}\text{Cl}$ cannot be explained with a fractionation factor of 1.00026. The range can be explained however with higher fractionation factors, and the most straightforward conclusion is that the chlorine isotope fractionation factor for the precipitation of halite from ocean water must be larger than 1.00026. The second problem is the reconstructed $\delta^{37}\text{Cl}$ of seawater based on modern salt samples. The mean value of the reconstructed $\delta^{37}\text{Cl}$ (based on fractionation factors 1.00035 and 1.00049) is +0.18‰, while the $\delta^{37}\text{Cl}$ of today's oceans is by definition 0‰. While the values obtained for ancient seawater seem to reflect the original $\delta^{37}\text{Cl}$ of those periods the recent samples seem not to, which might reflect differences in the precipitation process. All historic samples are precipitated from evaporating seawater in a static way, where a batch of seawater evaporated until it became saturated with halite and halite will precipitate to the bottom of the evaporite basin. The modern samples on the other hand (except MO3) were precipitated in an active way, where the precipitation of salt from seawater was as quickly as possible to improve the precipitation rate, especially by keeping the ponds as shallow as possible and to remove the salt immediately upon precipitation so that it can be dried in the sun. These effects considerably increase the kinetics of salt precipitation and this might result in possible non-equilibrium precipitation of halite from these seawaters as well as the significant isotope variation among these samples, including some that are from the same location. It has to be realised that all calculations above were made as if the chemical composition of ocean water had not changed during geologic history, while this composition obviously has changed (Babel and Schreiber, 2014). We have decided to work in this preliminary study using the modern composition of ocean water in order to simplify the calculations, although, as sulphate concentrations in the past were generally lower than they are today the halite only phase may have been more extended and might have been up to 86.9% when carnallite ($\text{KMgCl}_3 \cdot 6\text{H}_2\text{O}$) starts to precipitate (Eggenkamp et al., 1995) for sulphate free brines.

5.1.2 Estimate based on $\delta^{37}\text{Cl}$ and Br/Cl ratios of halite

It is well established that during precipitation of salt from seawater brine not only the $\delta^{37}\text{Cl}$ value of the brine decreases due to a Rayleigh type isotope fractionation, but also that the Br/Cl ratio increases. Because the Br/Cl ratio of precipitated halite is significantly lower than the Br/Cl ratio in seawater, controlled by the distribution coefficient, the Br/Cl ratios of the precipitated salt and the remaining brine evolve in a fashion very similar to that of the $\delta^{37}\text{Cl}$, following a Rayleigh fractionation process. This effect has been studied extensively in the past (e.g. Boeke, 1908; Kühn, 1955; Valyasko, 1956; Braitsch, 1962; Herrmann, 1972; Herrmann et al., 1973). Eggenkamp et al. (2019) have shown that a clear relationship between $\delta^{37}\text{Cl}$ and Br/Cl ratios is observed in a well-developed salt sequence. Figure 3 shows the relationship between the $\delta^{37}\text{Cl}$ and the Br/Cl ratios of the salt samples that were measured for the present study. The sample set can be separated into three populations. To the left a series of samples with a large variation in low Br/Cl ratios and very constant $\delta^{37}\text{Cl}$ values around -0.1‰, to the right a group of samples with high Br/Cl values and relatively high $\delta^{37}\text{Cl}$ values, and in the centre, which is the largest set of samples, a group of samples showing an inverse correlation between $\delta^{37}\text{Cl}$ values and Br/Cl ratios.

Figure 3

477

478 In more detail, the first group of samples (with a large variation in very low Br/Cl ratios and nearly
479 constant and low $\delta^{37}\text{Cl}$ values) are all Orosirian samples from the Onega parametric well in Russia.
480 These two billion years old evaporites show extremely low Br contents, but also very similar $\delta^{37}\text{Cl}$
481 values. We can explain this by repeated dissolution and reprecipitation cycles in which the Br
482 content decreased in each cycle (due to Br^- enrichment in the brine that for a large part disappeared
483 from the deposit), while the $\delta^{37}\text{Cl}$ values became homogenised during this process. This
484 interpretation is consistent with the Sr and S isotope data (Krupenik and Shesnikova, 2011; Blättler
485 et al., 2018), indicating a depositional system largely disconnected from the open ocean and
486 potential dissolution-reprecipitation and mixing related to diapir growth.

487 The second group of samples (with high Br/Cl ratios and high $\delta^{37}\text{Cl}$ values), are all modern “table”
488 salts that were produced with modern industrial production techniques as described above. The high
489 Br/Cl ratios in these salts might reflect kinetic rather than equilibrium fractionation since still wet
490 salt is removed from the salt pans and put aside to dry in the sun. Consequently, wet salt contains
491 significant amounts of brine with very high Br/Cl ratios, increasing the Br content of the final salt.
492 The high $\delta^{37}\text{Cl}$ ratios of industrial salt samples indicate much larger kinetic compared to
493 equilibrium fractionation factor as precipitates were removed from the brine well before the
494 thermodynamic equilibrium could have been reached. Similarly, this large difference between
495 kinetic and equilibrium fractionation factors might explain the large range of fractionation factors
496 involved in halite precipitation from brine discussed above. The fact that the modern salt stands
497 aside from ancient primary salt deposits shows however that the calculations done in the previous
498 section confirm that the reconstructed $\delta^{37}\text{Cl}$ of the modern ocean does not agree with the actual
499 $\delta^{37}\text{Cl}$ of the seawater from which it precipitates.

500 The third and largest group of samples, which contains all the samples from ancient primary salt
501 deposits, shows promising relationships. These samples fall on a trend showing a negative
502 correlation between $\delta^{37}\text{Cl}$ values and the Br/Cl ratios. Using this relationship, it might be possible to
503 retrieve the original $\delta^{37}\text{Cl}$ values of the seawater for each geological period. This was tested for
504 each period by applying the relationships between Br/Cl ratio and $\delta^{37}\text{Cl}$. Seven plots are produced
505 (Figure 4) that show the expected negative relationship between $\delta^{37}\text{Cl}$ values and the logarithm of
506 the Br/Cl ratio with varying degrees of uncertainties that are reflected by hyperbolas. Extrapolation
507 to the logarithm of the Br/Cl ratio of the first precipitating halite yields an estimate of $\delta^{37}\text{Cl}$ of the
508 first precipitated halite and from that the $\delta^{37}\text{Cl}$ of the seawater can be (in theory)
509 recovered/retrieved.

510 The Br content of the first precipitated halite can be obtained theoretically from the bromide content
511 in the brine at the stage of the first halite precipitation and from the Br distribution coefficient
512 between halite and the brine. This distribution coefficient (defined as $b = \text{mass\% Br in salt} / \text{mass\%}$
513 Br in brine) is 0.14 (Braitsch, 1962). Since the Br content in the brine at the moment of first halite
514 precipitation is about 0.053%, the Br content in the first precipitated halite is 0.0074%, and the
515 Br/Cl ratio in this halite is 0.00012. However, this is only correct if we assume that seawater had
516 the same chemical composition as the modern ocean. Yet, the chemical composition of seawater has
517 changed considerable over geological history (see e.g. Horita et al., 2002; Lowenstein et al., 2014).
518 These changes in seawater composition also had a significant influence on the amount of Br that is
519 incorporated in the first precipitated halite (cf. Siemann and Schramm, 2000; Siemann, 2003).
520 These studies have shown that in most of the Phanerozoic the bromide content in the first halite that
521 precipitated was lower than at present. According to their results, in the geological periods of
522 interest, the first precipitated halite should show Br/Cl ratios of 0.00017 (Neogene), 0.00010
523 (Paleogene), 0.00015 (Triassic), 0.00014 (Permian), 0.00008 (Ordovician-Devonian) and 0.00017
524 (Ediacaran-Cambrian). The ratio is not known for the Tonian. These values were recalculated from
525 $\mu\text{g Br/g NaCl}$ ratios as presented by Siemann (2003) to Br/Cl mass ratios. It is, however, important
526 to consider these Br/Cl ratio calculations with caution (Lowenstein et al., 2014), because Br

527 concentrations reported from the first precipitated halite in modern marine settings vary
528 substantially from study to study. For comparison, 38 ppm in halite grown experimentally from
529 Mediterranean seawater (Bloch and Scherb, 1953) to 50 ppm in modern halite from Baja California,
530 Mexico (Holser, 1966), to 100 ppm from evaporated North Sea seawater (Siemann, 2003). Br
531 concentrations in the recent commercial salt samples measured in this study are even higher than
532 these observations, but as discussed above this is probably due to non-equilibrium processes by
533 which these salts were produced.

534 The same uncertainties are also notable in our set of samples. The global relationship between Br/Cl
535 ratios and $\delta^{37}\text{Cl}$ values on Figure 3 shows that in our dataset the lowermost Br/Cl limit of primary
536 samples (thus excluding the Paleoproterozoic samples) can be as low as 0.00005 for a Triassic
537 sample, comparable to the ratio expected for the periods with the lowest suggested Br/Cl ratio by
538 Siemann (2003), but unfortunately not the Triassic, which should have a two to three times higher
539 Br/Cl ratio for first precipitated halite. These results indicate that model Br/Cl data for the first
540 precipitated halite as determined by Siemann (2003) must be used with caution and for the purpose
541 of the present study we will use the lowest Br/Cl ratio measured in our dataset (0.00005) to estimate
542 the original $\delta^{37}\text{Cl}$ of the ocean for the different geologic periods.

543

544

545

Figure 4

546 On figure 4 the regression lines as well as the uncertainty hyperbolas are extrapolated to a Br/Cl
547 ratio of 0.00005 (= -4.3 in log units) for samples from all geological period samples that were
548 available in this study. The resulting $\delta^{37}\text{Cl}$ values (and uncertainties) are summarised in Table 3.

549

550

Table 3

551

552 At first approximation these values can be considered as the $\delta^{37}\text{Cl}$ of the first precipitated halite for
553 each geologic period. The original seawater $\delta^{37}\text{Cl}$ can then be determined by subtracting $10^3\ln\alpha$ (α =
554 fractionation factor) from these extrapolated $\delta^{37}\text{Cl}$ values, using α values of 1.00026, 1.00035 and
555 1.00049 (Eggenkamp et al., 1995, 2016; Luo et al., 2012). This results in lower reconstructed $\delta^{37}\text{Cl}$
556 values for larger fractionation factors. Importantly, no large variations are observed between the
557 different secular $\delta^{37}\text{Cl}$ values of the ocean, and the average secular values are about 0.01‰
558 assuming a fractionation factor of 1.00026, -0.08‰ assuming a fractionation factor of 1.00035 and -
559 0.22‰ assuming a fractionation factor of 1.00049. These data thus suggest an only slightly negative
560 $\delta^{37}\text{Cl}$ value for the seawater during the last billion years with little temporal variation. The low
561 inferred (average) $\delta^{37}\text{Cl}$ value for a fractionation factor of 1.00049 with respect to the modern
562 seawater composition again indicates that this fractionation factor is non-realistically high as it
563 would imply a drastic change in $\delta^{37}\text{Cl}$ of the ocean between the Miocene and the present, which is
564 not sensible. Note that the calculations are made using the lowermost first halite Br/Cl ratio. As
565 there is a negative relationship between the $\delta^{37}\text{Cl}$ and the Br/Cl ratio, the calculated $\delta^{37}\text{Cl}$ values for
566 the ocean become even lower if higher first halite precipitated Br/Cl ratios, such as those suggested
567 by Siemann (2003), are used in the calculations. This may indicate that the initial Br/Cl ratios of the
568 first precipitated halite have always been lower than those suggested by Siemann (2003).

569

570 *5.1.3 Comparison of the two approaches to establish the $\delta^{37}\text{Cl}$ of seawater from precipitated halite*
571 *and the most probable seawater $\delta^{37}\text{Cl}$ values over geological history*

572

573 The two approaches to estimate the $\delta^{37}\text{Cl}$ values of the ocean during the geological past yield
574 different results, but combined together they are able to constrain the approximate value of $\delta^{37}\text{Cl}$ of
575 the ocean during the geological past. The combined results of the two approaches are summarised in
576 Figure 5. The results obtained for the recent salt-pan samples are omitted as they do not reflect the

577 $\delta^{37}\text{Cl}$ composition of current seawater. The $\delta^{37}\text{Cl}$ value of the ocean during the Paleoproterozoic
578 could not be determined via the second approach (with Br/Cl ratio) due to their extremely low Br
579 contents, but the results of the first approach (range of possible $\delta^{37}\text{Cl}$ in seawater) are shown. The
580 first “Cl only” approach is shown as coloured bands in the background of the figure as it is not
581 possible to give an average value but only a range of overlapping possible $\delta^{37}\text{Cl}$ ranges for all
582 samples within a specific geologic period. This range gets larger if higher fractionation factors are
583 assumed. Estimated $\delta^{37}\text{Cl}$ values of the ocean from the second “Br/Cl ratio” approach are shown as
584 three lines with increasing fractionation factors with uncertainties shown as 2σ error bars. There is
585 considerable overlap between the two approaches. It is clear however that assuming a fractionation
586 factor of 1.00049 the $\delta^{37}\text{Cl}$ range determination with the second approach falls really at the lower
587 end of the first approach. This seems to indicate again that our data do not support a Cl isotopic
588 fractionation factor as large as 1.00049 between brine and precipitating halite.
589 The overlap between the two approaches is much better for fractionation factors of 1.00026 and
590 1.00035. However, as a fractionation factor of 1.00026 leads to the impossibility to determine the
591 ocean’s $\delta^{37}\text{Cl}$ for the Neogene it is not likely that the fractionation factor is so small and it is likely
592 close to the recently published value of 1.00035 (Eggenkamp et al., 2016).
593

594 Figure 5
595

596 The data suggest small variations in the $\delta^{37}\text{Cl}$ of the ocean during the geological past that are
597 smaller than the uncertainties in the data. Variations are largest in the reconstructions of the first
598 approach that might originate in the speculation that in these periods samples are more biased
599 towards early or late stage halite. The second approach corrects for this bias as it extrapolates to the
600 $\delta^{37}\text{Cl}$ values of the first precipitated halite.

601 In summary we conclude that $\delta^{37}\text{Cl}$ variations of the ocean during the geologic past were small, as
602 has been suggested by Eastoe et al. (2007). The first approach suggests $\delta^{37}\text{Cl}$ values between about
603 +0.2 and -0.4‰, and these are confirmed by the second approach. Overall $\delta^{37}\text{Cl}$ values of the ocean
604 can be estimated to have fallen into the range $-0.10 \pm 0.25\text{‰}$ for the past two billion years (see figure
605 5).
606

607 *5.1.4 Comparison with $\delta^{37}\text{Cl}$ estimates reconstructed by Eggenkamp et al. (2016)* 608

609 Eggenkamp et al. (2016) reconstructed the $\delta^{37}\text{Cl}$ history of the past billion years based on
610 theoretical constraints of the isotope fractionation between brine and salt of NaCl (halite) in
611 combination with deposition and subsidence of salt deposits as reconstructed by Hay et al. (2006).
612 Eggenkamp et al. (2016) concluded that the $\delta^{37}\text{Cl}$ of the ocean should have decreased by about
613 0.25‰ during the last billion years since during that time period more halite has been removed from
614 the ocean than has been returned to it via subsidence. Net removal of halite should result in a
615 decrease in the $\delta^{37}\text{Cl}$ of the ocean as the heavier chlorine isotope preferentially precipitates out of
616 the brine. The results of this study however suggest that this decrease in $\delta^{37}\text{Cl}$ is not empirically
617 supported, and it seems even more likely that the $\delta^{37}\text{Cl}$ of the ocean was slightly lower than today.
618 The prediction of Eggenkamp et al. (2016) was based on the assumption that precipitation of halite
619 and subsidence of salt deposits are the only processes that determine the $\delta^{37}\text{Cl}$ of the ocean over
620 geological periods of time, but several other processes could also impact it such as removal of
621 chlorine at subduction zones and addition of chlorine during volcanic activity. To evaluate the
622 isotopic mass balance of the chlorine cycle on the geologic time scale, it is necessary to carry a
623 comprehensive isotopic study of the chlorine cycle and ensure that the isotope composition and
624 isotope fractionation of the various chlorine fluxes is taken into account. Although the chlorine
625 cycle is fairly well understood (see e.g. Jarrard, 2003) addition of the isotope compositions and
626 fractionations to the fluxes will surely improve our understanding.

627

628 5.2 Estimate of the secular $\delta^{81}\text{Br}$ values of seawater

629

630 Unlike chlorine isotopes, behaviour of bromine isotopes during the precipitation of salt is not yet
631 well understood. Eggenkamp et al. (2016) suggested very little fractionation based on experimental
632 precipitation of pure bromide salts. However, this interpretation could not explain the highly
633 positive Br isotope values of formation waters that had likely acquired their Br from dissolving
634 evaporites (Eggenkamp, 2015b). Subsequently, it was found that Br isotope compositions of a fully
635 developed salt sequence (halite to bischofite) do have large and systematic Br isotope variations and
636 it was concluded that isotope fractionation of Br when it precipitates with halite must be much
637 larger than previously expected, and that its fractionation might be as large as 1.0013 (Eggenkamp
638 et al., 2019). This large fractionation factor makes it difficult to infer the original $\delta^{81}\text{Br}$ of the ocean
639 based on the Br isotope composition alone. With a Br isotope fractionation factor of 1.0013, the first
640 halite to precipitate from seawater would have a $\delta^{81}\text{Br}$ of 1.3‰, which would progressively
641 decrease to -1.0‰ when the last halite to precipitate. The original $\delta^{81}\text{Br}$ of seawater would then fall
642 between 1.3‰ lower to 1.0‰ higher than the measured $\delta^{81}\text{Br}$ of a halite sample, which is a
643 considerable range. Based on the $\delta^{81}\text{Br}$ values of samples measured in this study, the $\delta^{81}\text{Br}$ value of
644 the ocean might have ranged between approximately -0.6 and +1.0‰ during the last 2 billion years.
645 Such a large plausible range is unfortunately not very useful to constrain the secular seawater $\delta^{81}\text{Br}$
646 evolution.

647 The second (Br/Cl ratio) approach that we applied to constrain seawater Br isotope variations
648 during the past shows ambiguous results. Figure 6 shows that the relationship between the $\delta^{81}\text{Br}$ and
649 the Br/Cl ratios of the whole set of halite samples is much more diffuse than that between the $\delta^{37}\text{Cl}$
650 and the Br/Cl ratios (Figure 2).

651

652 Figure 6

653

654 However, it is clear from Figure 6 that some relationship between $\delta^{81}\text{Br}$ and Br/Cl ratio exists. The
655 lowest possible $\delta^{81}\text{Br}$ value is a function of the Br/Cl ratio. Figure 6 shows that the lower $\delta^{81}\text{Br}$ limit
656 decreases with increasing Br/Cl ratio, pointing a minimum $\delta^{81}\text{Br}$ value of +0.33‰ vs SMOB at a
657 Br/Cl ratio of 0.00005. This suggests a minimum possible isotope fractionation between Br^- in
658 solution and Br^- in solid NaCl of about 1.0003. Note that the two samples with the lowest Br/Cl
659 ratios in this Figure are from the Russian sample set and, as their Br content has been decreased
660 considerably after salt deposition they should not be taken into account when the lowest possible
661 $\delta^{81}\text{Br}$ is determined. Nonetheless, in three of the nine sample groups (Permian, Ordovician-Silurian
662 and Ediacaran-Cambrian) a reasonably high correlation coefficient is observed with a negative
663 Br/Cl vs. $\delta^{81}\text{Br}$ trend, and these three sample groups point to $\delta^{81}\text{Br}$ values of halite (at a Br/Cl ratio
664 of 0.00005, = -4.3 in log units) between 0.6 and 0.8‰ (Figure 7).

665

666 Figure 7

667

668 Figure 7 shows the reconstructed relationships with uncertainty hyperbolas for these three sample
669 groups with high correlation coefficients. These three subsets point to $\delta^{81}\text{Br}$ values in the first
670 precipitated salt between 0.6 and 0.8‰ and the line showing the lowermost $\delta^{81}\text{Br}$ value suggests a
671 value higher than 0.3‰. As a result, these data suggest a lower bromine isotope fractionation factor
672 than suggested by Eggenkamp et al. (2019). Figure 8 shows a visual interpretation of these data in a
673 manner similar to that utilised for Cl in Figure 5. It shows the possible range in $\delta^{81}\text{Br}$ values
674 following the first, isotope only approach, for fractionation factors of 1.003, 1.007 and 1.013,
675 combined with the data for three periods following the second approach that takes the Br/Cl ratio in
676 account, for the same isotope fractionation factors.

677

678

679

Figure 8

680 Considering the fractionation factor of 1.0013 as suggested by Eggenkamp et al. (2019) this
681 translates to an original $\delta^{81}\text{Br}$ value of seawater between -0.7 and -0.5‰. Although this range is
682 close to the lowest possible $\delta^{81}\text{Br}$ values of seawater following the total possible range as indicated
683 in Figure 8 they seem not realistic as values more within the central part of the total range would
684 have been expected. From Figure 8 it is also deductible that a fractionation factor of 1.003 is not
685 realistic. With such a low isotope fractionation factor it is mostly not possible to reconstruct the
686 $\delta^{81}\text{Br}$ values of seawater using the $\delta^{81}\text{Br}$ only approach for all but the oldest Russian samples. For
687 all younger geologic periods the minimum possible value is higher than the maximum possible
688 value. The reconstruction based on an isotope fractionation factor of 1.007 seems however feasible.
689 Following the $\delta^{81}\text{Br}$ only approach $\delta^{81}\text{Br}$ of the ocean then has always been in the range between
690 approximately 0 and +0.5‰ vs. SMOB. Adding the three possible computations of the combined
691 $\delta^{81}\text{Br}$ and Br/Cl ratio approach, which point to a $\delta^{81}\text{Br}$ value of seawater (at least during most of the
692 Palaeozoic) that was close to 0‰ (Figure 8), suggest that the $\delta^{81}\text{Br}$ of the ocean has been at its
693 present value. The combination of the two approaches thus suggest that the Br isotope fractionation
694 between bromide in brine and halite is about 1.007 and that the Br isotope composition of the
695 oceans has always been close to (or very slightly larger) its current value. Considering the small
696 number of data, combined with a considerable scatter in $\delta^{81}\text{Br}$ data of evaporites, these values
697 certainly need further refinement along with future research on the Br isotope fractionation during
698 seawater evaporation.

699 It is clear that, to better understand secular seawater variations in $\delta^{81}\text{Br}$ further research is needed on
700 this isotope system. This includes not only more measurements of Br isotope ratios in salt samples,
701 but also considerable experimental research to precisely determine the isotope fractionation factor
702 for Br precipitation with NaCl under various conditions such as different Br/Cl ratios, different
703 initial seawater compositions and during precipitation of salt from complex brines, as the
704 composition of these brines changes during salt precipitation. Finally theoretical (ab-initio)
705 calculations are also needed to understand the thermodynamics and other properties of the processes
706 studied, such as the competition between Br^- and other major and trace ions for incorporation into
707 halites.

708

709 6. CONCLUSIONS

710

711 We have measured the Cl and Br isotope values for a large set of halite samples in order to better
712 constrain Cl isotope compositions and variations in the oceans during the Earth's history than
713 Eastoe et al. (2007) were able to, as well as the first constraints on the secular seawater Br isotope
714 variations. Based on two different approaches, the Cl isotope variations were small to negligible,
715 with average values in the range -0.10 ± 0.25 ‰ vs. SMOC during the last 2 Ga. Although with a
716 larger degree of uncertainty, it was also possible to obtain an indication of the seawater Br isotope
717 variations during this period. The data obtained in this study suggest a Br isotope fractionation
718 between bromide in brine and bromide in halite of about 1.0007. Combined with the possible Br
719 isotope range of the ocean obtained through the $\delta^{81}\text{Br}$ only approach, the range of Br isotope
720 compositions in the ocean may have been between 0,00 and +0.25‰ vs. SMOB (Figure 8) for at
721 least the last billion years with very little variation.

722

723 Acknowledgements

724

725 This research is part of the project "BRISOACTIONS" that has received funding from the European
726 Union's Horizon 2020 research and innovation programme under the Marie Skłodowska-Curie

727 grant agreement No 702001. We are grateful to Gilian Schout (Utrecht University), Alex Klomp and
728 Jan-Willem Weegink (both TNO Geological Survey) for their help in sample selection from the
729 Triassic and Upper Permian. We thank Pierre Burckel (IPGP) for Cl and Br analyses by ICP-MS
730 and Laure Cordier (IPGP) for the analyses by ICP-OES. Parts of this work were supported by the
731 IPGP multidisciplinary program PARI, by Paris–IdF region SESAME Grant no. 12015908, NSERC
732 Discovery and Accelerator Grant to AB, and by Australian Research Council Grant DP160100607
733 to JJB. This is IPGP contribution No. 3962.

734

735 **References**

736

737 Alavi M. (2004) Regional stratigraphy of the Zagros fold-thrust belt of Iran and its proforeland
738 evolution. *Am. J. Sc.* **304**, 1–20.

739 Alijani N. (2000) Petrography and geochemistry of evaporate deposits in Garmsar region. MSc
740 thesis, Tehran University.

741 Babel M. and Schreiber B.C. (2014) Geochemistry of evaporites and evolution of seawater. *Treat.*
742 *Geochem.* 2nd ed. 483-560.

743 Bagheri R., Nadri A., Raeisi E., Eggenkamp H.G.M., Kazemi G.A. and Montaseri A. (2014)
744 Hydrochemistry and isotope ($\delta^{18}\text{O}$, $\delta^2\text{H}$, $^{87}\text{Sr}/^{86}\text{Sr}$, $\delta^{37}\text{Cl}$ and $\delta^{81}\text{Br}$) applications: clues to the
745 origin of saline produced water in a gas reservoir. *Chem. Geol.* **384**, 62–75.

746 Blättler C.L., Claire M.W., Prave A.R., Kirsimäe K., Higgins J.A., Medvedev P.V., Romashkin A.E.,
747 Rychanchik D.V., Zerkle A.L., Paiste K., Kreitsmann T., Millar I.L., Hayles J.A., Bao H.,
748 Turchyn A.V., Warke M.R. and Lepland A. (2018) Two-billion-year-old evaporites capture
749 Earth's great oxidation. *Science* **360**, 320-323.

750 Bloch M.R. and Schnerb J. (1953) On the Cl⁻/Br⁻-ratio and the distribution of Br-ions in liquids and
751 solids during evaporation of bromide containing chloride solutions. *Bull. Res. Council Israel* **3**,
752 151-158.

753 Boeke H.E. (1908) Über das Krystallisationsschema der Chloride, Bromide, Jodide von Natrium,
754 Kalium und Magnesium, sowie über das Vorkommen des Broms und das Fehlen von Jod in den
755 Kalisalzlagerstätten. *Z. Kristallogr.* **45**, 346–391.

756 Boschetti T., Toscani L., Shouakar-Stash O., Iacumin P., Venturelli G., Mucchino C. and Frapé S.K.
757 (2011) Salt waters of the Northern Apennine Foredeep Basin (Italy): origin and evolution. *Aquat.*
758 *Geochem.* **17**, 71–108.

759 Braitsch O. (1962) Entstehung und Stoffbestand der Salzlagerstätten. Springer.

760 Buyze D. and Lorenzen H. (1986) Solution mining of multi-component magnesium-bearing salts: a
761 realization in the Netherlands. *CIM Bull.* **79**, 52-60.

762 Coeleweij P. A. J., Haug G. M. W., and van Kuijk H. (1978) Magnesium-salt exploration in the
763 Northeastern Netherlands. *Geol. Mijnb.* **57**, 487-502.

764 Eastoe, C.J. (2016) Stable chlorine isotopes in arid non-marine basins: Instances and possible
765 fractionation mechanisms. *Appl. Geochem.* **74**, 1-12.

766 Eastoe, C.J. and Peryt T. (1999) Stable chlorine isotope evidence for non-marine chloride in
767 Bedenian evaporites, Carpatian mountain region. *Terra Nova* **11**, 118-123.

768 Eastoe, C.J., Long, A. and Knauth, L.P. (1999) Stable chlorine isotopes in the Palo Duro Basin,
769 Texas: evidence for preservation of Permian evaporite brines. *Geochim. Cosmochim. Acta* **63**,
770 1375–1382.

771 Eastoe, C.J., Long, A., Land, L.S., and Kyle, R. (2001) Stable chlorine isotopes in halite and brine
772 from the Gulf Coast Basin: brine genesis and evolution. *Chem. Geol.* **176**, 343-360.

773 Eastoe, C.J., Peryt, T.M., Petrychenko, O.Y., and Geisler-Cussey, D. (2007) Stable chlorine isotopes
774 in Phanerozoic evaporites. *Appl. Geochem.* **22**, 575-588.

775 Eggenkamp H.G.M. (1994) $\delta^{37}\text{Cl}$: The geochemistry of chlorine isotopes. PhD Thesis, Utrecht.

- 776 Eggenkamp H.G.M. (1995) Bromine stable isotope fractionation: Experimental determination on
777 evaporites. EUG, 8th Congress. *Terra Abs., Abs. Suppl. to Terra Nova* **7**, p. 331 (Available from
778 http://www.eggenkamp.info/personal/Eggenkamp_Poster_EUG_1995.pdf).
- 779 Eggenkamp H.G.M. (2014) The geochemistry of stable chlorine and bromine isotopes. Springer.
- 780 Eggenkamp H.G.M. (2015a) Comment on “Stable isotope fractionation of chlorine during the
781 precipitation of single chloride minerals“ by Luo, C.-g., Xiao, Y.-k., Wen, H.-j., Ma, H.-z., Ma,
782 Y.-q., Zhang, Y.-l., Zhang, Y.-x. And He, M.-y. [Applied Geochemistry 47 (2014) 141-149]. *Appl.*
783 *Geochem.* **54**, 111–116.
- 784 Eggenkamp H.G.M. (2015b) Why are variations in bromine isotope compositions in the Earth's
785 history larger than chlorine isotope compositions? *Annales UMCS, Sectio AAA* **70**, 183–194.
- 786 Eggenkamp H.G.M. and Coleman M.L. (2000) Rediscovery of classical methods and their
787 application to the measurement of stable bromine isotopes in natural samples. *Chem. Geol.* **167**,
788 393–402.
- 789 Eggenkamp H.G.M. and Louvat P. (2018) A simple distillation method to extract bromine from
790 natural water and salt samples for isotope analysis by multi collector inductively coupled plasma
791 mass spectrometry. *Rapid Comm. Mass Spectr.* **32**, 612-618.
- 792 Eggenkamp H.G.M., Kreulen R. and Koster van Groos A.F. (1995) Chlorine stable isotope
793 fractionation in evaporites. *Geochim. Cosmochim. Acta* **59**, 5169-5175.
- 794 Eggenkamp, H.G.M., Bonifacie, M., Ader, M. and Agrinier, P. (2016) Experimental determination
795 of stable chlorine and bromine isotope fractionation during precipitation of salt from a saturated
796 solution. *Chem. Geol.* **433**, 46-56.
- 797 Eggenkamp H.G.M., Louvat P., Griffioen J., Agrinier P. (2019) Chlorine and bromine isotope
798 evolution within a fully developed Upper Permian natural salt sequence. *Geochim. Cosmochim.*
799 *Acta* **245**, 316-326.
- 800 Glushanin L.V., Sharov N.V. and Shchiptsov V.V. (2011) The Onega Palaeoproterozoic Structure
801 (Geology, Tectonics, Deep Structure and Minerogeny) (in Russian). Institute of Geology,
802 Karelian Research Centre of the Russian Academy of Sciences.
- 803 Godon A., Jendrzewski N., Eggenkamp H.G.M., Banks D.A., Ade, M., Coleman M.L. and Pineau,
804 F. (2004) A cross calibration of chlorine isotopic measurements and suitability of seawater as the
805 international reference material. *Chem. Geol.* **207**, 1–12.
- 806 Gorbachev V.I., Petrov O.V., Tarkhanov G.V., Erinchek Y.M., Akhmedov A.M., Krupenik V.A.,
807 Narkisova V.V. and Sveshnikova, K.Y. (2011) Rock salts in the Paleoproterozoic of the Onega
808 Trough of the Baltic Shield. *Regional Geology and Metallogeny* **45**, 90-97 (in Russian).
- 809 Grobe M. (2000) Distribution and thickness of salt within the Devonian Elk Point group, western
810 Canada sedimentary basin. *Alberta Geol. Surv. Earth Sc. Rep.* **2000-02**.
- 811 Haines P.W. (2009) The Carribuddy Group and Worrall Formation, Canning basin, Western
812 Australia: stratigraphy, sedimentology, and petroleum potential. *Geol. Surv. West. Australia Rep.*
813 **105**, 60p.
- 814 Hay W.H., Migdisov A., Bulukhovskiy A.N., Wold C.N., Flögel S. and Söding E. (2006) Evaporites
815 and the salinity of the ocean during the Phanerozoic: implications for climate, ocean circulation
816 and life. *Palaeogeogr. Palaeoclimatol. Palaeoecol.* **240**, 3–46.
- 817 Herrmann A.G. (1972) Bromine distribution coefficients for halite precipitated from modern sea
818 water under natural conditions. *Contr. Mineral. Petrol.* **37**, 249-252.
- 819 Herrmann A.G., Knake D., Schneider J. and Peters H. (1973) Geochemistry of modern seawater and
820 brines from salt pans: main components and bromine distribution. *Contrib. Mineral. Petrol.* **40**,
821 1–24.
- 822 Holser W.T. (1966) Bromide geochemistry of salt rocks. In: Rau JL (ed.) Proceedings of the Second
823 Symposium on Salt, 248–275. Cleveland, OH: Northern Ohio Geological Society.

- 824 Horita J., Zimmermann H. and Holland H.D. (2002) The chemical evolution of seawater during the
825 Phanerozoic: Implications from the record of marine evaporites. *Geochim. Cosmochim. Acta* **66**,
826 3733–3756.
- 827 Jarrard R.D. (2003) Subduction fluxes of water, carbon dioxide, chlorine, and potassium. *Geochem.*
828 *Geophys. Geosystems* **4**. doi:10.1029/2002GC000392.
- 829 Kaufmann R.S. (1984) Chlorine in ground water: Stable isotope distribution. PhD thesis, Tucson.
- 830 Kaufmann R.S., Long A., Bentley H. and Davis S. (1984) Natural chlorine isotope variations.
831 *Nature* **309**, 338-340.
- 832 Kent P.E. (1979) The emergent Hormuz salt plugs of southern Iran. *J. Petrol. Geol.* **2**, 117–144.
- 833 Krupenik V.A. and Sveshnikova K.Y. (2011) “Correlation of the Onega Parametric Hole with the
834 reference sections of the Onega Structure,” in *The Onega Palaeoproterozoic Structure (Geology,*
835 *Tectonics, Deep Structure and Minerogeny)* (in Russian), L. V. Glushanin, N. V. Sharov, V. V.
836 Shchiptsov, Eds. (Institute of Geology, Karelian Research Centre of the Russian Academy of
837 Sciences, 2011), 190–195.
- 838 Kühn R. (1955) Über den Bromgehalt von Salzgesteinen, insbesondere die quantitative Ableitung
839 des Bromgehaltes nichtprimärer Hartsalze oder Sylvinit aus Carnallit. *Kali u. Steinsalz* **1(9)**, 3-
840 16
- 841 Liu, W.G., Xiao, Y.K., Wang, Q.Z., Qi, H.P., Wang, Y.H., Zhou, Y.M. and Shirodkar, P.V. (1997)
842 Chlorine isotopic geochemistry of salt lakes in the Qaidam Basin, China. *Chem. Geol.* **136**, 271–
843 279.
- 844 Louvat P., Bonifacie M., Giunta T., Michel A. and Coleman M. (2016) Determination of bromine
845 stable isotope ratios from saline solutions by "wet plasma" MC-ICPMS including a comparison
846 between high- and high-resolution modes, and three introduction systems. *Anal. Chem.* **88**, 3891-
847 3898.
- 848 Lowenstein T.K., Kendall B. and Anbar A.D. (2014) The geologic history of seawater. *Treat.*
849 *Geochem.* 2nd ed. 569-621.
- 850 Luo C.G., Xiao Y.K., Ma H.Z., Ma Y.Q., Zhang Y.L. and He M.Y. (2012) Stable isotope
851 fractionation of chlorine during evaporation of brine from a saline lake. *Chin. Sci. Bull.* **57**,
852 1833–1843.
- 853 Luo C.G., Xiao Y.K., Wen H.J., Ma H.H., Ma Y.Q., Zhang Y.L., Zhang Y.X. and He M.Y. (2014)
854 Stable isotope fractionation of chloride during the precipitation of single chloride minerals. *Appl.*
855 *Geochem.* **47**, 141–149.
- 856 Luo C.G., Xiao Y.K., Wen H.J., Ma H.H., Ma Y.Q., Zhang Y.L. and He M.Y. (2015) Reply to the
857 comment on the paper “Stable isotope fractionation of chlorine during the precipitation of single
858 chloride minerals”. *Appl. Geochem.* **54**, 117–118.
- 859 Maley V.C. and Huffington R.M. (1953) Cenozoic fill and evaporate [evaporite] solution in the
860 Delaware basin, Tex. And N. Mex. *Geol. Soc. Am. Bull.* **64**, 539-545.
- 861 Mattes B.W. and Conway Morris S. (1990) Carbonate/evaporite deposition in the Late Precambrian
862 - Early Cambrian Ara Formation of Southern Oman. *Geol Soc London Sp. Publ.* **49**, 617-636.
- 863 McCaffrey M.A., Lazar, B. and Holland H.D. (1987) The evaporation path of seawater and the
864 coprecipitation of Br⁻ and K⁺ with halite. *J. Sed. Petrol.* **57**, 928-937.
- 865 Morozov A.F., Khakhaev B.N., Petrov O.V., Gorbachev V.I., Tarkhanov G.V., Tsvetkov L.D.,
866 Erinchek Yu.M., Akhmedov A.M., Krupenik V.A. and Sveshnikova K.Yu. (2010) Rock Salt Mass
867 in the Paleoproterozoic Sequence of the Onega Trough in Karelia (from the Onega Parametric
868 Well Data). *Dokl. Earth Sc.* **432**, 1483-1486.
- 869 Murphy T.J., Clabaugh W.S. and Gilchrist R. (1954) Separation of iodide, bromide and chloride
870 from one another and their subsequent determination. *J. Res. Nat. Bur. Stand.* **53**, 13-18.
- 871 Naughton D.A., Quinlan T., Hopkins R.M. and Wells A.T. (1968) Evolution of salt anticlines and
872 salt domes in the Amadeus Basin, Central Australia. *Geol. Soc. Am., Spec. Pap.* **88**, 229-247.

- 873 Paris G., Gaillardet J., and Louvat P. (2010) Geological evolution of seawater boron isotope
874 composition recorded in evaporites. *Geology* **38**, 1035-1038.
- 875 Petrychenko O.Y., Peryt T.M. and Chechel E.I. (2005) Early Cambrian seawater chemistry from
876 fluid inclusions in halite from Siberian evaporites. *Chem. Geol.* **219**, 149–161.
- 877 Pierce W.G. and Rich E.I. (1962) Summary of rock salt deposits in the United States as possible
878 Storage sites for radioactive waste materials. *USGS Bulletin* **1148**, 91pp.
- 879 Schröder S, Grotzinger JP, Amthor JE and Matter A (2005) Carbonate deposition and hydrocarbon
880 reservoir development at the Precambrian- Cambrian boundary: the Ara Group in South Oman.
881 *Sedim. Geol.* **180**, 1–28.
- 882 Sharp Z. D., Barnes J. D., Brearley A. J., Fischer T. P., Chaussidon M. and Kamenetsky V. S. (2007)
883 Chlorine isotope homogeneity of the mantle, crust and carbonaceous chondrites. *Nature* **446**,
884 1062–1065.
- 885 Sharp Z.D., Mercer J.A., Jones R.H., Brearley A.J., Selverstone J., Bekker A. and Stachel T. (2013)
886 The chlorine isotope composition of chondrites and Earth. *Geochim. Cosmochim. Acta* **107**, 189-
887 204.
- 888 Shouakar-Stash O., Alexeev S.V., Frapce S.K., Alexeeva L.P., and Drimmie R. J. (2007)
889 Geochemistry and stable isotope signatures, including chlorine and bromine isotopes, of the deep
890 groundwaters of the Siberian Platform. *Appl. Geochem.* **22**, 589–605.
- 891 Siemann M.G. (2003) Extensive and rapid changes in seawater chemistry during the Phanerozoic:
892 evidence from Br contents in basal halite. *Terra Nova* **15**, 243-248.
- 893 Siemann M.G. and Schramm M. (2000) Thermodynamic modelling of the Br partition between
894 aqueous solutions and halite. *Geochim. Cosmochim. Acta* **64**, 1681-1693.
- 895 Stein M., Starinsky A., Agnon A., Katz A., Raab M., Spiro B. and Zak I. (2000) The impact of
896 brine-rock interaction during marine evaporite formation on the isotopic Sr record in the oceans:
897 Evidence from Mt. Sedom, Israel. *Geochim. Cosmochim. Acta* **64**, 2039-2053.
- 898 Stewart A.J. (1979) A barred-basin marine evaporite in Upper Proterozoic of the Amadeus Basin,
899 Central Australia. *Sedimentology* **26**, 33-62.
- 900 Tan, H.B., Ma, H.Z., Xiao, Y.K., Wei, H.Z., Zhang, X.Y. and Ma, W.D. (2005) Characteristics of
901 chlorine isotope distribution and analysis on sylvinitic deposit formation based on ancient salt
902 rock in western Tarim basin. *Sci. China, Ser. D Earth Sci.* **48**, 1913–1920.
- 903 Tan H.B., Ma H.Z., Wei H.Z., Xu J.X. and Li T.W. (2006) Chlorine, sulfur and oxygen isotopic
904 constraints on ancient evaporite deposit in the Western Tarim Basin, China. *Geochem. J.* **40**,
905 569–577.
- 906 Tan H.B., Ma H.Z., Zhang X.Y., Xu J.X. and Xiao Y.K. (2009) Fractionation of chlorine isotope in
907 salt mineral sequences and application: research on sedimentary stage of ancient salt rock deposit
908 in Tarim Basin and western Qaidam Basin. *Acta Petrol. Sin.* **25**, 955–962 (in Chinese with
909 English abstract).
- 910 Valyashko M.G. (1956) Geochemistry of bromine in the processes of salt deposition and the use of
911 the bromine content as a genetic and prospecting criterion. *Geochemistry (Geokhimiya)* **1956**,
912 570-589.
- 913 Weinberger R., Agnon A., and Ron H. (1997) Paleomagnetic reconstruction of the structure of Mt.
914 Sedom, Dead Sea rift. *J. Geophys. Res.* **102(B3)**, 5173–5192.
- 915 Xiao, Y.K., Liu, W.G. and Zhang, C.G. (1994) The preliminary investigation on chlorine isotopic
916 fractionation during the crystallization of saline minerals in salt lake. *Salt Lake Sci.* **2**, 35–40 (in
917 Chinese with English abstract).
- 918 Xiao, Y.K., Liu, W.G. and Zhou, Y.M. (1997) Isotopic compositions of chlorine in brine and saline
919 minerals. *Chin. Sci. Bull.* **42**, 406–409.
- 920 Xiao, Y.K., Liu, W.G., Zhou, Y.M., Wang, Y.H. and Shirodkar, P.V. (2000) Variations in isotopic
921 compositions of chlorine in evaporation controlled salt lake brines of Qaidam Basin, China.
922 *Chin. J. Oceanol. Limnol.* **18**, 169–177.

923 Zak I. (1997) Evolution of the Dead Sea brines. In *The Dead Sea, the lake and its settings* (ed. T. M.
924 Niemi, Z. Ben Avraham and J. R. Gat), **36**, 133–144. Oxford Monogr. on Geology and
925 Geophysics.
926

1 **The bromine and chlorine isotope compositions of primary halite deposits and**
2 **their significances for the secular isotope compositions of seawater**

3
4 HGM Eggenkamp^{a,b,*}, P Louvat^a, P. Agrinier^a, M Bonifacie^a, A Bekker^c, V Krupenik^d, J Griffioen^{e,f},
5 J Horita^g, JJ Brocks^h, R Bagheriⁱ

6
7 a Institut de Physique du Globe de Paris, Sorbonne Paris Cité, UMR 7154, CNRS, 1 rue Jussieu,
8 75238 Paris Cedex 05, France

9 b Eberhard Karls Universität [Tübingen](#), FB Geowissenschaften, [AG Petrologie](#), Wilhelmstraße 56,
10 72074 Tübingen, Germany

11 c Department of Earth Sciences, University of California, Riverside, CA 92521, USA

12 d Sector of Precambrian Geology, A.P. Karpinsky Russian Geological Research Institute, 74
13 Sredny Prospect, 199106, St. Petersburg, Russia

14 e TNO Geological Survey of the Netherlands, P.O. Box 80015, Utrecht, the Netherlands

15 f Copernicus Institute of Sustainable Development, Utrecht University, P.O. Box 80115, Utrecht,
16 the Netherlands

17 g Department of Geosciences, Texas Tech University, Texas, 79409-1053, USA

18 h Research School of Earth Sciences, The Australian National University, Canberra, ACT 2601,
19 Australia

20 i Faculty of Earth Sciences, Shahrood University of Technology, Shahrood, Iran

21
22 *Corresponding author, email hans@eggenkamp.info

23
24 Keywords: Bromine isotopes, chlorine isotopes, isotope fractionation, halite, secular variation, salt
25 deposits
26

27 **Abstract**

28
29 We determined the chlorine and bromine isotope compositions of 83 halite samples from nine
30 different geological periods between the Orosirian and the Pliocene in order to study the secular Cl
31 and Br isotope variations in the ocean during the last 2 billion years. Relatively large Cl (-0.24 to
32 +0.51‰ vs. SMOC) and Br (-0.24 to +1.08‰ vs. SMOB) isotope variations are found in these
33 halite samples. Two different methods, one in which the isotope fractionation between the brine and
34 the salt is used, and a second in which the relationship between the isotope compositions and the
35 Br/Cl ratios in the halite samples is used were applied to establish the original Cl and Br isotope
36 compositions of the ocean. Both approaches showed that the Cl and Br isotope compositions of the
37 ocean have always been close to the modern value (which is by definition 0‰ for both isotope
38 systems) and that at most very small variations in Br and Cl isotope composition of seawater have
39 occurred during the last 2 billion years. This indicates that, unlike in other isotope systems that
40 often show significant isotope variations over geologic time, Cl and Br isotope compositions can be
41 used directly to determine processes that occurred in the deposits of interest without need for
42 correction for secular variations.

43
44 **1. INTRODUCTION**

45
46 Of the geochemically significant halogen elements (fluorine, chlorine, bromine and iodine) only
47 chlorine (Cl) and bromine (Br) have two stable isotopes. It is only of these two that the stable
48 isotope geochemistry can be studied. Chlorine consists of the isotopes, ³⁵Cl and ³⁷Cl which exist in a
49 ratio of approximately 3:1. Bromine consists of the isotopes ⁷⁹Br and ⁸¹Br which exists at about
50 equal abundances. For both elements the internationally accepted standard is the isotope ratio of
51 seawater (Standard Mean Ocean Chloride, SMOC (Kaufmann, 1984) for chlorine and Standard
52 Mean Ocean Bromide (Eggenkamp and Coleman, 2000) for bromine. Their isotope variations are
53 reported as δ³⁷Cl and δ⁸¹Br values that indicate the per mil (‰) difference of the ratio of the isotope
54 of interest, relative to that ratio in the international standard. δ³⁷Cl is defined as:

Formatted: Superscript

Formatted: Superscript

Formatted: Superscript

Formatted: Superscript

Formatted: Superscript

Formatted: Superscript

55
56
$$\delta^{37}\text{Cl} = \left(\frac{^{37}\text{Cl}/^{35}\text{Cl}}{(^{37}\text{Cl}/^{35}\text{Cl})_{\text{standard}}} - 1 \right)$$

Formatted: Superscript

Formatted: Superscript

57
58 where (³⁷Cl/³⁵Cl)_{sample} is the Cl isotope ratio in the sample and (³⁷Cl/³⁵Cl)_{standard} in the standard.
59 δ⁸¹Br is defined as:

Formatted: Subscript

Formatted: Superscript

60
61
$$\delta^{81}\text{Br} = \left(\frac{^{81}\text{Br}/^{79}\text{Br}}{(^{81}\text{Br}/^{79}\text{Br})_{\text{standard}}} - 1 \right)$$

Formatted: Superscript

Formatted: Subscript

62
63 where (⁸¹Br/⁷⁹Br)_{sample} is the Br isotope ratio in the sample and (⁸¹Br/⁷⁹Br)_{standard} in the standard.

64 The chlorine isotope geochemistry of evaporite deposits has been studied extensively. The chlorine
65 isotope fractionation has been studied experimentally in individual evaporite minerals and brines
66 (Eggenkamp et al., 1995, 2016, Luo et al., 2012, 2014) and isotope variations have been studied in
67 detail both in marine evaporites (Eastoe and Peryt, 1999, Eastoe et al., 1999; 2001, 2007,
68 Eggenkamp et al., 2019) and terrestrial evaporites (Xiao et al., 1994; 1997; 2000; Liu et al., 1997,
69 Tan et al., 2005; 2006; 2009; Luo et al., 2012; Eastoe, 2016) ~~in detail~~. As a result, the chlorine
70 isotope behaviour of an evaporating seawater body is now quite well understood. During
71 evaporation of modern seawater, the chlorine isotope ratio of the precipitated halite decreases from
72 slightly positive values in the first precipitated halite to fairly negative values when other salts ~~after~~
73 ~~halite~~ start to precipitate after halite. This effect is due to a Rayleigh-type fractionation because the
74 precipitated halite has a higher chlorine isotope ratio than the brine. As the heavier chlorine isotope
75 is removed preferentially from the brine the remaining brine becomes lighter, and halite that
76 precipitates later have thus lighter isotope compositions. This effect has recently been confirmed to

77 exist in natural salt sequences by Eggenkamp et al. (2019) in a study on Cl and Br isotope variations
78 in a fully developed Zechstein (Upper Permian) salt sequence from the Netherlands. The Cl isotope
79 data observed in both natural salt deposits (Eggenkamp et al., 1995; 2019) and experimental
80 evaporation of seawater (Eastoe et al., 1999) indicate that salt precipitates from brine in an open
81 system. If salt were to precipitate in a closed system this would indicate that its isotope ratio could
82 not be lower than the original isotope ratio of the brine, and these studies already showed that lower
83 ratios are possible in significantly evolved salt deposits.

84 The chlorine isotope composition of an extensive set of Late Proterozoic to Miocene salts has been
85 previously measured by Eastoe et al. (2007) who concluded that the chlorine isotope composition of
86 the ocean could not have varied significantly from its modern composition. They observed that all
87 $\delta^{37}\text{Cl}$ values of marine evaporites were in the range of $0.0\pm 0.9\%$ relative to SMOC (Standard Mean
88 Ocean Chloride, equivalent to the Cl isotope composition of the modern ocean) with most of the
89 data in the range of $0.0\pm 0.5\%$, but with larger ranges observed in smaller basins. On average, lower
90 Cl isotope values were found in potash-rich basins. These data suggest that no detectable change in
91 Cl isotope ratio of seawater has taken place during the Phanerozoic. Cl isotope values measured in
92 Precambrian cherts, barite, dolomite and halite confirmed that values must have been relatively
93 constant during the Precambrian too, although the data suggest a possibly wider range than for the
94 Phanerozoic (Sharp et al., 2007, 2013).

95 The isotope fractionation of chlorine during precipitation of chloride salts from saturated solutions
96 has been studied extensively (Eggenkamp et al., 1995, 2016; Luo et al., 2012, 2014). Based on the
97 isotope fractionation factors for halite (NaCl), it is possible to estimate, within an approximate
98 range of 0.5% , what was the original Cl isotope composition of seawater if the Cl isotope
99 composition of halite salts of a marine evaporite deposit is measured. This approach makes it
100 possible to impose a better constraint on and explore some limited variations in the original Cl
101 isotope composition of the ocean during the Phanerozoic and to resolve whether limited Cl isotope
102 variations in the seawater compositions occurred.

103 In their recent paper Eggenkamp et al. (2019) showed that the chlorine isotope composition within a
104 single salt sequence correlates very well with its Br/Cl ratio. As a consequence, the combination of
105 the Cl isotope ratio with the Br/Cl ratio for a sample makes it possible to estimate the original Cl
106 isotope composition of the brine from which a salt precipitated as the Br/Cl ratio of the first
107 precipitating halite is known for the Phanerozoic (Siemann, 2003). Consequently, combining Cl
108 isotope values and Br/Cl ratios, it might be possible to determine the original Cl isotope ratio of a
109 brine more precisely than with other techniques.

110 Compared to Cl, our knowledge of the Br isotope composition of evaporites and ancient seawater is
111 very limited. This knowledge was only based on a small number of Br isotope determinations of
112 formation waters with very low Br/Cl ratios (Eggenkamp, 2014), which, as a consequence, should
113 have most of their Cl and Br content from the dissolution of Br-poor (and halite-rich) evaporite
114 deposits. Only eight such samples were recognised and published prior to 2016 (Shouakar-Stash et
115 al., 2007; Boschetti et al., 2011; Bagheri et al., 2014) and they suggest an average $\delta^{81}\text{Br}$ value of
116 $+0.60\pm 0.29\%$ for evaporites. This value is at first sight not consistent with Br precipitation from
117 modern seawater with a value of 0% vs. SMOB, as an almost negligible Br isotope fractionation
118 was expected (Eggenkamp, 1995, Eggenkamp et al., 2016), indicating either a significantly more
119 positive Br isotope ratio in ancient seawater or a significant isotope fractionation accompanying
120 incorporation of bromide into chloride minerals during precipitation of salt from brine. The Br
121 isotopes in a salt sequence from the Dutch Zechstein deposit seems even more complex
122 (Eggenkamp et al., 2019). From slightly positive $\delta^{81}\text{Br}$ values ($+0.2\%$) in the samples with the
123 lowest Br/Cl ratios, $\delta^{81}\text{Br}$ values decreased sharply (to -0.5%) in samples with slightly higher Br/Cl
124 values, and increases again (to $0.1 \pm 0.3\%$) in samples with very high Br/Cl ratios (carnallite- and
125 bischofite-dominated samples). This effect was explained as a competition effect between Br^- and
126 Cl^- ions in solution for incorporation into a chloride salt. Due to its slightly larger size, Br^- ions are

127 more difficult to be incorporated into the salt and will thus concentrate in the brine. This effect has
128 been explained to produce a considerably larger isotope fractionation factor than the equilibrium
129 between Br^- in solution and Br^- in a pure bromide salt (Eggenkamp et al., 2016, 2019). This effect
130 must be related to the fact that there is only 1 Br^- ion for 600 Cl^- ions in seawater as compared to Br^-
131 ions only in pure bromide brine.

132 For the present study, we collected a total of 83 presumably primary (unaltered) salt samples
133 dominated by halite so that it could be expected that they were precipitated during early stages in
134 salt precipitation. The geologic ages of the samples range from the Paleoproterozoic to recent salt
135 pans, covering approximately 2 billion years. For all samples, chemical compositions and Cl and if
136 possible Br isotopic compositions were determined in order: 1/ to assess if it were possible to
137 constrain the Cl isotope variations to a narrower band than had been done before by Eastoe et al.
138 (2007); 2/ to assess if the Br isotope composition of the ocean was as stable as the Cl isotope
139 composition; and 3/ to refine the understanding on the Br isotope variations observed in halite-
140 dominated salt samples.

141

142 **2. MATERIAL**

143

144 We collected 73 salt samples from various evaporite deposits from Pliocene to Orosirian ages, as
145 well as 10 recent salt pan samples for comparison with the ancient samples. The ancient samples are
146 from 16 different geological stages and were sampled from different locations in North America,
147 Europe, Asia, and Australia. Some samples were individual samples, while others were related
148 samples taken from a single drill-core or from within a restricted area. A brief description of the
149 samples used in this study follows, sorted by age from the most recent to the most ancient. The
150 analytical results are presented in Table 1. In the discussion, the samples from each geological
151 period are combined in order to have a large enough set of samples per time period to properly
152 estimate Cl and Br isotope trends. The samples often originate from several subperiods as discussed
153 below.

154

155 **2.1 Recent samples**

156

157 10 samples of modern sea salts were mostly bought from supermarkets in France and the
158 Netherlands. The salts are from different locations, most of them in Europe with a focus on France.
159 Of these MO1 is JOZO salt (AKZONobel) of unknown origin, MO2 is from the Mediterranean
160 coast of France (La Baleine), MO3 is Maldon salt from the United Kingdom, MO4 is from the
161 South Coast of Portugal (Atlantis salt), MO5 and EVA27 are Fleur de Sel from Guérande, MO6 is
162 from Le Saunier, and MO7 is from Noirmoutier. The last three are from France, MO6 from the
163 Mediterranean coast (Camargue), while MO5 and MO7 are from the Atlantic coast. EVA 6 and
164 EVA10 are from Sicily (Mediterranean Sea). All samples except MO3 are produced from salt pans,
165 where seawater is introduced into individual pans and left to evaporate by the sun. Evaporation is
166 enhanced by regularly turning the salt. MO3 is produced by seething, a process by which seawater
167 is filtered and boiled in salt pans until it crystallises (see [http://www.maldonsalt.co.uk/The-Story-
168 How-Maldon-Salt-is-made.html](http://www.maldonsalt.co.uk/The-Story-How-Maldon-Salt-is-made.html)).

169

170 **2.2 Neogene**

171

172 *2.2.1 Plio-Pleistocene (about 2.6 Ma)*

173

174 One sample (H1) was taken from the Sedom salt deposit in Israel (Zak, 1967; Weinberger et al.,
175 1997; Stein et al., 2000).

176

177 2.2.2 *Messinian (about 6.3 Ma)*

178
179 Nine samples from Messinian salt deposits were analysed. EVA2, EVA9, EVA12, and EVA24 are
180 from Sicily in Italy: EVA 2 (Pe38 3D) and EVA12 (Pe38 6D) from borehole Porto Empedocle 38,
181 (Caltanissetta basin), EVA9 (Mess1) from Realmonte Mine and EVA24 (Cat5) from Cattolica
182 Eraclea borehole. EVA15 (L4 212) and EVA23 (L4 228) are from Lorca in Spain (Paris et al.,
183 2010). IR1, IR2 and IR3 are from the Garmsar Salt Dome in North Iran (Alijani, 2000), deposited in
184 a lagoon during the Ghom sea regression. Upon analysis, sample IR1 happened to be a KCl salt and
185 was not used as a primary source in the following study to determine the original Cl isotope
186 composition of the Messinian Ocean.

187
188 2.2.3 *Serravalian (about 12.7 Ma)*

189
190 Two samples (EVA5 and EVA7) from Serravalian salt deposits in Poland, taken from the section
191 Woszycze IG-1, were analysed (Paris et al., 2010).

192
193 **2.3 Paleogene**

194
195 2.3.1 *Eocene-Oligocene transition (about 33.9 Ma)*

196
197 The three samples EVA8 (EZ8 1229), EVA14 (EZ8 1230.7) and EVA18 (EZ8 1400) were from the
198 Eocene-Oligocene salt deposits from Bresse in Eastern France (Paris et al., 2010).

199
200 2.3.2 *Priabonian (about 35.9 Ma)*

201
202 The three samples EVA16 (BI 436/1), EVA20 (BI 436/2) and EVA21 (BI 427) were from
203 Priabonian salt deposits from the Lower Evaporite Unit of the Biurrun borehole in Navarra, Spain
204 (Paris et al., 2010).

205
206 **2.4 Triassic**

207
208 2.4.1 *Carmian/Norian (about 227 Ma)*

209
210 One French Keuper sample from the Paris Basin was analysed (H2).

211
212 2.4.2 *Anisian (about 245 Ma)*

213
214 Seven samples (NL02 to NL08) were taken from the drill-core TWR-515 from depths between
215 418.3 and 424.2 m. These samples are from Röt (Triassic) deposits of Anisian age. The core was
216 drilled in 2000 by AKZO in order to explore for table salt. The description of the core can be found
217 at the Dutch Oil and Gas Portal (<http://www.nlog.nl/en>): click on "boreholes" and "listing boreholes"
218 then search for TWR-515. The purest halite samples were selected from this core based on their
219 translucency.

220
221 **2.5 Permian**

222
223 2.5.1 *Changhsingian (about 253 Ma)*

224
225 One sample (H3) is taken from the Changhsingian Salado salt deposit in New Mexico (Maley and
226 Huffington, 1953; Pierce and Rich, 1962).

227

228 2.5.2 *Wuchiapingian (about 257 Ma)*

229

230 Six of the samples described in Eggenkamp et al. (2019), which are halite salt samples are
231 incorporated in this study. These samples were recently taken the core TCI-2, which was described
232 and studied earlier by Eggenkamp et al. (1995). A general description of this core was given in
233 Coeleweij et al. (1978) and Buyze and Lorenzen (1986).

234

235 **2.6 Late Ordovician to Middle Devonian**

236

237 2.6.1 *Givetian (about 385 Ma)*

238

239 The three samples EVA1 (15.34.93.24W4), EVA4 (6.80.36.13W4) and H4 were taken from the
240 Givetian (Mid-Devonian) Canadian Prairie Formation (Grobe, 2000). EVA1 and EVA4 were made
241 available from the collection of the Muséum Nationale de Histoire Naturelle in Paris.

242

243 2.6.2 *Late Ordovician / Early Silurian (about 444 Ma)*

244

245 One sample (H5) was taken from the Western Australian Caribuddy Formation of the Late
246 Ordovician to Early Silurian age (Haines, 2009). As this sample was visibly heterogeneous,
247 containing white and red parts, it was split into two, H5a containing the white salt and H5b
248 containing the red salt.

249

250 **2.7 Ediacaran to Early Cambrian**

251

252 2.7.1 *Terreneuvian (about 531 Ma)*

253

254 One sample (H6) was taken from the East Siberian Angarskaya Formation (Petrychenko et al.,
255 2005).

256

257 2.7.2 *Ediacaran (about 545 Ma)*

258

259 One sample (H7) is taken from the Ara Formation in Oman (Mattes and Conway Morris, 1990;
260 Schröder et al., 2005) and three (IR4, IR5 and IR6) from the Iranian Hormuz Formation (Kent,
261 1979; Alavi, 2004). These samples are of comparable age are lateral equivalent to each other.

262

263 **2.8 Tonian (about 820 Ma)**

264

265 Six samples (AU1 to AU6) were collected from the Gillen Formation of the Bitter Springs Group,
266 Amadeus Basin in central Australia. The Gillen Formation was, until recently, the oldest known
267 massive salt deposit (Naughton et al., 1968; Stewart, 1979). Samples AU1 AU3 were collected from
268 drill core Mt Charlotte-1 at depths of 1875.34 to 1875.44, 1877.85 to 1877.92 and 2060.14 m
269 respectively. Samples AU4 to AU6 were collected at depths of 556', 306' and 600' from diamond
270 drill core Mt Liebig-1 and represent massive, orange-coloured halite.

271

272 **2.9 Orosirian (about 2000 Ma)**

273

274 This deposit represents a recently discovered massive and thick evaporite (halite and anhydrite)
275 deposit that is only recognised in the Onega parametric well in Russia (Morozov et al., 2010;
276 Krupenik and Sveshnikova, 2011; Gorbachev et al., 2011; Glushanin et al., 2011). These are the

277 oldest currently known massive halite deposits on Earth. They are described as marine evaporites
278 (Blätter et al., 2018). It is not known yet if their thickness in the drill core represents stratigraphic
279 thickness or the thickness of the evaporite interval in a salt diapir. 23 samples from this core were
280 available for this study. Magnesium and calcium isotopes of this evaporite deposit have recently
281 been studied and interpreted to record the Great Oxidation Event that can explain the high sulphate
282 contents in these deposits (Blättler et al., 2018). Several of the samples analysed in the study from
283 this deposit were previously measured for their Cl isotope composition by Sharp et al. (2013).

284 3. METHODS

285 All samples, except those labelled "EVA" were available as solid salt samples. The "EVA" samples
286 were available as solutions prepared previously with approximately seawater chloride
287 concentrations (see Paris et al., 2010). Solid salt samples were dissolved in water in a ratio of 1:9 (1
288 gram of salt and 9 grams of distilled water) for Cl and Br isotope measurements. This 1:9 solution
289 was diluted by an extra 1000 times to obtain solutions diluted enough for ICP-OES and ICP-MS
290 measurement of the chemical composition. All dissolved samples were analysed for the
291 determination of chemical (Cl^- , Br^- , SO_4^{2-} , Na^+ , K^+ , Mg^{2+} and Ca^{2+}) and isotopic ($\delta^{37}\text{Cl}$ and $\delta^{81}\text{Br}$)
292 compositions at the Institut de Physique du Globe de Paris, France.

293 Cl^- and Br^- concentrations were measured by ICP-MS on an Agilent Technologies 7900 ICP-MS.
294 The cations and sulphate (measured as S) were analysed by ICP-OES on a Thermo Scientific iCAP
295 6000 Series ICP Spectrometer. The results were calculated back to the chemical composition of the
296 salts and are reported in Table 1 in the unit of g per kg salt.

297 The chlorine isotope composition was measured according to the method described by Kaufmann
298 (1984), Eggenkamp (1994) and Godon et al. (2004). In short, Cl^- is precipitated as AgCl by adding
299 AgNO_3 , which was reacted with CH_3I to form CH_3Cl . CH_3Cl is separated from CH_3I by two gas
300 chromatograph runs using a Périchrom IGC-11 gas chromatograph (with dry pure He at 130°C,
301 2.1 bar and 15 ml/min) in two identical packed columns (Porapak-Q 80–100 mesh, 2 m length and
302 3.175 mm outer diameter). A thermal conductivity detector is used to check the progress of this
303 purification and to detect any leaks. $^{37}\text{Cl}/^{35}\text{Cl}$ ratios were subsequently determined on the CH_3Cl
304 with dual-inlet mass spectrometry on a ThermoFisher Delta PlusXP mass spectrometer (IRMS). The
305 results are reported in the δ notation (as $\delta^{37}\text{Cl}$) in ‰ relative to SMOC (Standard Mean Ocean
306 Chloride, Kaufmann et al., 1984), with a standard deviation (1σ) of 0.05‰.

307 The bromine isotope composition was measured on a Neptune (ThermoFisher) multicollector ICP
308 mass spectrometer (MC-ICP-MS). Due to the low Br/Cl ratios of the halite samples, it was not
309 possible to extract the bromide using the classic ion-exchange method (Louvat et al., 2016);
310 bromine was extracted through oxidative distillation following Murphy et al. (1954) as described by
311 Eggenkamp and Louvat (2018). Bromide is oxidised to bromine gas by a 14% boiling nitric acid
312 solution and distilled into a 0.5N ammonia solution, where bromine is trapped and
313 disproportionated into bromide and bromate. Due to the reducing nature of the ammonia solution,
314 bromate is reduced to bromide. The extraction efficiency of this distillation is about 50%. As shown
315 by Eggenkamp and Louvat (2018) no isotope fractionation was observed during the distillation
316 process. This solution can be measured directly by MC-ICP-MS as a wet plasma as described by
317 Louvat et al. (2016). Results are reported in the δ notation (as $\delta^{81}\text{Br}$) in ‰ relative to SMOB
318 (Standard Mean Ocean Bromide, Eggenkamp and Coleman, 2000) with an average standard
319 deviation (1σ) of about 0.1‰.

320 For both Cl and Br isotope measurements ocean water sampled in the Indian Ocean (sampled in
321 January 2010 during the MD 175 cruise, latitude 32.45°S, longitude 84.01°E) was prepared and
322 measured 13 times for its $\delta^{37}\text{Cl}$ composition (with better than 0.05‰ 1σ standard deviation, which
323 is comparable to the typical long-term external reproducibility of $\delta^{37}\text{Cl}$ measurements obtained at
324 IGP on both seawater and unknown samples; e.g., Godon et al., 2004 and Bonifacie et al., 2005)

Formatted: Left, Hyphenate, Don't adjust space between Latin and Asian text, Don't adjust space between Asian text and numbers

Formatted: Font: (Default) Times New Roman, 12 pt

Formatted: Font: (Default) Times New Roman, 12 pt

Formatted: Font: (Default) Times New Roman, 12 pt

Formatted: Superscript

Formatted: Font: (Default) Times New Roman, 12 pt

Formatted: Superscript

Formatted: Superscript

327 and prepared and measured 5 times for its $\delta^{81}\text{Br}$ composition (with better than 0.10‰ 1 σ standard
328 deviation).

329 Results of the $\delta^{37}\text{Cl}$ and $\delta^{81}\text{Br}$ measurements are also reported in Table 1. The accuracy of the
330 measurements is indicated in the Table showing the 1 σ standard deviation of multiple (mostly two)
331 preparations and measurements of the same sample.

333 4. RESULTS

334
335 Data reported in Table 1 show that all samples except one (IR1) are predominately composed of
336 halite. Varying amounts of K, Mg and Ca are present, indicating that the evaporates formed during
337 various stages of halite-dominated precipitation. As the Br/Cl ratio can be used as a proxy for the
338 evaporation stage (Valyasko, 1956; Braitsch, 1962; Herrmann et al., 1973; McCaffrey et al., 1987;
339 Eggenkamp et al., 2019), it was calculated for all samples and included in table 1. The samples
340 show a considerable range in Br/Cl ratios, from <0.00001 to 0.00091. All samples with very low
341 Br/Cl ratios (<0.00005) are taken from the Omega parametric well in Russia (A02 to A21), and due
342 to their low Br content and insufficient amount of sample available it was only possible to analyse
343 two of these samples for Br isotopes. The total range of Cl isotope ratios in the sample set ranges
344 from -0.24 to +0.51‰, while the range of Br isotope ratios is from -0.24 to +1.08‰. The total range
345 of Br isotope ratios is thus considerably larger than that for Cl isotope ratios.

346
347 Table 1

349 5. DISCUSSION

350
351 Based on a set of 132 salt samples with ages ranging from the Late Neoproterozoic (ca. 550 Ma) to
352 the Messinian (ca. 6.3 Ma), Eastoe et al. (2007) concluded that significant variations in the Cl
353 isotope composition of the ocean were unlikely during this period. They reported no range within
354 which the Cl isotope composition could have varied (however small it may have been), which was
355 based on the observation that the overwhelming majority of salt samples had $\delta^{37}\text{Cl}$ values between -
356 0.50 and +0.50‰ relative to SMOC. We expect that it should be possible to constrain the $\delta^{37}\text{Cl}$
357 secular trend of the ocean within a narrower limit using our recent constraints for the isotope
358 fractionation of chloride during chloride salt precipitation from saturated brine. There are several
359 studies that determined the isotope fractionation of chlorine during precipitation from saturated
360 brine (Eggenkamp et al., 1995, 2016, Luo et al., 2012, 2014). The fractionation factors obtained in
361 these studies varied considerably. Eggenkamp et al. (1995) reported a value of $\alpha=1.00026$,
362 Eggenkamp et al. (2016) reported 1.00035 and the average of the values reported by Luo et al.
363 (2012, 2014) is 1.00049. This relatively large variability has to be taken into account, if the original
364 $\delta^{37}\text{Cl}$ of seawater is to be determined. If the fractionation factor is larger, the $\delta^{37}\text{Cl}$ values of the
365 precipitated halite diverge progressively with precipitation (see e.g. the discussion by Eggenkamp
366 (2015a) and Luo et al. (2015)). Thus, the estimate of secular seawater $\delta^{37}\text{Cl}$ values requires
367 relatively large corrections, if the larger fractionation factors are assumed. The Br isotope data in
368 the present paper are the first of a notable number of halite samples, and the seawater record of the
369 Br isotopes will be discussed despite our limited knowledge of Br isotope fractionation during sea-
370 salt precipitation.

372 5.1 Estimate of the secular $\delta^{37}\text{Cl}$ values of seawater

373
374 Here we apply two methods to estimate the original $\delta^{37}\text{Cl}$ of the ocean based on the $\delta^{37}\text{Cl}$ values of
375 the analysed halite samples. At first, an approach solely based on $\delta^{37}\text{Cl}$ values is applied, and the
376

377 | second approach is based on the Br/Cl ratio used as a parameter in combination with the $\delta^{37}\text{Cl}$ of
378 | the samples to infer the original $\delta^{37}\text{Cl}$ of the ocean from which the halite was precipitated.

380 | 5.1.1 Estimate based on $\delta^{37}\text{Cl}$ of halite salt only

381
382 | When salt precipitates from a saturated solution it removes heavy chlorine isotope from the brine
383 | that, as a result, becomes enriched in the lighter isotope. This effect is a classic Rayleigh effect that
384 | has been described before (Eggenkamp et al., 1995, Luo et al., 2014, Eggenkamp 2015). As long as
385 | halite is the only chloride-precipitating mineral, this process is gradual. The previous studies have
386 | demonstrated that the first halite that precipitates is heavier in Cl isotopes than that of seawater, and
387 | that it becomes progressively lighter until 82.5% of all chloride is precipitated and the first
388 | potassium chloride (kainite $[\text{K}_4\text{Mg}_4\text{Cl}_4(\text{SO}_4)_4 \cdot 11\text{H}_2\text{O}]$) starts to precipitate (Braitsch, 1962). From
389 | this stage, precipitating salt is no longer a pure halite so that isotope fractionation, as well as Br
390 | distribution, will be different from there on. Thus, if we use the $\delta^{37}\text{Cl}$ of a primary halite to infer the
391 | seawater composition it must have precipitated before 82.5% of the chloride present in the brine has
392 | been precipitated. The $\delta^{37}\text{Cl}$ composition of salt that precipitated from modern seawater with a
393 | $\delta^{37}\text{Cl}$ value of 0‰ decreases depending on the fractionation factor that is used. For example, if we
394 | assume a fractionation factor of 1.00026, the halite precipitated initially will have a $\delta^{37}\text{Cl}$ of
395 | +0.26‰ and the last batch (when potassium-bearing chloride starts to precipitate) will have a $\delta^{37}\text{Cl}$
396 | of -0.19‰. If we use a fractionation factor of 1.00035, $\delta^{37}\text{Cl}$ of the precipitated halite decreases
397 | from +0.35‰ to -0.26‰ due to the Rayleigh effect. Similarly, if we use a fractionation factor of
398 | 1.00049, the $\delta^{37}\text{Cl}$ of the halite decreases from +0.49‰ to -0.36‰. To know the $\delta^{37}\text{Cl}$ composition
399 | of the original seawater, these $\delta^{37}\text{Cl}_{\text{halite}}$ values need to be reversed/inverted. That means that in the
400 | case of a fractionation factor of 1.00026 the original $\delta^{37}\text{Cl}$ value of the ocean was somewhere
401 | between 0.26‰ lower and 0.19‰ higher than the $\delta^{37}\text{Cl}$ of the halite sample, depending on where
402 | the sample was precipitated on the Rayleigh curve. For higher fractionation factors, these numbers
403 | are between 0.35‰ lower and 0.26‰ higher for $\alpha=1.00035$ and between 0.49‰ lower and 0.36‰
404 | higher for $\alpha=1.00049$. This result in fairly large potential ranges for the original $\delta^{37}\text{Cl}$ of the oceans,
405 | as it is unknown at what point on the Rayleigh curve the samples precipitated. Figure 1 shows how
406 | this process is applied to seawater with a $\delta^{37}\text{Cl}$ of 0‰ and halite with a fractionation factor of
407 | 1.00035. However, since we have measured multiple halite samples for each geological period, it is
408 | possible to decrease the calculated range of $\delta^{37}\text{Cl}$ in seawater.

410 | Figure 1

411
412 | Indeed, assuming primary, unaltered $\delta^{37}\text{Cl}$ values of the salt samples, the possible range of $\delta^{37}\text{Cl}$ in
413 | the ocean must be the overlapping part of all the $\delta^{37}\text{Cl}$ ranges from the individual samples
414 | corresponding to the concerned geological period. Figure 2 illustrates how this works for one of the
415 | geological periods, the Permian, a period from which we analysed eight samples. For each of the
416 | eight samples we calculate the maximum range of possible original $\delta^{37}\text{Cl}$ of the seawater for
417 | $\alpha=1.00035$. This figure shows that the range, within which the original $\delta^{37}\text{Cl}$ must have layed,
418 | decreases significantly when more samples from a period were measured. In the case a smaller or
419 | larger value for α used the original $\delta^{37}\text{Cl}$ range will be smaller or larger. It is clear from this figure
420 | that the effective range of $\delta^{37}\text{Cl}$ of the seawater is where all eight $\delta^{37}\text{Cl}$ of the seawater ranges of the
421 | samples overlap. In the case of the Permian the figure shows that assuming a fractionation factor α
422 | of 1.00035 the original $\delta^{37}\text{Cl}$ of the oceans must have been between -0.10‰ and +0.14‰. This
423 | range would be smaller (between -0.01‰ and +0.07‰) assuming $\alpha=1.00026$, or larger (between -
424 | 0.24‰ and +0.24‰) assuming $\alpha=1.00049$.

425 | Figure 2

427
428
429
430
431
432
433
434
435
436
437
438
439
440
441
442
443
444
445
446
447
448
449
450
451
452
453
454
455
456
457
458
459
460
461
462
463
464
465
466
467
468
469
470
471
472
473
474
475
476

Table 2

These calculations were made for all the geologic periods considered here and the results are summarised in Table 2. This table highlights also weaknesses of this approach. For two periods, the Recent and the Neogene, the range in $\delta^{37}\text{Cl}$ of the seawater was larger than the possible isotope variation if we assume $\alpha=1.00026$. As a consequence, the minimum value in this approach is higher than the maximum value, and that means that the seawater $\delta^{37}\text{Cl}$ cannot be explained with a fractionation factor of 1.00026. The range can be explained however with higher fractionation factors, and the most straightforward conclusion is that the chlorine isotope fractionation factor for the precipitation of halite from ocean water must be larger than 1.00026. The second problem is the reconstructed $\delta^{37}\text{Cl}$ of seawater based on modern salt samples. The mean value of the reconstructed $\delta^{37}\text{Cl}$ (based on fractionation factors 1.00035 and 1.00049) is +0.18‰, while the $\delta^{37}\text{Cl}$ of today's oceans is by definition 0‰. While the values obtained for ancient seawater seem to reflect the original $\delta^{37}\text{Cl}$ of those periods the recent samples seem not to, which might reflect differences in the precipitation process. All historic samples are precipitated from evaporating seawater in a static way, where a batch of seawater evaporated until it became saturated with halite and halite will precipitate to the bottom of the evaporite basin. The modern samples on the other hand (except MO3) were precipitated in an active way, where the precipitation of salt from seawater was as quickly as possible to improve the precipitation rate, especially by keeping the ponds as shallow as possible and to remove the salt immediately upon precipitation so that it can be dried in the sun. These effects considerably increase the kinetics of salt precipitation and this might result in possible non-equilibrium precipitation of halite from these seawaters as well as the significant isotope variation among these samples, including some that are from the same location. It has to be realised that all calculations above were made as if the [chemical](#) composition of ocean water had not changed during geologic history, while ~~the~~-this composition obviously has changed (Babel and Schreiber, 2014). We have decided to work in this preliminary study using the modern composition of ocean water in order to simplify the calculations, although, as sulphate concentrations in the past were generally lower than they are today the halite only phase may have been more extended and might have been up to 86.9% when carnallite ($\text{KMgCl}_3 \cdot 6\text{H}_2\text{O}$) starts to precipitate (Eggenkamp et al., 1995) for sulphate free brines.

5.1.2 Estimate based on $\delta^{37}\text{Cl}$ and Br/Cl ratios of halite

It is well established that during precipitation of salt from seawater brine not only the $\delta^{37}\text{Cl}$ value of the brine decreases due to a Rayleigh type isotope fractionation, but also that the Br/Cl ratio increases. Because the Br/Cl ratio of precipitated halite is significantly lower than the Br/Cl ratio in seawater, controlled by the distribution coefficient, the Br/Cl ratios of the precipitated salt and the remaining brine evolve in a fashion very similar to that of the $\delta^{37}\text{Cl}$, following a Rayleigh fractionation process. This effect has been studied extensively in the past (e.g. Boeke, 1908; Kühn, 1955; Valyasko, 1956; Braitsch, 1962; Herrmann, 1972; Herrmann et al., 1973). Eggenkamp et al. (2019) have shown that a clear relationship between $\delta^{37}\text{Cl}$ and Br/Cl ratios is observed in a well-developed salt sequence. Figure 3 shows the relationship between the $\delta^{37}\text{Cl}$ and the Br/Cl ratios of the salt samples that were measured for the present study. The sample set can be separated into three populations. To the left a series of samples with a large variation in low Br/Cl ratios and very constant $\delta^{37}\text{Cl}$ values around -0.1‰, to the right a group of samples with high Br/Cl values and relatively high $\delta^{37}\text{Cl}$ values, and in the centre, which is the largest set of samples, a group of samples showing an inverse correlation between $\delta^{37}\text{Cl}$ values and Br/Cl ratios.

Figure 3

477
478 In more detail, the first group of samples (with a large variation in very low Br/Cl ratios and nearly
479 constant and low $\delta^{37}\text{Cl}$ values) are all Orosirian samples from the Onega parametric well in Russia.
480 These two billion years old evaporites show extremely low Br contents, but also very similar $\delta^{37}\text{Cl}$
481 values. We can explain this by repeated dissolution and reprecipitation cycles in which the Br
482 content decreased in each cycle (due to Br^- enrichment in the brine that for a large part disappeared
483 from the deposit), while the $\delta^{37}\text{Cl}$ values became homogenised during this process. This
484 interpretation is consistent with the Sr and S isotope data (Krupenik and Shesnikova, 2011; Blättler
485 et al., 2018), indicating a depositional system largely disconnected from the open ocean and
486 potential dissolution-reprecipitation and mixing related to diapir growth.
487 The second group of samples (with high Br/Cl ratios and high $\delta^{37}\text{Cl}$ values), are all modern “table”
488 salts that were produced with modern industrial production techniques as described above. The high
489 Br/Cl ratios in these salts might reflect kinetic rather than equilibrium fractionation since still wet
490 salt is removed from the salt pans and put aside to dry in the sun. Consequently, wet salt contains
491 significant amounts of brine with very high Br/Cl ratios, increasing the Br content of the final salt.
492 The high $\delta^{37}\text{Cl}$ ratios of industrial salt samples indicate much larger kinetic compared to
493 equilibrium fractionation factor as precipitates were removed from the brine well before the
494 thermodynamic equilibrium could have been reached. Similarly, this large difference between
495 kinetic and equilibrium fractionation factors might explain the large range of fractionation factors
496 involved in halite precipitation from brine discussed above. The fact that the modern salt stands
497 aside from ancient primary salt deposits shows however that the calculations done in the previous
498 section confirm that the reconstructed $\delta^{37}\text{Cl}$ of the modern ocean does not agree with the actual
499 $\delta^{37}\text{Cl}$ of the seawater from which it precipitates.
500 The third and largest group of samples, which contains all the samples from ancient primary salt
501 deposits, shows promising relationships. These samples fall on a trend showing a negative
502 correlation between $\delta^{37}\text{Cl}$ values and the Br/Cl ratios. Using this relationship, it might be possible to
503 retrieve the original $\delta^{37}\text{Cl}$ values of the seawater for each geological period. This was tested for
504 each period by applying the relationships between Br/Cl ratio and $\delta^{37}\text{Cl}$. Seven plots are produced
505 (Figure 4) that show the expected negative relationship between $\delta^{37}\text{Cl}$ values and the logarithm of
506 the Br/Cl ratio with varying degrees of uncertainties that are reflected by hyperbolas. Extrapolation
507 to the logarithm of the Br/Cl ratio of the first precipitating halite yields an estimate of $\delta^{37}\text{Cl}$ of the
508 first precipitated halite and from that the $\delta^{37}\text{Cl}$ of the seawater can be (in theory)
509 recovered/retrieved.
510 The Br content of the first precipitated halite can be obtained theoretically from the bromide content
511 in the brine at the stage of the first halite precipitation and from the Br distribution coefficient
512 between halite and the brine. This distribution coefficient (defined as $b = \text{mass\% Br in salt} / \text{mass\%}$
513 Br in brine) is 0.14 (Braitsch, 1962). Since the Br content in the brine at the moment of first halite
514 precipitation is about 0.053%, the Br content in the first precipitated halite is 0.0074%, and the
515 Br/Cl ratio in this halite is 0.00012. However, this is only correct if we assume that seawater had
516 the same chemical composition as the modern ocean. Yet, the chemical composition of seawater has
517 changed considerable over geological history (see e.g. Horita et al., 2002; Lowenstein et al, 2014).
518 These changes in seawater composition also had a significant influence on the amount of Br that is
519 incorporated in the first precipitated halite (cf. Siemann and Schramm, 2000; Siemann, 2003).
520 These studies have shown that in most of the Phanerozoic the bromide content in the first halite that
521 precipitated was lower than at present. According to their results, in the geological periods of
522 interest, the first precipitated halite should show Br/Cl ratios of 0.00017 (Neogene), 0.00010
523 (Paleogene), 0.00015 (Triassic), 0.00014 (Permian), 0.00008 (Ordovician-Devonian) and 0.00017
524 (Ediacaran-Cambrian). The ratio is not known for the Tonian. These values were recalculated from
525 $\mu\text{g Br/g NaCl}$ ratios as presented by Siemann (2003) to Br/Cl mass ratios. It is, however, important
526 to consider these Br/Cl ratio calculations with caution (Lowenstein et al., 2014), because Br

527 concentrations reported from the first precipitated halite in modern marine settings vary
528 substantially from study to study. For comparison, 38 ppm in halite grown experimentally from
529 Mediterranean seawater (Bloch and Scherb, 1953) to 50 ppm in modern halite from Baja California,
530 Mexico (Holser, 1966), to 100 ppm from evaporated North Sea seawater (Siemann, 2003). Br
531 concentrations in the recent commercial salt samples measured in this study are even higher than
532 these observations, but as discussed above this is probably due to non-equilibrium processes by
533 which these salts were produced.

534 The same uncertainties are also notable in our set of samples. The global relationship between Br/Cl
535 ratios and $\delta^{37}\text{Cl}$ values on Figure 3 shows that in our dataset the lowermost Br/Cl limit of primary
536 samples (thus excluding the Paleoproterozoic samples) can be as low as 0.00005 for a Triassic
537 sample, comparable to the ratio expected for the periods with the lowest suggested Br/Cl ratio by
538 Siemann (2003), but unfortunately not the Triassic, which should have a two to three times higher
539 Br/Cl ratio for first precipitated halite. These results indicate that model Br/Cl data for the first
540 precipitated halite as determined by Siemann (2003) must be used with caution and for the purpose
541 of the present study we will use the lowest Br/Cl ratio measured in our dataset (0.00005) to estimate
542 the original $\delta^{37}\text{Cl}$ of the ocean for the different geologic periods.

543
544
545

Figure 4

546 On figure 4 the regression lines as well as the uncertainty hyperbolas are extrapolated to a Br/Cl
547 ratio of 0.00005 (= -4.3 in log units) for samples from all geological period samples that were
548 available in this study. The resulting $\delta^{37}\text{Cl}$ values (and uncertainties) are summarised in Table 3.

549
550
551

Table 3

552 At first approximation these values can be considered as the $\delta^{37}\text{Cl}$ of the first precipitated halite for
553 each geologic period. The original seawater $\delta^{37}\text{Cl}$ can then be determined by subtracting $10^3 \ln \alpha$ (α =
554 fractionation factor) from these extrapolated $\delta^{37}\text{Cl}$ values, using α values of 1.00026, 1.00035 and
555 1.00049 (Eggenkamp et al., 1995, 2016; Luo et al., 2012). This results in lower reconstructed $\delta^{37}\text{Cl}$
556 values for larger fractionation factors. Importantly, no large variations are observed between the
557 different secular $\delta^{37}\text{Cl}$ values of the ocean, and the average secular values are about 0.01‰
558 assuming a fractionation factor of 1.00026, -0.08‰ assuming a fractionation factor of 1.00035 and -
559 0.22‰ assuming a fractionation factor of 1.00049. These data thus suggest an only slightly negative
560 $\delta^{37}\text{Cl}$ value for the seawater during the last billion years with little temporal variation. The low
561 inferred (average) $\delta^{37}\text{Cl}$ value for a fractionation factor of 1.00049 with respect to the modern
562 seawater composition again indicates that this fractionation factor is non-realistically high as it
563 would imply a drastic change in $\delta^{37}\text{Cl}$ of the ocean between the Miocene and the present, which is
564 not sensible. Note that the calculations are made using the lowermost first halite Br/Cl ratio. As
565 there is a negative relationship between the $\delta^{37}\text{Cl}$ and the Br/Cl ratio, the calculated $\delta^{37}\text{Cl}$ values for
566 the ocean become even lower if higher first halite precipitated Br/Cl ratios, such as those suggested
567 by Siemann (2003), are used in the calculations. This may indicate that the initial Br/Cl ratios of the
568 first precipitated halite have always been lower than those suggested by Siemann (2003).

569
570 *5.1.3 Comparison of the two approaches to establish the $\delta^{37}\text{Cl}$ of seawater from precipitated halite*
571 *and the most probable seawater $\delta^{37}\text{Cl}$ values over geological history*

572
573 The two approaches to estimate the $\delta^{37}\text{Cl}$ values of the ocean during the geological past yield
574 different results, but combined together they are able to constrain the approximate value of $\delta^{37}\text{Cl}$ of
575 the ocean during the geological past. The combined results of the two approaches are summarised in
576 Figure 5. The results obtained for the recent salt-pan samples are omitted as they do not reflect the

577 $\delta^{37}\text{Cl}$ composition of current seawater. The $\delta^{37}\text{Cl}$ value of the ocean during the Paleoproterozoic
578 could not be determined via the second approach (with Br/Cl ratio) due to their extremely low Br
579 contents, but the results of the first approach (range of possible $\delta^{37}\text{Cl}$ in seawater) are shown. The
580 first “Cl only” approach is shown as coloured bands in the background of the figure as it is not
581 possible to give an average value but only a range of overlapping possible $\delta^{37}\text{Cl}$ ranges for all
582 samples within a specific geologic period. This range gets larger if higher fractionation factors are
583 assumed. Estimated $\delta^{37}\text{Cl}$ values of the ocean from the second “Br/Cl ratio” approach are shown as
584 three lines with increasing fractionation factors with uncertainties shown as 2σ error bars. There is
585 considerable overlap between the two approaches. It is clear however that assuming a fractionation
586 factor of 1.00049 the $\delta^{37}\text{Cl}$ range determination with the second approach falls really at the lower
587 end of the first approach. This seems to indicate again that our data do not support a Cl isotopic
588 fractionation factor as large as 1.00049 between brine and precipitating halite.
589 The overlap between the two approaches is much better for fractionation factors of 1.00026 and
590 1.00035. However, as a fractionation factor of 1.00026 leads to the impossibility to determine the
591 ocean’s $\delta^{37}\text{Cl}$ for the Neogene it is not likely that the fractionation factor is so small and it is likely
592 close to the recently published value of 1.00035 (Eggenkamp et al., 2016).
593

594 Figure 5
595

596 The data suggest small variations in the $\delta^{37}\text{Cl}$ of the ocean during the geological past that are
597 smaller than the uncertainties in the data. Variations are largest in the reconstructions of the first
598 approach that might originate in the speculation that in these periods samples are more biased
599 towards early or late stage halite. The second approach corrects for this bias as it extrapolates to the
600 $\delta^{37}\text{Cl}$ values of the first precipitated halite.

601 In summary we conclude that $\delta^{37}\text{Cl}$ variations of the ocean during the geologic past were small, as
602 has been suggested by Eastoe et al. (2007). The first approach suggests $\delta^{37}\text{Cl}$ values between about
603 +0.2 and -0.4‰, and these are confirmed by the second approach. Overall $\delta^{37}\text{Cl}$ values of the ocean
604 can be estimated to have fallen into the range $-0.10 \pm 0.25\text{‰}$ for the past two billion years (see figure
605 5).
606

607 5.1.4 Comparison with $\delta^{37}\text{Cl}$ estimates reconstructed by Eggenkamp et al. (2016) 608

609 Eggenkamp et al. (2016) reconstructed the $\delta^{37}\text{Cl}$ history of the past billion years based on
610 theoretical constraints of the isotope fractionation between brine and salt of NaCl (halite) in
611 combination with deposition and subsrosion of salt deposits as reconstructed by Hay et al. (2006).
612 Eggenkamp et al. (2016) concluded that the $\delta^{37}\text{Cl}$ of the ocean should have decreased by about
613 0.25‰ during the last billion years since during that time period more halite has been removed from
614 the ocean than has been returned to it via subsrosion. Net removal of halite should result in a
615 decrease in the $\delta^{37}\text{Cl}$ of the ocean as the heavier chlorine isotope preferentially precipitates out of
616 the brine. The results of this study however suggest that this decrease in $\delta^{37}\text{Cl}$ is not empirically
617 supported, and it seems even more likely that the $\delta^{37}\text{Cl}$ of the ocean was slightly lower than today.
618 The prediction of Eggenkamp et al. (2016) was based on the assumption that precipitation of halite
619 and subsrosion of salt deposits are the only processes that determine the $\delta^{37}\text{Cl}$ of the ocean over
620 geological periods of time, but several other processes could also impact it such as removal of
621 chlorine at subduction zones and addition of chlorine during volcanic activity. To evaluate the
622 isotopic mass balance of the chlorine cycle on the geologic time scale, it is necessary to carry a
623 comprehensive isotopic study of the chlorine cycle and ensure that the isotope composition and
624 isotope fractionation of the various chlorine fluxes is taken into account. Although the chlorine
625 cycle is fairly well understood (see e.g. Jarrard, 2003) addition of the isotope compositions and
626 fractionations to the fluxes will surely improve our understanding.

627

628

5.2 Estimate of the secular $\delta^{81}\text{Br}$ values of seawater

629

630

631

632

633

634

635

636

637

638

639

640

641

642

643

644

645

646

647

648

649

650

651

652

653

654

655

656

657

658

659

660

661

662

663

664

665

666

667

668

669

670

671

672

673

674

675

676

Unlike chlorine isotopes, behaviour of bromine isotopes during the precipitation of salt is not yet well understood. Eggenkamp et al. (2016) suggested very little fractionation based on experimental precipitation of pure bromide salts. However, this interpretation could not explain the highly positive Br isotope values of formation waters that had likely acquired their Br from dissolving evaporites (Eggenkamp, 2015b). Subsequently, it was found that Br isotope compositions of a fully developed salt sequence (halite to bischofite) do have large and systematic Br isotope variations and it was concluded that isotope fractionation of Br when it precipitates with halite must be much larger than previously expected, and that its fractionation might be as large as 1.0013 (Eggenkamp et al., 2019). This large fractionation factor makes it difficult to infer the original $\delta^{81}\text{Br}$ of the ocean based on the Br isotope composition alone. With a Br isotope fractionation factor of 1.0013, the first halite to precipitate from seawater would have a $\delta^{81}\text{Br}$ of 1.3‰, which would progressively decrease to -1.0‰ when the last halite to precipitate. The original $\delta^{81}\text{Br}$ of seawater would then fall between 1.3‰ lower to 1.0‰ higher than the measured $\delta^{81}\text{Br}$ of a halite sample, which is a considerable range. Based on the $\delta^{81}\text{Br}$ values of samples measured in this study, the $\delta^{81}\text{Br}$ value of the ocean might have ranged between approximately -0.6 and +1.0‰ during the last 2 billion years. Such a large plausible range is unfortunately not very useful to constrain the secular seawater $\delta^{81}\text{Br}$ evolution.

The second (Br/Cl ratio) approach that we applied to constrain seawater Br isotope variations during the past shows ambiguous results. Figure 6 shows that the relationship between the $\delta^{81}\text{Br}$ and the Br/Cl ratios of the whole set of halite samples is much more diffuse than that between the $\delta^{37}\text{Cl}$ and the Br/Cl ratios (Figure 2).

Figure 6

However, it is clear from Figure 6 that some relationship between $\delta^{81}\text{Br}$ and Br/Cl ratio exists. The lowest possible $\delta^{81}\text{Br}$ value is a function of the Br/Cl ratio. Figure 6 shows that the lower $\delta^{81}\text{Br}$ limit decreases with increasing Br/Cl ratio, pointing a minimum $\delta^{81}\text{Br}$ value of +0.33‰ vs SMOB at a Br/Cl ratio of 0.00005. This suggests a minimum possible isotope fractionation between Br⁻ in solution and Br⁻ in solid NaCl of about 1.0003. Note that the two samples with the lowest Br/Cl ratios in this Figure are from the Russian sample set and, as their Br content has been decreased considerably after salt deposition they should not be taken into account when the lowest possible $\delta^{81}\text{Br}$ is determined. Nonetheless, in three of the nine sample groups (Permian, Ordovician-Silurian and Ediacaran-Cambrian) a reasonably high correlation coefficient is observed with a negative Br/Cl vs. $\delta^{81}\text{Br}$ trend, and these three sample groups point to $\delta^{81}\text{Br}$ values of halite (at a Br/Cl ratio of 0.00005, = -4.3 in log units) between 0.6 and 0.8‰ (Figure 7).

Figure 7

Figure 7 shows the reconstructed relationships with uncertainty hyperbolas for these three sample groups with high correlation coefficients. These three subsets point to $\delta^{81}\text{Br}$ values in the first precipitated salt between 0.6 and 0.8‰ and the line showing the lowermost $\delta^{81}\text{Br}$ value suggests a value higher than 0.3‰. As a result, these data suggest a lower bromine isotope fractionation factor than suggested by Eggenkamp et al. (2019). Figure 8 shows a visual interpretation of these data in a manner similar to that utilised for Cl in Figure 5. It shows the possible range in $\delta^{81}\text{Br}$ values following the first, isotope only approach, for fractionation factors of 1.003, 1.007 and 1.013, combined with the data for three periods following the second approach that takes the Br/Cl ratio in account, for the same isotope fractionation factors.

677
678
679

Figure 8

680 Considering the fractionation factor of 1.0013 as suggested by Eggenkamp et al. (2019) this
681 translates to an original $\delta^{81}\text{Br}$ value of seawater between -0.7 and -0.5‰. Although this range is
682 close to the lowest possible $\delta^{81}\text{Br}$ values of seawater following the total possible range as indicated
683 in Figure 8 they seem not realistic as values more within the central part of the total range would
684 have been expected. From Figure 8 it is also deductible that a fractionation factor of 1.003 is not
685 realistic. With such a low isotope fractionation factor it is mostly not possible to reconstruct the
686 $\delta^{81}\text{Br}$ values of seawater using the $\delta^{81}\text{Br}$ only approach for all but the oldest Russian samples. For
687 all younger geologic periods the minimum possible value is higher than the maximum possible
688 value. The reconstruction based on an isotope fractionation factor of 1.007 seems however feasible.
689 Following the $\delta^{81}\text{Br}$ only approach $\delta^{81}\text{Br}$ of the ocean then has always been in the range between
690 approximately 0 and +0.5‰ vs. SMOB. Adding the three possible computations of the combined
691 $\delta^{81}\text{Br}$ and Br/Cl ratio approach, which point to a $\delta^{81}\text{Br}$ value of seawater (at least during most of the
692 Palaeozoic) that was close to 0‰ (Figure 8), suggest that the $\delta^{81}\text{Br}$ of the ocean has been at its
693 present value. The combination of the two approaches thus suggest that the Br isotope fractionation
694 between bromide in brine and halite is about 1.007 and that the Br isotope composition of the
695 oceans has always been close to (or very slightly larger) its current value. Considering the small
696 number of data, combined with a considerable scatter in $\delta^{81}\text{Br}$ data of evaporites, these values
697 certainly need further refinement along with future research on the Br isotope fractionation during
698 seawater evaporation.

699 It is clear that, to better understand secular seawater variations in $\delta^{81}\text{Br}$ further research is needed on
700 this isotope system. This includes not only more measurements of Br isotope ratios in salt samples,
701 but also considerable experimental research to precisely determine the isotope fractionation factor
702 for Br precipitation with NaCl under various conditions such as different Br/Cl ratios, different
703 initial seawater compositions and during precipitation of salt from complex brines, as the
704 composition of these brines changes during salt precipitation. Finally theoretical (ab-initio)
705 calculations are also needed to understand the thermodynamics and other properties of the processes
706 studied, such as the competition between Br^- and other major and trace ions for incorporation into
707 halites.

708

709 6. CONCLUSIONS

710

711 We have measured the Cl and Br isotope values for a large set of halite samples in order to better
712 constrain Cl isotope compositions and variations in the oceans during the Earth's history than
713 Eastoe et al. (2007) were able to, as well as the first constraints on the secular seawater Br isotope
714 variations. Based on two different approaches, the Cl isotope variations were small to negligible,
715 with average values in the range $-0.10 \pm 0.25\%$ vs. SMOC during the last 2 Ga. Although with a
716 larger degree of uncertainty, it was also possible to obtain an indication of the seawater Br isotope
717 variations during this period. The data obtained in this study suggest a Br isotope fractionation
718 between bromide in brine and bromide in halite of about 1.0007. Combined with the possible Br
719 isotope range of the ocean obtained through the $\delta^{81}\text{Br}$ only approach, the range of Br isotope
720 compositions in the ocean may have been between 0,00 and +0.25‰ vs. SMOB (Figure 8) for at
721 least the last billion years with very little variation.

722

723 Acknowledgements

724

725 This research is part of the project "BRISOACTIONS" that has received funding from the European
726 Union's Horizon 2020 research and innovation programme under the Marie Skłodowska-Curie

727 grant agreement No 702001. We are grateful to Gilian Schout (Utrecht University), Alex Klomp and
728 Jan-Willem Weegink (both TNO Geological Survey) for their help in sample selection from the
729 Triassic and Upper Permian. We thank Pierre Burckel (IPGP) for Cl and Br analyses by ICP-MS
730 and Laure Cordier (IPGP) for the analyses by ICP-OES. Parts of this work were supported by the
731 IPGP multidisciplinary program PARI, by Paris–IdF region SESAME Grant no. 12015908, NSERC
732 Discoverery and Accelerator Grant to AB, and by Australian Research Council Grant DP160100607
733 to JJB. This is IPGP contribution No. 3962.

734

735 References

736

737 Alavi M. (2004) Regional stratigraphy of the Zagros fold-thrust belt of Iran and its proforeland
738 evolution. *Am. J. Sc.* **304**, 1–20.

739 Alijani N. (2000) Petrography and geochemistry of evaporate deposits in Garmsar region. MSc
740 thesis, Tehran University.

741 Babel M. and Schreiber B.C. (2014) Geochemistry of evaporites and evolution of seawater. *Treat.*
742 *Geochem.* 2nd ed. 483-560.

743 Bagheri R., Nadri A., Raeisi E., Eggenkamp H.G.M., Kazemi G.A. and Montaseri A. (2014)
744 Hydrochemistry and isotope ($\delta^{18}\text{O}$, $\delta^2\text{H}$, $^{87}\text{Sr}/^{86}\text{Sr}$, $\delta^{37}\text{Cl}$ and $\delta^{81}\text{Br}$) applications: clues to the
745 origin of saline produced water in a gas reservoir. *Chem. Geol.* **384**, 62–75.

746 Blättler C.L., Claire M.W., Prave A.R., Kirsimäe K., Higgins J.A., Medvedev P.V., Romashkin A.E.,
747 Rychanchik D.V., Zerkle A.L., Paiste K., Kreitsmann T., Millar I.L., Hayles J.A., Bao H.,
748 Turchyn A.V., Warke M.R. and Lepland A. (2018) Two-billion-year-old evaporites capture
749 Earth's great oxidation. *Science* **360**, 320-323.

750 Bloch M.R. and Schnerb J. (1953) On the Cl/Br⁻-ratio and the distribution of Br-ions in liquids and
751 solids during evaporation of bromide containing chloride solutions. *Bull. Res. Council Israel* **3**,
752 151-158.

753 Boeke H.E. (1908) Über das Krystallisationsschema der Chloride, Bromide, Jodide von Natrium,
754 Kalium und Magnesium, sowie über das Vorkommen des Broms und das Fehlen von Jod in den
755 Kalisalzlagern. *Z. Kristallogr.* **45**, 346–391.

756 Boschetti T., Toscani L., Shouakar-Stash O., Iacumin P., Venturelli G., Mucchino C. and Frappe S.K.
757 (2011) Salt waters of the Northern Apennine Foredeep Basin (Italy): origin and evolution. *Aquat.*
758 *Geochem.* **17**, 71–108.

759 Braitsch O. (1962) Entstehung und Stoffbestand der Salzlagerstätten. Springer.

760 Buyze D. and Lorenzen H. (1986) Solution mining of multi-component magnesium-bearing salts: a
761 realization in the Netherlands. *CIM Bull.* **79**, 52-60.

762 Coeleweij P. A. J., Haug G. M. W., and van Kuijk H. (1978) Magnesium-salt exploration in the
763 Northeastern Netherlands. *Geol. Mijnb.* **57**, 487-502.

764 Eastoe, C.J. (2016) Stable chlorine isotopes in arid non-marine basins: Instances and possible
765 fractionation mechanisms. *Appl. Geochem.* **74**, 1-12.

766 Eastoe, C.J. and Peryt T. (1999) Stable chlorine isotope evidence for non-marine chloride in
767 Bedenian evaporites, Carpatian mountain region. *Terra Nova* **11**, 118-123.

768 Eastoe, C.J., Long, A. and Knauth, L.P. (1999) Stable chlorine isotopes in the Palo Duro Basin,
769 Texas: evidence for preservation of Permian evaporite brines. *Geochim. Cosmochim. Acta* **63**,
770 1375–1382.

771 Eastoe, C.J., Long, A., Land, L.S., and Kyle, R. (2001) Stable chlorine isotopes in halite and brine
772 from the Gulf Coast Basin: brine genesis and evolution. *Chem. Geol.* **176**, 343-360.

773 Eastoe, C.J., Peryt, T.M., Petrychenko, O.Y., and Geisler-Cussey, D. (2007) Stable chlorine isotopes
774 in Phanerozoic evaporites. *Appl. Geochem.* **22**, 575-588.

775 Eggenkamp H.G.M. (1994) $\delta^{37}\text{Cl}$: The geochemistry of chlorine isotopes. PhD Thesis, Utrecht.

- 776 Eggenkamp H.G.M. (1995) Bromine stable isotope fractionation: Experimental determination on
777 evaporites. EUG, 8th Congress. *Terra Abs., Abs. Suppl. to Terra Nova* **7**, p. 331 (Available from
778 http://www.eggenkamp.info/personal/Eggenkamp_Poster_EUG_1995.pdf).
- 779 Eggenkamp H.G.M. (2014) The geochemistry of stable chlorine and bromine isotopes. Springer.
- 780 Eggenkamp H.G.M. (2015a) Comment on “Stable isotope fractionation of chlorine during the
781 precipitation of single chloride minerals“ by Luo, C.-g., Xiao, Y.-k., Wen, H.-j., Ma, H.-z., Ma,
782 Y.-q., Zhang, Y.-l., Zhang, Y.-x. And He, M.-y. [Applied Geochemistry 47 (2014) 141-149]. *Appl.*
783 *Geochem.* **54**, 111–116.
- 784 Eggenkamp H.G.M. (2015b) Why are variations in bromine isotope compositions in the Earth's
785 history larger than chlorine isotope compositions? *Annales UMCS, Sectio AAA* **70**, 183–194.
- 786 Eggenkamp H.G.M. and Coleman M.L. (2000) Rediscovery of classical methods and their
787 application to the measurement of stable bromine isotopes in natural samples. *Chem. Geol.* **167**,
788 393–402.
- 789 Eggenkamp H.G.M. and Louvat P. (2018) A simple distillation method to extract bromine from
790 natural water and salt samples for isotope analysis by multi collector inductively coupled plasma
791 mass spectrometry. *Rapid Comm. Mass Spectr.* **32**, 612-618.
- 792 Eggenkamp H.G.M., Kreulen R. and Koster van Groos A.F. (1995) Chlorine stable isotope
793 fractionation in evaporites. *Geochim. Cosmochim. Acta* **59**, 5169-5175.
- 794 Eggenkamp, H.G.M., Bonifacie, M., Ader, M. and Agrinier, P. (2016) Experimental determination
795 of stable chlorine and bromine isotope fractionation during precipitation of salt from a saturated
796 solution. *Chem. Geol.* **433**, 46-56.
- 797 Eggenkamp H.G.M., Louvat P., Griffioen J., Agrinier P. (2019) Chlorine and bromine isotope
798 evolution within a fully developed Upper Permian natural salt sequence. *Geochim. Cosmochim.*
799 *Acta* **245**, 316-326.
- 800 Glushanin L.V., Sharov N.V. and Shchiptsov V.V. (2011) The Onega Palaeoproterozoic Structure
801 (Geology, Tectonics, Deep Structure and Minerogeny) (in Russian). Institute of Geology,
802 Karelian Research Centre of the Russian Academy of Sciences.
- 803 Godon A., Jendrzewski N., Eggenkamp H.G.M., Banks D.A., Ade, M., Coleman M.L. and Pineau,
804 F. (2004) A cross calibration of chlorine isotopic measurements and suitability of seawater as the
805 international reference material. *Chem. Geol.* **207**, 1–12.
- 806 Gorbachev V.I., Petrov O.V., Tarkhanov G.V., Erinchek Y.M., Akhmedov A.M., Krupenik V.A.,
807 Narkisova V.V. and Sveshnikova, K.Y. (2011) Rock salts in the Paleoproterozoic of the Onega
808 Trough of the Baltic Shield. *Regional Geology and Metallogeny* **45**, 90-97 (in Russian).
- 809 Grobe M. (2000) Distribution and thickness of salt within the Devonian Elk Point group, western
810 Canada sedimentary basin. *Alberta Geol. Surv. Earth Sc. Rep.* **2000-02**.
- 811 Haines P.W. (2009) The Carribuddy Group and Worrall Formation, Canning basin, Western
812 Australia: stratigraphy, sedimentology, and petroleum potential. *Geol. Surv. West. Australia Rep.*
813 **105**, 60p.
- 814 Hay W.H., Migdisov A., Bulukhovskiy A.N., Wold C.N., Flögel S. and Söding E. (2006) Evaporites
815 and the salinity of the ocean during the Phanerozoic: implications for climate, ocean circulation
816 and life. *Palaeogeogr. Palaeoclimatol. Palaeoecol.* **240**, 3–46.
- 817 Herrmann A.G. (1972) Bromine distribution coefficients for halite precipitated from modern sea
818 water under natural conditions. *Contr. Mineral. Petrol.* **37**, 249-252.
- 819 Herrmann A.G., Knake D., Schneider J. and Peters H. (1973) Geochemistry of modern seawater and
820 brines from salt pans: main components and bromine distribution. *Contrib. Mineral. Petrol.* **40**,
821 1–24.
- 822 Holser W.T. (1966) Bromide geochemistry of salt rocks. In: Rau JL (ed.) Proceedings of the Second
823 Symposium on Salt, 248–275. Cleveland, OH: Northern Ohio Geological Society.

- 824 Horita J., Zimmermann H. and Holland H.D. (2002) The chemical evolution of seawater during the
825 Phanerozoic: Implications from the record of marine evaporites. *Geochim. Cosmochim. Acta* **66**,
826 3733–3756.
- 827 Jarrard R.D. (2003) Subduction fluxes of water, carbon dioxide, chlorine, and potassium. *Geochem.*
828 *Geophys. Geosystems* **4**. doi:10.1029/2002GC000392.
- 829 Kaufmann R.S. (1984) Chlorine in ground water: Stable isotope distribution. PhD thesis, Tucson.
- 830 Kaufmann R.S., Long A., Bentley H. and Davis S. (1984) Natural chlorine isotope variations.
831 *Nature* **309**, 338-340.
- 832 Kent P.E. (1979) The emergent Hormuz salt plugs of southern Iran. *J. Petrol. Geol.* **2**, 117–144.
- 833 Krupenik V.A. and Sveshnikova K.Y. (2011) “Correlation of the Onega Parametric Hole with the
834 reference sections of the Onega Structure,” in *The Onega Palaeoproterozoic Structure (Geology,*
835 *Tectonics, Deep Structure and Minerogeny)* (in Russian), L. V. Glushanin, N. V. Sharov, V. V.
836 Shchiptsov, Eds. (Institute of Geology, Karelian Research Centre of the Russian Academy of
837 Sciences, 2011), 190–195.
- 838 Kühn R. (1955) Über den Bromgehalt von Salzgesteinen, insbesondere die quantitative Ableitung
839 des Bromgehaltes nichtprimärer Hartsalze oder Sylvinit aus Carnallit. *Kali u. Steinsalz* **1(9)**, 3-
840 16
- 841 Liu, W.G., Xiao, Y.K., Wang, Q.Z., Qi, H.P., Wang, Y.H., Zhou, Y.M. and Shirodkar, P.V. (1997)
842 Chlorine isotopic geochemistry of salt lakes in the Qaidam Basin, China. *Chem. Geol.* **136**, 271–
843 279.
- 844 Louvat P., Bonifacie M., Giunta T., Michel A. and Coleman M. (2016) Determination of bromine
845 stable isotope ratios from saline solutions by "wet plasma" MC-ICPMS including a comparison
846 between high- and high-resolution modes, and three introduction systems. *Anal. Chem.* **88**, 3891-
847 3898.
- 848 Lowenstein T.K., Kendall B. and Anbar A.D. (2014) The geologic history of seawater. *Treat.*
849 *Geochem.* 2nd ed. 569-621.
- 850 Luo C.G., Xiao Y.K., Ma H.Z., Ma Y.Q., Zhang Y.L. and He M.Y. (2012) Stable isotope
851 fractionation of chlorine during evaporation of brine from a saline lake. *Chin. Sci. Bull.* **57**,
852 1833–1843.
- 853 Luo C.G., Xiao Y.K., Wen H.J., Ma H.H., Ma Y.Q., Zhang Y.L., Zhang Y.X. and He M.Y. (2014)
854 Stable isotope fractionation of chloride during the precipitation of single chloride minerals. *Appl.*
855 *Geochem.* **47**, 141–149.
- 856 Luo C.G., Xiao Y.K., Wen H.J., Ma H.H., Ma Y.Q., Zhang Y.L. and He M.Y. (2015) Reply to the
857 comment on the paper “Stable isotope fractionation of chlorine during the precipitation of single
858 chloride minerals”. *Appl. Geochem.* **54**, 117–118.
- 859 Maley V.C. and Huffington R.M. (1953) Cenozoic fill and evaporate [evaporite] solution in the
860 Delaware basin, Tex. And N. Mex. *Geol. Soc. Am. Bull.* **64**, 539-545.
- 861 Mattes B.W. and Conway Morris S. (1990) Carbonate/evaporite deposition in the Late Precambrian
862 - Early Cambrian Ara Formation of Southern Oman. *Geol Soc London Sp. Publ.* **49**, 617-636.
- 863 McCaffrey M.A., Lazar, B. and Holland H.D. (1987) The evaporation path of seawater and the
864 coprecipitation of Br⁻ and K⁺ with halite. *J. Sed. Petrol.* **57**, 928-937.
- 865 Morozov A.F., Khakhaev B.N., Petrov O.V., Gorbachev V.I., Tarkhanov G.V., Tsvetkov L.D.,
866 Erinchek Yu.M., Akhmedov A.M., Krupenik V.A. and Sveshnikova K.Yu. (2010) Rock Salt Mass
867 in the Paleoproterozoic Sequence of the Onega Trough in Karelia (from the Onega Parametric
868 Well Data). *Dokl. Earth Sc.* **432**, 1483-1486.
- 869 Murphy T.J., Clabaugh W.S. and Gilchrist R. (1954) Separation of iodide, bromide and chloride
870 from one another and their subsequent determination. *J. Res. Nat. Bur. Stand.* **53**, 13-18.
- 871 Naughton D.A., Quinlan T., Hopkins R.M. and Wells A.T. (1968) Evolution of salt anticlines and
872 salt domes in the Amadeus Basin, Central Australia. *Geol. Soc. Am., Spec. Pap.* **88**, 229-247.

- 873 Paris G., Gaillardet J., and Louvat P. (2010) Geological evolution of seawater boron isotope
874 composition recorded in evaporites. *Geology* **38**, 1035-1038.
- 875 Petrychenko O.Y., Peryt T.M. and Chechel E.I. (2005) Early Cambrian seawater chemistry from
876 fluid inclusions in halite from Siberian evaporites. *Chem. Geol.* **219**, 149–161.
- 877 Pierce W.G. and Rich E.I. (1962) Summary of rock salt deposits in the United States as possible
878 Storage sites for radioactive waste materials. *USGS Bulletin* **1148**, 91pp.
- 879 Schröder S, Grotzinger JP, Amthor JE and Matter A (2005) Carbonate deposition and hydrocarbon
880 reservoir development at the Precambrian- Cambrian boundary: the Ara Group in South Oman.
881 *Sedim. Geol.* **180**, 1–28.
- 882 Sharp Z. D., Barnes J. D., Brearley A. J., Fischer T. P., Chaussidon M. and Kamenetsky V. S. (2007)
883 Chlorine isotope homogeneity of the mantle, crust and carbonaceous chondrites. *Nature* **446**,
884 1062–1065.
- 885 Sharp Z.D., Mercer J.A., Jones R.H., Brearley A.J., Selverstone J., Bekker A. and Stachel T. (2013)
886 The chlorine isotope composition of chondrites and Earth. *Geochim. Cosmochim. Acta* **107**, 189-
887 204.
- 888 Shouakar-Stash O., Alexeev S.V., Frapce S.K., Alexeeva L.P., and Drimmie R. J. (2007)
889 Geochemistry and stable isotope signatures, including chlorine and bromine isotopes, of the deep
890 groundwaters of the Siberian Platform. *Appl. Geochem.* **22**, 589–605.
- 891 Siemann M.G. (2003) Extensive and rapid changes in seawater chemistry during the Phanerozoic:
892 evidence from Br contents in basal halite. *Terra Nova* **15**, 243-248.
- 893 Siemann M.G. and Schramm M. (2000) Thermodynamic modelling of the Br partition between
894 aqueous solutions and halite. *Geochim. Cosmochim. Acta* **64**, 1681-1693.
- 895 Stein M., Starinsky A., Agnon A., Katz A., Raab M., Spiro B. and Zak I. (2000) The impact of
896 brine-rock interaction during marine evaporite formation on the isotopic Sr record in the oceans:
897 Evidence from Mt. Sedom, Israel. *Geochim. Cosmochim. Acta* **64**, 2039-2053.
- 898 Stewart A.J. (1979) A barred-basin marine evaporite in Upper Proterozoic of the Amadeus Basin,
899 Central Australia. *Sedimentology* **26**, 33-62.
- 900 Tan, H.B., Ma, H.Z., Xiao, Y.K., Wei, H.Z., Zhang, X.Y. and Ma, W.D. (2005) Characteristics of
901 chlorine isotope distribution and analysis on sylvinite deposit formation based on ancient salt
902 rock in western Tarim basin. *Sci. China, Ser. D Earth Sci.* **48**, 1913–1920.
- 903 Tan H.B., Ma H.Z., Wei H.Z., Xu J.X. and Li T.W. (2006) Chlorine, sulfur and oxygen isotopic
904 constraints on ancient evaporite deposit in the Western Tarim Basin, China. *Geochem. J.* **40**,
905 569–577.
- 906 Tan H.B., Ma H.Z., Zhang X.Y., Xu J.X. and Xiao Y.K. (2009) Fractionation of chlorine isotope in
907 salt mineral sequences and application: research on sedimentary stage of ancient salt rock deposit
908 in Tarim Basin and western Qaidam Basin. *Acta Petrol. Sin.* **25**, 955–962 (in Chinese with
909 English abstract).
- 910 Valyashko M.G. (1956) Geochemistry of bromine in the processes of salt deposition and the use of
911 the bromine content as a genetic and prospecting criterion. *Geochemistry (Geokhimiya)* **1956**,
912 570-589.
- 913 Weinberger R., Agnon A., and Ron H. (1997) Paleomagnetic reconstruction of the structure of Mt.
914 Sedom, Dead Sea rift. *J. Geophys. Res.* **102(B3)**, 5173–5192.
- 915 Xiao, Y.K., Liu, W.G. and Zhang, C.G. (1994) The preliminary investigation on chlorine isotopic
916 fractionation during the crystallization of saline minerals in salt lake. *Salt Lake Sci.* **2**, 35–40 (in
917 Chinese with English abstract).
- 918 Xiao, Y.K., Liu, W.G. and Zhou, Y.M. (1997) Isotopic compositions of chlorine in brine and saline
919 minerals. *Chin. Sci. Bull.* **42**, 406–409.
- 920 Xiao, Y.K., Liu, W.G., Zhou, Y.M., Wang, Y.H. and Shirodkar, P.V. (2000) Variations in isotopic
921 compositions of chlorine in evaporation controlled salt lake brines of Qaidam Basin, China.
922 *Chin. J. Oceanol. Limnol.* **18**, 169–177.

923 Zak I. (1997) Evolution of the Dead Sea brines. In *The Dead Sea, the lake and its settings* (ed. T. M.
924 Niemi, Z. Ben Avraham and J. R. Gat), **36**, 133–144. Oxford Monogr. on Geology and
925 Geophysics.
926

Table 1

Sample	Stage	Age (Ma)	$\delta^{37}\text{Cl}$ (‰)	$\delta^{81}\text{Br}$ (‰)	Na^+ (g/kg)	K^+ (g/kg)	Mg^{2+} (g/kg)	Ca^{2+} (g/kg)	Cl^- (g/kg)	Br^- (g/kg)	SO_4^{2-} (g/kg)	Br/Cl (g/g)
EVA06	Recent	0	+0.37±0.01	-0.24±0.12	401	3.0	8.5	0.9	520	0.47	13.9	0.00091
EVA10	Recent	0	+0.33±0.04	+0.05±0.13	392	1.5	3.9	1.2	605	0.33	7.8	0.00054
EVA27	Recent	0	+0.31±0.02	+0.21±0.03	375	1.7	7.1	1.7	623	0.44	16.0	0.00071
M1	Recent	0	+0.21±0.01	+0.16±0.05	414	0.2	0.1	0.5	636	0.12	1.6	0.00019
M2	Recent	0	+0.26±0.01	+0.18±0.09	429	0.1	0.0	0.4	657	0.12	1.2	0.00018
M3	Recent	0	-0.07±0.01	-0.02±0.09	390	0.2	0.6	1.5	601	0.09	5.3	0.00016
M4	Recent	0	+0.18±0.03	+0.71±0.08	404	0.7	1.8	1.2	625	0.22	6.1	0.00035
M5	Recent	0	+0.51±0.02	+0.51±0.11	326	0.9	3.4	2.3	508	0.25	11.4	0.00050
M6	Recent	0	+0.25±0.01	-0.02±0.07	379	0.1	0.9	0.5	586	0.20	1.8	0.00034
M7	Recent	0	+0.42±0.01	+0.19±0.08	376	1.6	6.8	4.2	593	0.42	20.7	0.00071
H1	Pliocene/Pleistocene	2.6	-0.07±0.01	+0.19±0.06	388	0.7	0.5	1.5	598	0.23	5.2	0.00038
EVA02	Messinian	6.3	+0.07±0.04	+0.05±0.02	397	0.1	0.2	0.1	625	0.07	0.7	0.00012
EVA09	Messinian	6.3	+0.07±0.02	+0.24±0.16	400	0.2	0.2	0.2	618	0.07	0.6	0.00011
EVA12	Messinian	6.3	+0.06±0.04	n.d.	402	0.1	0.1	0.3	608	0.07	1.2	0.00011
EVA15	Messinian	6.3	-0.05±0.05	+0.17±0.11	388	0.7	1.7	4.4	610	0.18	12.5	0.00029
EVA23	Messinian	6.3	+0.03±0.01	+0.21±0.04	402	0.2	0.6	1.7	595	0.13	4.9	0.00022
EVA24	Messinian	6.3	-0.24±0.06	0.00±0.07	399	0.2	0.0	0.2	621	0.20	0.8	0.00032
IR1	Messinian	6.3	-0.53±0.01	-0.11±0.14	200	261	0.0	0.7	538	0.84	2.2	0.00156
IR2	Messinian	6.3	+0.22±0.04	+0.24±0.09	400	0.1	0.0	2.4	607	0.04	6.2	0.00007
IR3	Messinian	6.3	+0.25±0.01	+0.32±0.09	401	0.1	0.0	1.3	610	0.03	3.5	0.00006
EVA05	Badenian/Serrevallian	12.7	+0.33±0.02	+0.32±0.08	366	0.3	0.1	0.3	615	0.04	2.0	0.00006
EVA07	Badenian/Serrevallian	12.7	+0.28±0.09	+1.08±0.13	395	0.1	0.1	0.2	630	0.03	0.8	0.00005
EVA08	Eocene/Oligocene	12.7	-0.20±0.10	+1.00±0.08	415	0.3	0.2	1.2	542	0.15	2.8	0.00028
EVA14	Eocene/Oligocene	33.9	-0.20±0.01	+0.91±0.18	392	0.4	0.4	1.4	628	0.26	3.1	0.00041
EVA18	Eocene/Oligocene	33.9	-0.15±0.01	+0.83±0.13	389	1.2	0.1	0.2	640	0.18	0.2	0.00028
EVA16	Priabonian	35.9	-0.03±0.03	+0.51±0.20	320	23.6	8.3	23.6	478	0.11	116	0.00024
EVA20	Priabonian	35.9	-0.05±0.04	+0.27±0.14	388	2.1	0.6	1.9	620	0.13	9.7	0.00021
EVA21	Priabonian	35.9	-0.12	+0.25±0.10	377	3.2	1.1	2.9	625	0.20	14.7	0.00031
H2	Carnian/Norian	227	+0.06±0.01	-0.16±0.15	394	0.0	0.1	2.4	607	0.10	6.3	0.00017
NL02	Anisian	245	+0.30±0.02	+0.28±0.11	403	0.0	0.0	0.3	618	0.04	1.0	0.00007
NL03	Anisian	245	+0.02±0.02	+0.11±0.05	408	0.1	0.1	0.0	624	0.18	0.1	0.00029
NL04	Anisian	245	+0.07±0.01	+0.31±0.05	392	0.0	0.0	0.0	603	0.19	0.0	0.00031
NL05	Anisian	245	+0.05±0.02	+0.07±0.04	399	1.2	1.4	1.0	611	0.21	9.5	0.00034
NL06	Anisian	245	+0.03±0.01	+0.38±0.04	408	0.3	0.1	0.1	622	0.32	0.7	0.00051
NL07	Anisian	245	+0.19	+0.06±0.03	407	0.3	0.1	4.5	621	0.07	11.9	0.00011
NL08	Anisian	245	+0.24±0.08	+0.51±0.11	412	0.0	0.0	0.4	628	0.03	1.0	0.00005
H3	Changhsingian	253	+0.25	+0.42±0.06	392	0.1	0.1	2.7	603	0.05	7.0	0.00008
EVA03	Wuchiapingian	257	-0.06±0.01	+0.02±0.05	393	1.9	1.2	2.2	605	0.29	10.3	0.00049
NL09	Wuchiapingian	257	-0.12±0.07	+0.27±0.07	391	1.4	2.5	0.8	601	0.21	10.5	0.00035
NL10	Wuchiapingian	257	-0.06±0.03	-0.10±0.05	393	1.2	0.7	0.1	603	0.32	0.4	0.00054
NL11	Wuchiapingian	257	+0.04±0.04	+0.26±0.05	394	2.5	4.1	1.5	609	0.22	12.5	0.00036
NL12	Wuchiapingian	257	+0.05±0.02	+0.23±0.10	397	5.1	4.8	0.4	618	0.24	8.3	0.00038
NL13	Wuchiapingian	257	-0.02±0.01	+0.16±0.05	361	0.2	14.3	0.4	561	0.14	54.1	0.00025
NL14	Wuchiapingian	257	-0.04±0.02	+0.11±0.11	324	0.2	18.8	1.2	517	0.20	107	0.00039
H4	Givetian	385	+0.23±0.01	+0.20±0.16	400	0.1	0.1	0.1	617	0.05	0.5	0.00008
EVA01	Givetian	385	+0.13±0.05	+0.97±0.16	411	0.2	0.1	3.0	543	0.05	7.3	0.00009
EVA04	Givetian	385	+0.14±0.01	+0.41±0.12	394	0.1	0.1	2.4	619	0.07	5.8	0.00011
H5a	Ordovician/Silurian	444	-0.06±0.02	-0.05±0.12	401	0.2	0.0	0.3	618	0.18	0.8	0.00028
H5b	Ordovician/Silurian	444	-0.04±0.04	-0.04±0.09	402	0.2	0.1	4.2	620	0.20	10.1	0.00032
H6	Terreneuvian	531	+0.03±0.03	-0.17±0.10	390	0.2	0.0	2.0	600	0.21	5.2	0.00034

H7	Ediacaran	545	-0.17±0.05	+0.06±0.08	389	2.4	0.9	1.8	600	0.14	10.1	0.00024
IR4	Ediacaran	545	+0.03±0.01	+0.52±0.10	400	0.2	0.0	2.0	608	0.08	5.2	0.00013
IR5	Ediacaran	545	+0.10±0.03	+0.24±0.15	402	0.3	0.0	0.9	611	0.07	2.4	0.00012
IR6	Ediacaran	545	+0.19±0.02	+0.17±0.08	401	0.2	0.0	1.2	610	0.07	3.1	0.00011
AU1	Tonian	820	-0.09±0.01	-0.03±0.05	363	0.3	0.2	3.6	558	0.18	9.0	0.00032
AU2	Tonian	820	-0.02±0.01	-0.02±0.13	385	0.3	0.1	1.6	594	0.17	4.0	0.00028
AU3	Tonian	820	-0.02±0.01	0.00±0.10	398	0.2	0.0	3.2	611	0.14	8.0	0.00023
AU4	Tonian	820	+0.01	-0.18±0.09	370	0.2	0.2	5.6	571	0.11	13.4	0.00019
AU5	Tonian	820	+0.01±0.01	0.00±0.01	377	0.2	0.2	3.4	581	0.12	8.4	0.00021
AU6	Tonian	820	+0.05±0.01	+0.69±0.04	336	0.1	0.2	37.2	517	0.10	92.5	0.00020
A02	Orosirian	2000	-0.10±0.03	n.d.	296	0.3	33.6	5.7	459	0.01	148	0.00003
A03	Orosirian	2000	-0.12±0.03	n.d.	375	1.1	6.8	0.6	579	0.02	30.6	0.00004
A04	Orosirian	2000	-0.15±0.05	n.d.	343	0.5	4.3	30.9	530	<0.01	91.2	<0.00001
A05	Orosirian	2000	-0.13±0.01	n.d.	296	2.2	35.2	20.8	460	0.02	186	0.00004
A06	Orosirian	2000	-0.10±0.02	n.d.	379	0.1	3.6	4.6	577	<0.01	35.4	<0.00001
A07	Orosirian	2000	-0.13±0.01	n.d.	380	0.3	2.7	6.8	592	0.01	19.0	0.00001
A08	Orosirian	2000	-0.10±0.03	n.d.	386	0.2	2.6	0.9	590	0.01	20.5	0.00001
A09	Orosirian	2000	-0.09±0.04	n.d.	294	2.2	4.1	52.8	322	<0.01	324	<0.00001
A09a	Orosirian	2000	-0.13±0.01	n.d.	378	3.0	0.0	9.0	582	<0.01	27.4	<0.00001
A10	Orosirian	2000	-0.07±0.03	n.d.	300	1.2	3.7	63.0	452	0.02	178	0.00003
A10a	Orosirian	2000	-0.11±0.01	n.d.	357	0.3	2.6	17.1	495	<0.01	128	<0.00001
A11	Orosirian	2000	-0.08±0.03	n.d.	353	0.2	9.8	13.6	523	<0.01	101	<0.00001
A12	Orosirian	2000	-0.08±0.01	n.d.	363	0.8	7.1	14.7	587	<0.01	27.9	<0.00001
A13	Orosirian	2000	-0.09±0.01	+0.69±0.06	353	8.1	6.6	2.6	545	0.02	42.5	0.00003
A14	Orosirian	2000	-0.07±0.07	n.d.	391	0.3	1.1	0.1	603	0.01	4.2	0.00002
A15	Orosirian	2000	-0.07±0.06	n.d.	240	54.4	30.0	33.3	348	<0.01	295	<0.00001
A15a	Orosirian	2000	-0.11±0.01	n.d.	325	25.7	8.0	21.5	490	<0.01	130	<0.00001
A16	Orosirian	2000	-0.09±0.02	+0.46±0.12	308	0.5	8.1	33.8	462	0.02	132	0.00004
A17	Orosirian	2000	-0.04±0.01	n.d.	302	1.2	1.5	72.4	537	<0.01	85.8	<0.00001
A17a	Orosirian	2000	-0.11±0.02	n.d.	333	0.2	2.8	46.8	568	<0.01	49.6	<0.00001
A18	Orosirian	2000	-0.07±0.02	n.d.	392	0.1	0.4	0.1	605	<0.01	2.0	<0.00001
A20	Orosirian	2000	-0.12±0.01	n.d.	381	0.1	0.3	8.2	583	<0.01	26.9	<0.00001
A21	Orosirian	2000	-0.09±0.03	n.d.	295	10.2	19.0	36.7	429	<0.01	210	<0.00001

Table 1: Chemical and isotopic composition of the salt samples studied in this research. n.d. means not determined (sample too small). The error in the isotope measurements is the 1 σ standard deviation of two measurements for Cl or the 2 σ standard deviation of five standard bracketing determinations for Br. When no error value is noted only a single measurement was possible.

		$\alpha=1.00026$		$\alpha=1.00035$		$\alpha=1.00049$		midpoint
		min	max	min	max	min	max	
Period	Age (Ma)							
Recent	0	<i>0.25</i>	<i>0.12</i>	0.16	0.19	0.02	0.29	0.19
Neogene	7	<i>0.07</i>	<i>-0.05</i>	-0.02	0.02	-0.16	0.12	0.07
Paleogene	35	-0.29	-0.01	-0.38	0.06	-0.52	0.16	-0.15
Triassic	243	0.04	0.21	-0.05	0.28	-0.19	0.38	0.13
Permian	256	-0.01	0.07	-0.10	0.14	-0.24	0.24	0.03
Ordov./Dev.	409	-0.03	0.13	-0.12	0.20	-0.26	0.30	0.05
Edia./Cambr.	542	-0.07	0.02	-0.16	0.09	-0.30	0.19	-0.03
Tonian	850	-0.21	0.10	-0.30	0.17	-0.44	0.27	-0.05
Orosirian	2000	-0.30	0.04	-0.39	0.11	-0.53	0.21	-0.13

Table 2: Minimum, maximum and midpoint values for the possible $\delta^{37}\text{Cl}$ values of the oceans in the past, without taking into account the Br/Cl ratios of the salt that precipitates from it. The possible values are determined for the three different fractionation factors discussed in the text. The table clearly shows that for the Recent and the Neogene it is not possible to reconstruct a possible $\delta^{37}\text{Cl}$ value as the minimum possible value is larger than the maximum possible value.

Table 2 revised with changes highlighted

		$\alpha=1.00026$		$\alpha=1.00035$		$\alpha=1.00049$		midpoint
		min	max	min	max	min	max	
Period	Age (Ma)							
Recent	0	0.25	0.12	0.16	0.19	0.02	0.29	0.19
Neocene Neogene	7	0.07	-0.05	-0.02	0.02	-0.16	0.12	0.07
Paleocene Paleogene	35	-0.29	-0.01	-0.38	0.06	-0.52	0.16	-0.15
Triassic	243	0.04	0.21	-0.05	0.28	-0.19	0.38	0.13
Permian	256	-0.01	0.07	-0.10	0.14	-0.24	0.24	0.03
Ordov./Dev.	409	-0.03	0.13	-0.12	0.20	-0.26	0.30	0.05
Edia./Cambr.	542	-0.07	0.02	-0.16	0.09	-0.30	0.19	-0.03
Tonian	850	-0.21	0.10	-0.30	0.17	-0.44	0.27	-0.05
Orosirian	2000	-0.30	0.04	-0.39	0.11	-0.53	0.21	-0.13

Table 2: Minimum, maximum and midpoint values for the possible $\delta^{37}\text{Cl}$ values of the oceans in the past, without taking into account the Br/Cl ratios of the salt that precipitates from it. The possible values are determined for the three different fractionation factors discussed in the text. The table clearly shows that for the Recent and the Neogene it is not possible to reconstruct a possible $\delta^{37}\text{Cl}$ value as the minimum possible value is larger than the maximum possible value.

Table 3

		Average	Range		Range	
			Student's t-test		95% probability	
		@ Br/Cl=0.00005	min	max	min	max
Period	Age (Ma)					
Neocene	7	0.26	0.13	0.39	0.10	0.42
Paleocene	35	0.25	0.05	0.45	0.04	0.47
Triassic	243	0.26	0.13	0.39	0.10	0.42
Permian	256	0.19	0.05	0.34	0.04	0.34
Ordov./Dev.	409	0.31	0.26	0.37	0.23	0.40
Edia./Cambr.	542	0.22	0.08	0.36	0.01	0.43
Tonian	850	0.40	0.30	0.50	0.29	0.50

Table 3: Average and possible range of $\delta^{37}\text{Cl}$ values of the oceans in the past when Br/Cl ratios are taken into account assuming that during the whole geological history the first precipitating halite has a Br/Cl ratio of 0.00005.

Figure 1
[Click here to download high resolution image](#)

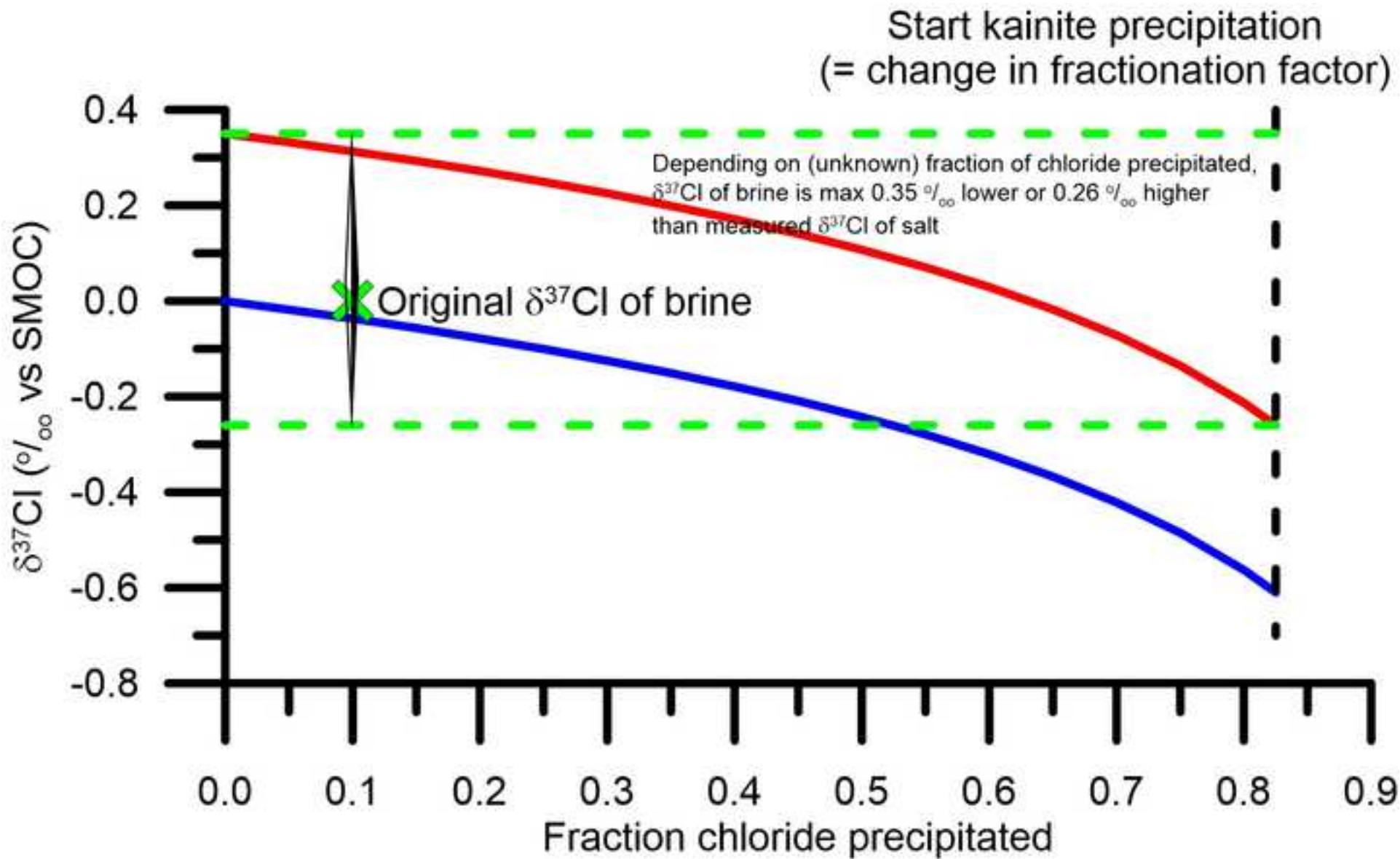


Figure 2
[Click here to download high resolution image](#)

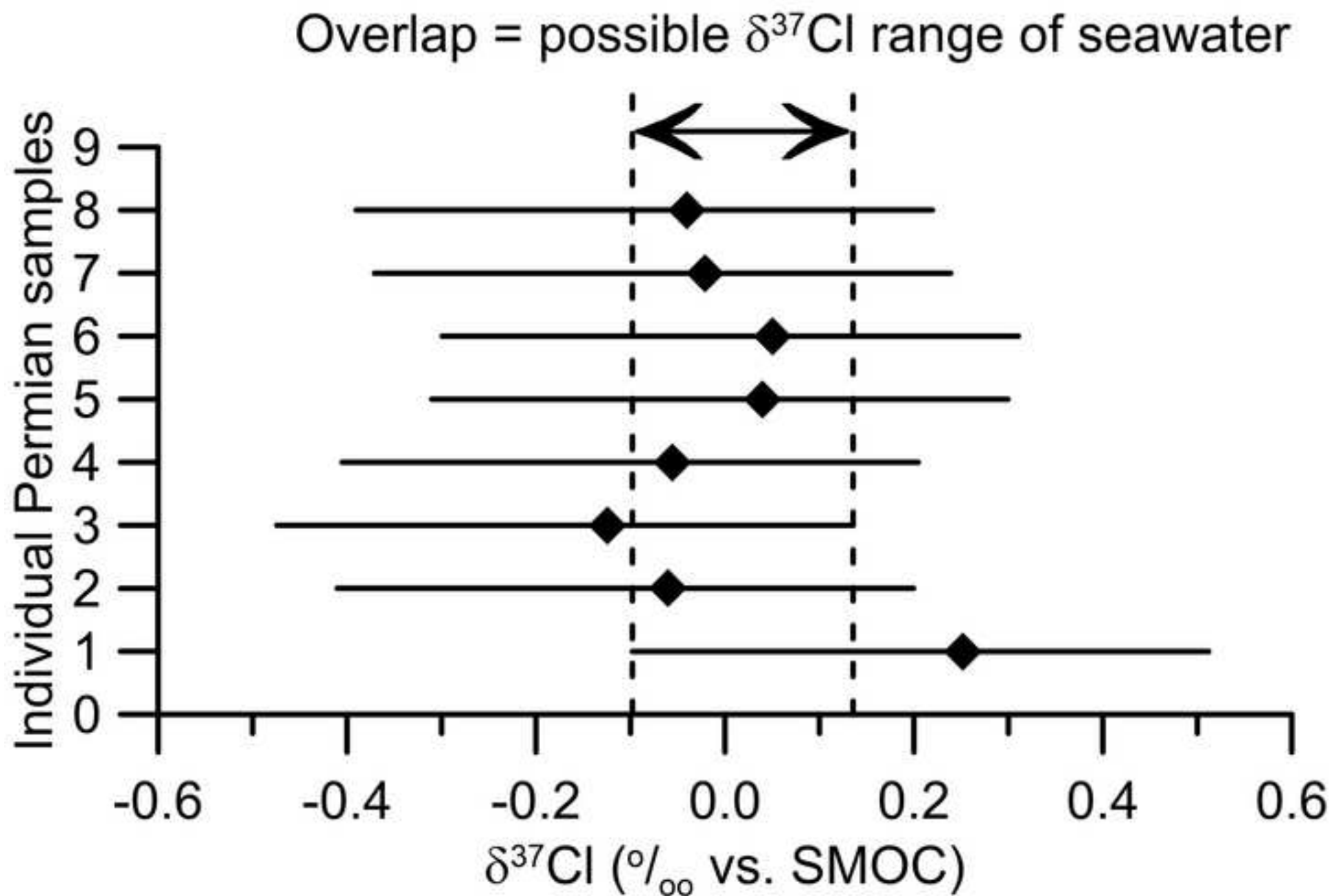


Figure 3
[Click here to download high resolution image](#)

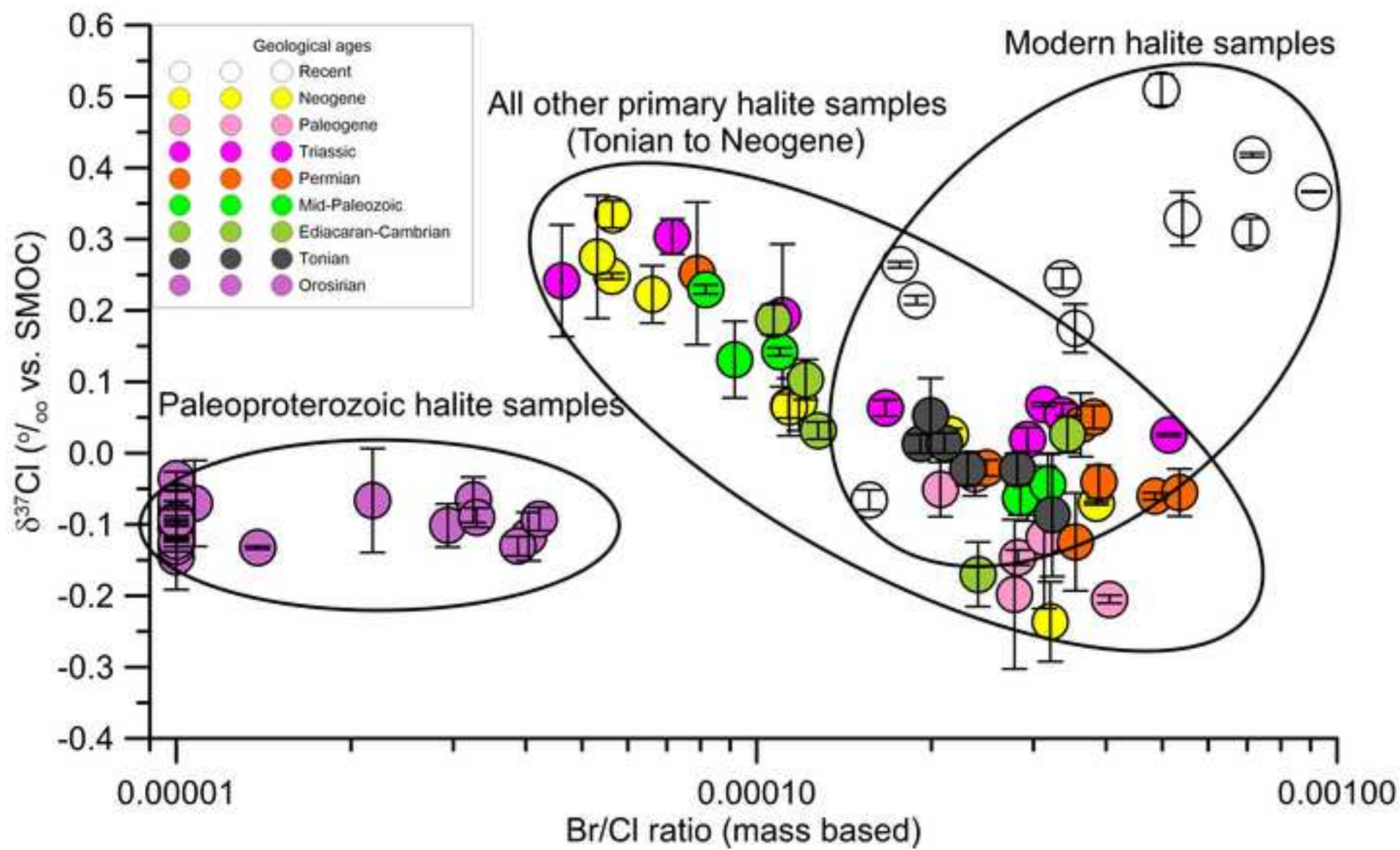


Figure 4
[Click here to download high resolution image](#)

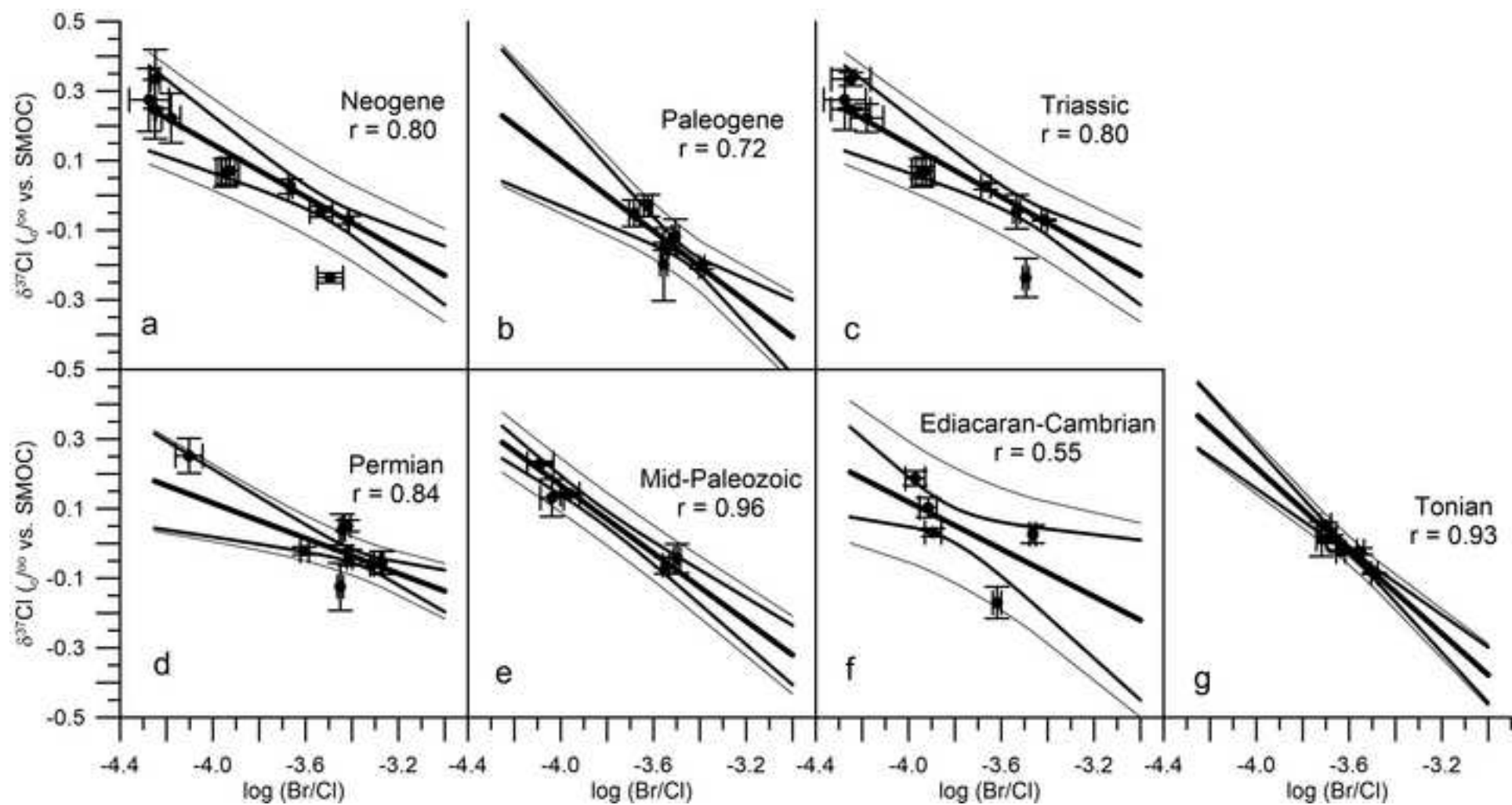


Figure 5
[Click here to download high resolution image](#)

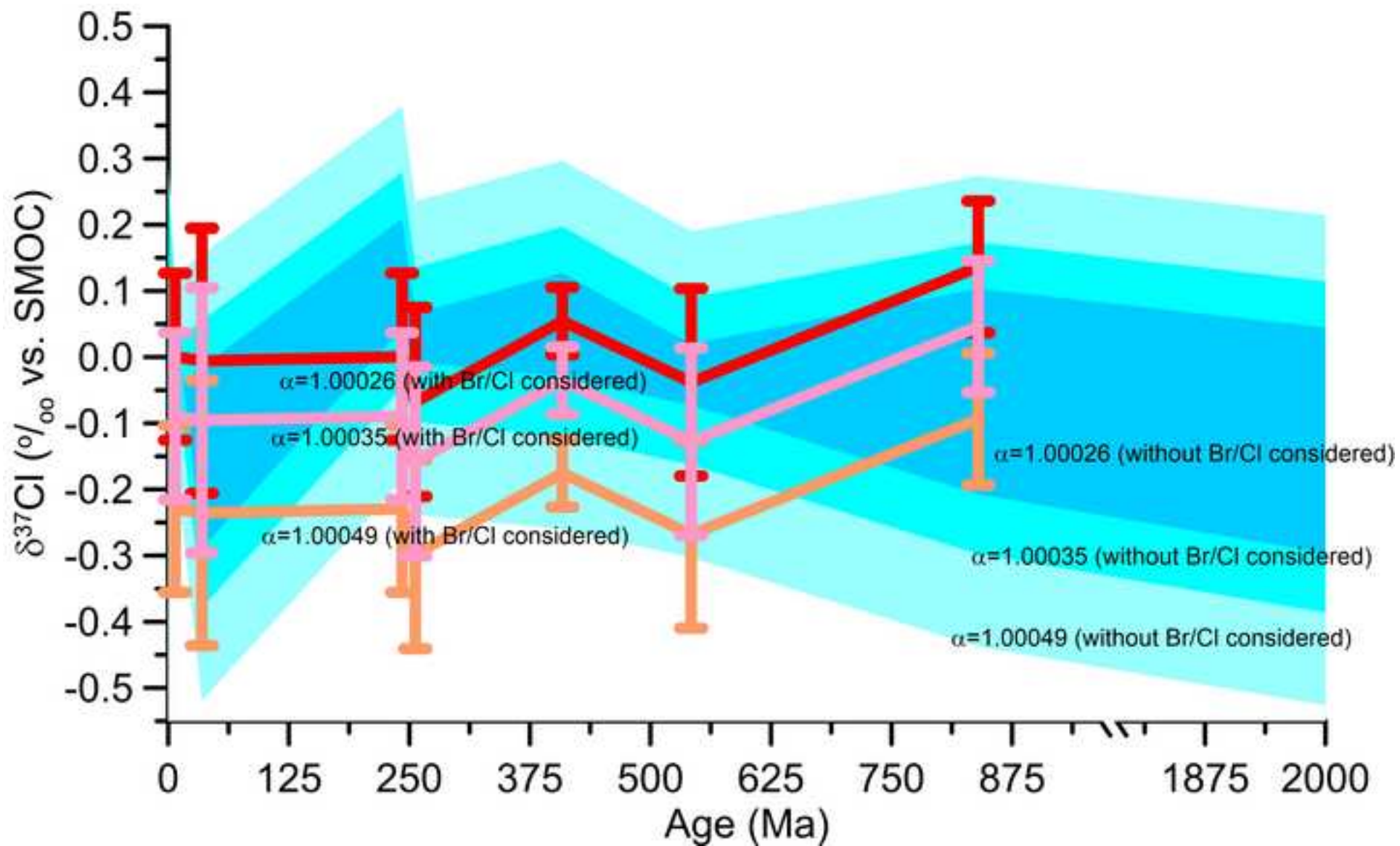


Figure 7
[Click here to download high resolution image](#)

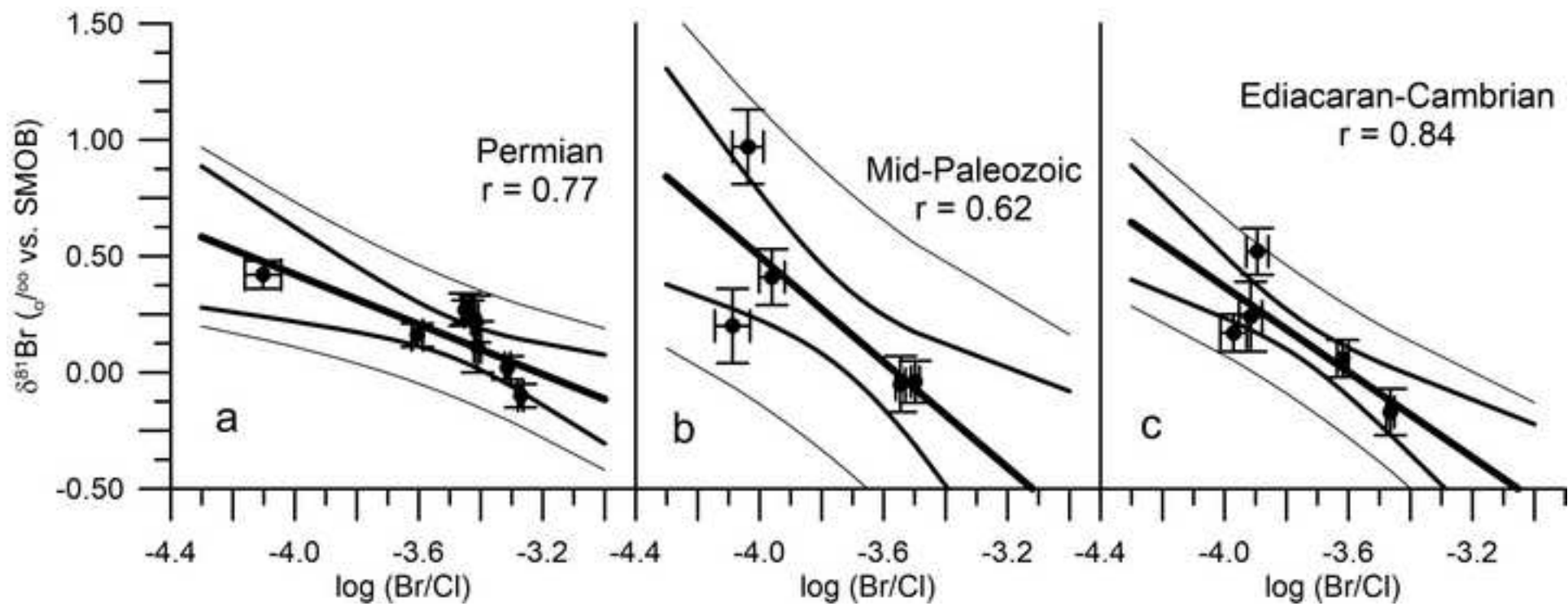


Figure 8
[Click here to download high resolution image](#)

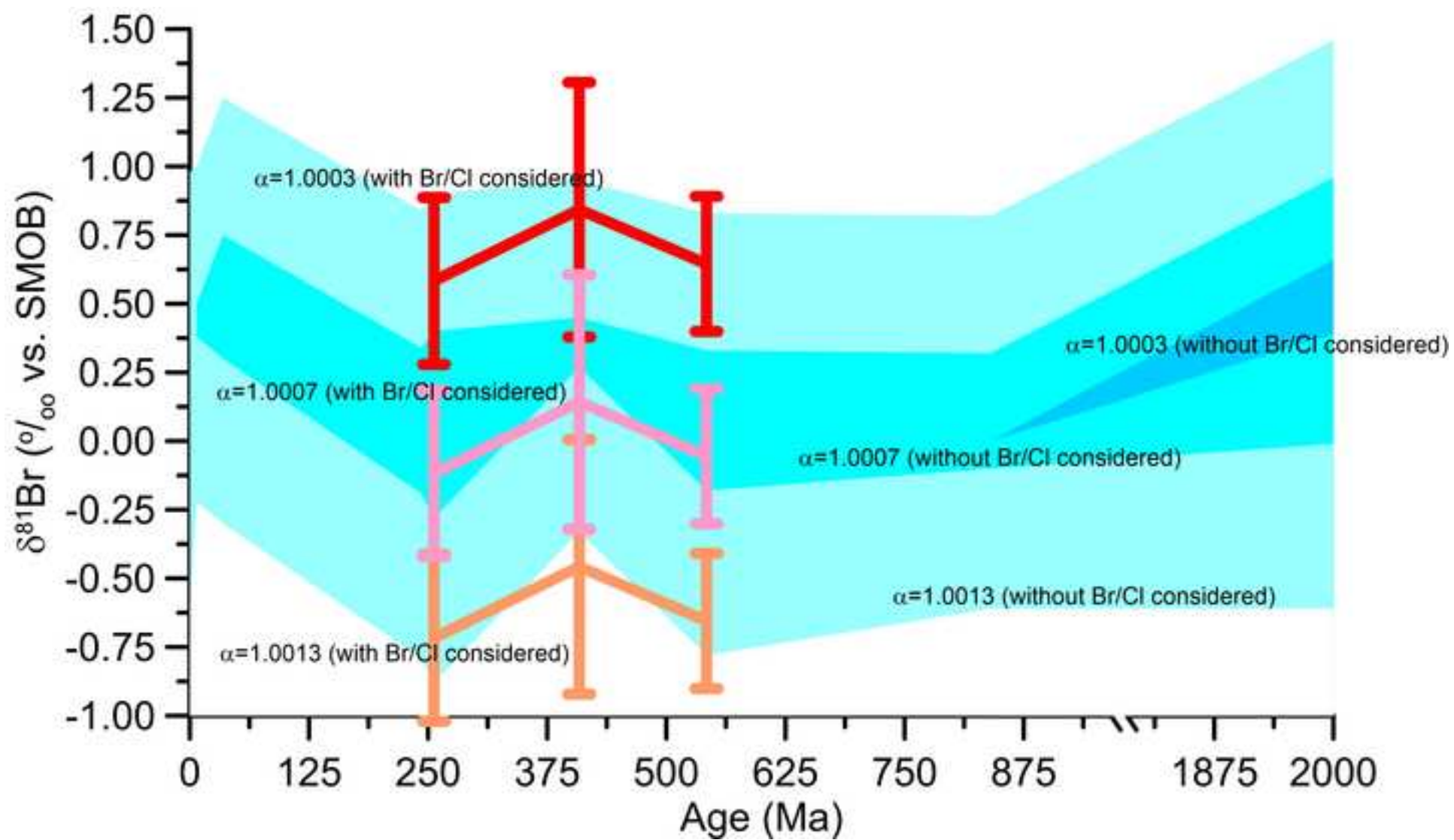


Figure captions

Figure 1: Estimate for the range of possible seawater $\delta^{37}\text{Cl}$ values based on the $\delta^{37}\text{Cl}$ value for halite samples. The blue (lower solid) line indicates the evolution of the brine, the red (upper solid) line that of the precipitate (which is always 0.35‰ higher). Figure shows how the $\delta^{37}\text{Cl}$ of a salt is related to the original $\delta^{37}\text{Cl}$ of the brine. In this case, the original $\delta^{37}\text{Cl}$ of the brine is 0‰, and the salt that precipitates from it is between the upper and the lower green lines, or between +0.35‰ and -0.38‰. An indication for the original brine $\delta^{37}\text{Cl}$ of 0‰ is plotted slightly to the right for visibility. As soon as salt starts to precipitate the $\delta^{37}\text{Cl}$ of the remaining brine starts to decrease. Inverted, it means that if the $\delta^{37}\text{Cl}$ of the salt is known the $\delta^{37}\text{Cl}$ of the original brine must be between 0.38‰ higher and 0.35‰ lower, which is indicated by the green dashed lines.

Figure 2: Possible $\delta^{37}\text{Cl}$ range for Permian seawater based on the maximum and minimum possible $\delta^{37}\text{Cl}$ values for the individual samples. The dashed lines indicate the possible $\delta^{37}\text{Cl}$ range the Permian seawater could have based on the measured $\delta^{37}\text{Cl}$ of the 8 Permian samples (diamonds) and the possible $\delta^{37}\text{Cl}$ range based on each of these 8 samples (horizontal lines). The possible $\delta^{37}\text{Cl}$ range of Permian seawater cannot be larger than the overlap of these horizontal lines.

Figure 3: Plot showing the $\delta^{37}\text{Cl}$ versus the Br/Cl ratio of the individual halite samples. The vertical error bars are the errors as defined in Table 1. Colours indicate samples from different geologic ages.

Figure 4: Correlations between $\delta^{37}\text{Cl}$ and $\log(\text{Br}/\text{Cl})$ for each geological period (except the Recent and the Orosirian samples). All figures are extrapolated to a lowest Br/Cl value of 0.00005 (= -4.3 in log units). The figures indicate that the $\delta^{37}\text{Cl}$ of the first precipitated salt is close to +0.35‰ indicating (within errors) only little possible $\delta^{37}\text{Cl}$ variation during Earth's history.

Figure 5: Possible $\delta^{37}\text{Cl}$ variations in the Earth's history for the different scenarios described in this paper. Blue areas define (from lighter to darker) the possible $\delta^{37}\text{Cl}$ ranges for higher to lower fractionation factors; the lines indicate the calculated $\delta^{37}\text{Cl}$ of the ocean depending on the isotope fractionation and the Br/Cl ratio of the samples. Although differences between the various scenarios are visible, it is obvious that the most logical scenario is defined by a Cl isotope fractionation factor of 1.00035, as the overlap between the scenarios with and without the Br/Cl ratio taking into account is best at this fractionation factor (overlap middle blue field with pink line).

Figure 6: Plot showing the $\delta^{81}\text{Br}$ versus the Br/Cl ratio of the individual halite samples. The vertical error bars are the errors as defined in Table 1. It is visible that the relationship between $\delta^{81}\text{Br}$ and Br/Cl is not as clear as between $\delta^{37}\text{Cl}$ and Br/Cl. Striking is the line showing that the lowest possible $\delta^{81}\text{Br}$ value for each given Br/Cl ratio increases with decreasing Br/Cl ratio.

Figure 7: Correlations between $\delta^{81}\text{Br}$ and Br/Cl ratios for the geological periods with high correlation coefficients between $\delta^{81}\text{Br}$ and Br/Cl ratio (Permian, Mid-Palaeozoic and Ediacaran-Cambrian). These relationships point to a negative ($\delta^{81}\text{Br}$ -Br/Cl) relationship with a $\delta^{81}\text{Br}$ value of approximately +0.7‰ at the lowest Br/Cl value of 0.00005 (= -4.3 in log units).

Figure 8: Possible $\delta^{81}\text{Br}$ variations in the Earth's history for the different scenarios described in this paper. Blue areas define (from darker to lighter) the possible $\delta^{81}\text{Br}$ ranges for lower to higher fractionation factors, the lines indicate the calculated $\delta^{81}\text{Br}$ values of seawater depending on the isotope fractionation and the Br/Cl ratio of the samples. Although differences between the various scenarios are visible, it is clear that the most reasonable scenario is defined by a Br isotope fractionation factor of 1.0007, as the overlap between the scenarios with and without the Br/Cl ratio taking into account is best at this fractionation factor (overlap middle blue field with pink line).

Figure captions

Figure 1: Estimate for the range of possible seawater $\delta^{37}\text{Cl}$ values based on the $\delta^{37}\text{Cl}$ value for halite samples. The blue (lower solid) line indicates the evolution of the brine, the red (upper solid) line that of the precipitate (which is always 0.35‰ higher). Figure shows how the $\delta^{37}\text{Cl}$ of a salt is related to the original $\delta^{37}\text{Cl}$ of the brine. In this case, the original $\delta^{37}\text{Cl}$ of the brine is 0‰, and the salt that precipitates from it is between the upper and the lower green lines, or between +0.35‰ and -0.38‰. An indication for the original brine $\delta^{37}\text{Cl}$ of 0‰ is plotted slightly to the right for visibility. As soon as salt starts to precipitate the $\delta^{37}\text{Cl}$ of the remaining brine starts to decrease. Reversed/Inverted, it means that if the $\delta^{37}\text{Cl}$ of the salt is known the $\delta^{37}\text{Cl}$ of the original brine must be between 0.38‰ higher and 0.35‰ lower, which is indicated by the green dashed lines.

Figure 2: Possible $\delta^{37}\text{Cl}$ range for Permian seawater based on the maximum and minimum possible $\delta^{37}\text{Cl}$ values for the individual samples. The dashed lines indicate the possible $\delta^{37}\text{Cl}$ range the Permian seawater could have based on the measured $\delta^{37}\text{Cl}$ of the 8 Permian samples (diamonds) and the possible $\delta^{37}\text{Cl}$ range based on each of these 8 samples (horizontal lines). The possible $\delta^{37}\text{Cl}$ range of Permian seawater cannot be larger than the overlap of these horizontal lines.

Figure 3: Plot showing the $\delta^{37}\text{Cl}$ versus the Br/Cl ratio of the individual halite samples. The vertical error bars are the errors as defined in Table 1. Colours indicate samples from different geologic ages.

Figure 4: Correlations between $\delta^{37}\text{Cl}$ and $\log(\text{Br}/\text{Cl})$ for each geological period (except the Recent and the Orosirian samples). All figures are extrapolated to a lowest Br/Cl value of 0.00005 (= -4.3 in log units). The figures indicate that the $\delta^{37}\text{Cl}$ of the first precipitated salt is close to +0.35‰ indicating (within errors) only little possible $\delta^{37}\text{Cl}$ variation during Earth's history.

Figure 5: Possible $\delta^{37}\text{Cl}$ variations in the Earth's history for the different scenarios described in this paper. Blue areas define (from lighter to darker) the possible $\delta^{37}\text{Cl}$ ranges for higher to lower fractionation factors; the lines indicate the calculated $\delta^{37}\text{Cl}$ of the ocean depending on the isotope fractionation and the Br/Cl ratio of the samples. Although differences between the various scenarios are visible, it is obvious that the most logical scenario is defined by a Cl isotope fractionation factor of 1.00035, as the overlap between the scenarios with and without the Br/Cl ratio taking into account is best at this fractionation factor (overlap middle blue field with pink line).

Figure 6: Plot showing the $\delta^{81}\text{Br}$ versus the Br/Cl ratio of the individual halite samples. The vertical error bars are the errors as defined in Table 1. It is visible that the relationship between $\delta^{81}\text{Br}$ and Br/Cl is not as clear as between $\delta^{37}\text{Cl}$ and Br/Cl. Striking is the line showing that the lowest possible $\delta^{81}\text{Br}$ value for each given Br/Cl ratio increases with decreasing Br/Cl ratio.

Figure 7: Correlations between $\delta^{81}\text{Br}$ and Br/Cl ratios for the geological periods with high correlation coefficients between $\delta^{81}\text{Br}$ and Br/Cl ratio (Permian, Mid-Palaeozoic and Ediacaran-Cambrian). These relationships point to a negative ($\delta^{81}\text{Br}$ -Br/Cl) relationship with a $\delta^{81}\text{Br}$ value of approximately +0.7‰ at the lowest Br/Cl value of 0.00005 (= -4.3 in log units).

Figure 8: Possible $\delta^{81}\text{Br}$ variations in the Earth's history for the different scenarios described in this paper. Blue areas define (from darker to lighter) the possible $\delta^{81}\text{Br}$ ranges for lower to higher fractionation factors, the lines indicate the calculated $\delta^{81}\text{Br}$ values of seawater depending on the isotope fractionation and the Br/Cl ratio of the samples. Although differences between the various scenarios are visible, it is clear that the most reasonable scenario is defined by a Br isotope fractionation factor of 1.0007, as the overlap between the scenarios with and without the Br/Cl ratio taking into account is best at this fractionation factor (overlap middle blue field with pink line).